



THE HONG KONG POLYTECHNIC UNIVERSITY
Department of Civil & Structural Engineering

Hung Hum, Kowloon, Hong Kong;
Email: cekslam@polyu.edu.hk

Fax No: 852-2334-6389;

Phone No: 2766-6071

September 23, 2004

Tender AM02 - 316

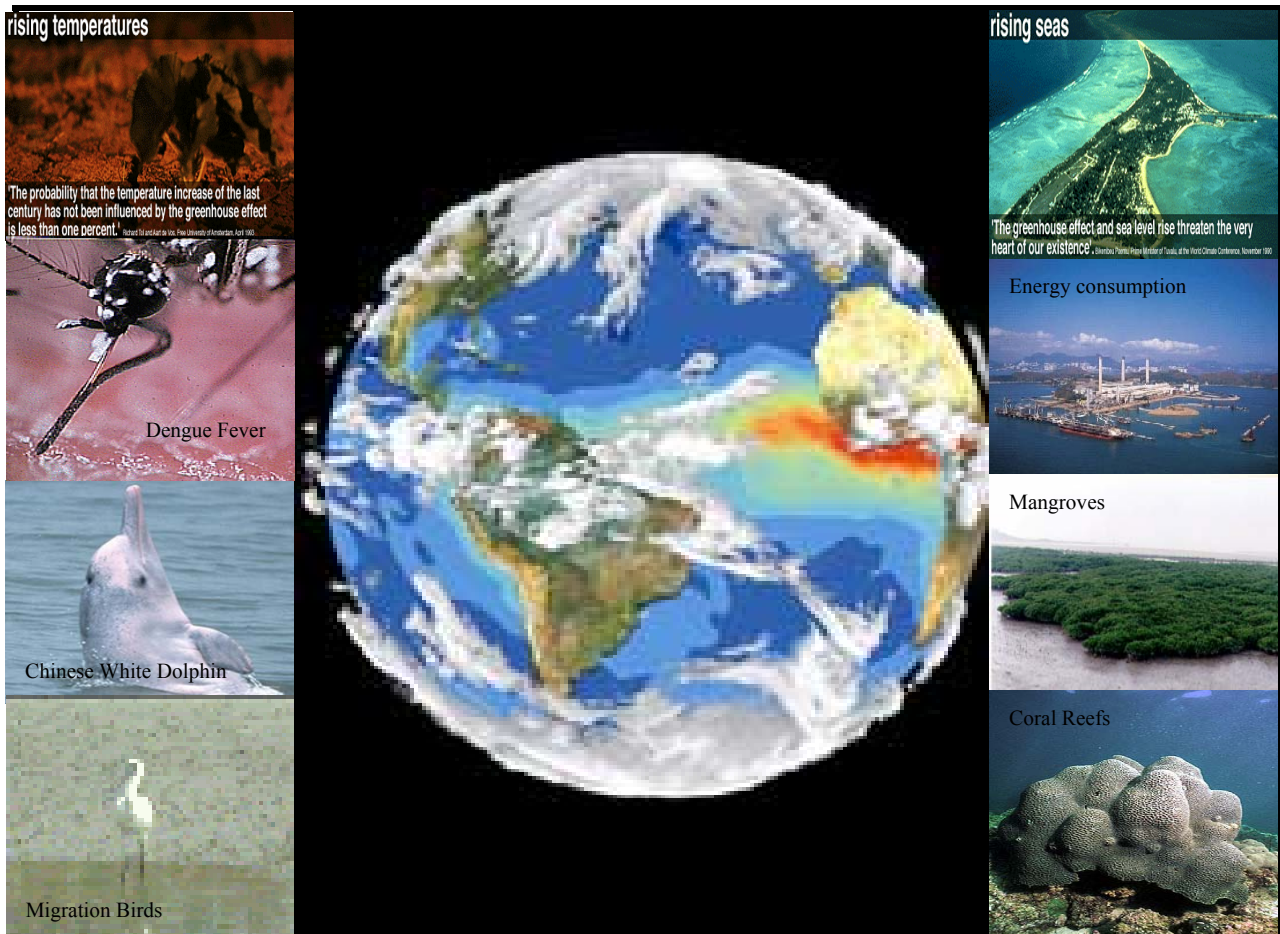
Provision of Service for Characterizing the Climate Change Impact in Hong Kong

Final report submitted to the

HKSAR – Environmental Protection Department

Written by: Miss Fung Wing Yee

Investigators: Dr. Lam Ka Se, Dr. Hung Wing Tat, Miss Fung Wing Yee



Content

<i>Content</i>	2
<i>Objectives</i>	11
<i>Part One: Urban Heat Island in the HKSAR</i>	12
<i>Chapter1: Hong Kong’s Urban Heat Island</i>	12
1.1 <i>Introduction</i>	12
1.2 <i>Methodology</i>	13
1.3 <i>Results and Discussion</i>	20
1.4 <i>Limitations of Temperature Scanning using Motor Cars</i> ..	26
1.5 <i>Conclusion</i>	33
1.6 <i>References</i>	33
<i>Part Two: Present and Future Climate in the HKSAR</i>	34
<i>Chapter2. Climatology for Hong Kong from The Hong Kong Observatory</i> 34	
2.1 <i>Past Climate Change in the HKSAR</i>	34
2.1.1 <i>Surface Temperature</i>	34
2.1.2 <i>Visibility</i>	36
2.1.3 <i>Cloud Amount</i>	37
2.1.4 <i>Global Solar Radiation</i>	37
2.1.5 <i>Evaporation</i>	38
2.1.6 <i>Rainfall / Thunderstorms / Tropical Cyclones</i>	38
2.1.7 <i>Mean Sea Level</i>	40
2.2 <i>Projected temperature in the 21st century</i>	41
2.3 <i>References</i>	42
<i>Part Three: The impacts of Climate Change and Adaptation Strategies in the HKSAR</i>	43
<i>Chapter3: Energy Industry</i>	43
3.1 <i>Introduction</i>	43
3.2 <i>Methodology</i>	44
3.3 <i>Results and Discussions</i>	46
3.3.1 <i>Electricity Consumption</i>	46
3.3.2 <i>Gas Consumption:</i>	53
3.3.3 <i>Oil Product Consumption:</i>	56
3.3.4 <i>Electricity Consumption for Government Office Buildings (Commercial Sector)</i>	57
3.4 <i>Conclusion:</i>	60
3.5 <i>References</i>	60
<i>Chapter4. Human Health</i>	61
4.1 <i>Introduction</i>	61
4.2 <i>Correlation between Mortality and Ambient Temperature in Hong Kong</i>	64
4.3 <i>Heat Stroke</i>	66

4.4 Dengue Fever (DEN)	67
4.5 Malaria.....	72
4.6 Present and Future Adaptation Measures in Hong Kong .	77
4.7 References	80
Chapter5: Air Pollution.....	81
5.1 Introduction.....	81
5.2 Ozone Study.....	81
5.2.1 Exceedance of Surface Ozone in Hong Kong.....	81
5.2.2 Results	83
5.3 Impacts and Possible Adaptations	86
5.4 References	87
Chapter6. Tourism Industry.....	88
6.1 Introduction (eco-tour)	88
6.2 Impacts on Migratory Birds Watching	89
6.3 Impacts on Dolphin Watching.....	89
6.4 Impacts on Mountain Related Tourism.....	90
6.5 Modeling of Economic Loss of Tourism	90
6.6 References	91
Chapter7. Agricultures and Water Resources	92
7.1 Agricultures.....	92
7.2 Water Resources.....	93
7.3 Flooding	96
7.4 References	101
Chapter8. Ecosystems	102
8.1 Introduction.....	102
8.2 Migratory and Local Birds	102
8.3 Hill Fires	104
8.4 References	108
Chapter9. Coastal Zones and Marine Life	109
9.1 Introduction.....	109
9.2 Impact on Coral reefs	109
9.3 Impact on Coastal Wetlands / Mangroves / Mudflats.....	112
9.4 Impact on Dolphins	113
9.5 References	115
Chapter10. Sea level Rise Extracted from “Guangdong Haipingmian Bianhua Jiqi Yingxiang Yu Duice”	116
10.1 Introduction.....	116
10.2 The Impact on Storm Tide.....	117
10.3 The impact on Water Level in the Pearl River Estuary .	119
10.4 The Impact of Sea Level Rise on Seawall and Dam	120

10.5 The Impact of Sea Level Rise on Saline Water Intrusion	124
10.6 The Impact of Sea Level Rise on Beach and Shore.....	124
10.7 The Impact of Sea Level Rise on Coastal Eco-system and Aquaculture	125
10.8 Conclusion.....	128
10.9 References	129
Chapter11 Conclusion.....	130

Content of Tables

Table 1.1 Correlation Formula for Each Temperature Sensor.....	17
Table 1.2 Temperature Adjustment for Diurnal Variation in Each Period in Summer	19
Table 1.3 Temperature Adjustment for Diurnal Variation in Each Period in Autumn.....	20
Table 1.4 Temperature Adjustment for Diurnal Variation in Each Period in Winter	20
Table 1.5 Summary of Field Sampling	25
Table 2.1 Summary of Climate Change in the HKSAR	34
Table 3.1 Polynomial and Linear Regression Results Between Electricity Consumption C and Ambient Temperature T.	48
Table 3.2 Computation of Increased Electricity Consumption of Domestic Sector due to 1°C, 2°C, and 3°C Increase in Ambient Temperature (2002 and 1996).	49
Table 3.3 Computation of Increased Electricity Consumption of Domestic Sector due to 1°C, 2°C, and 3°C Increase in Ambient Temperature (1990).	50
Table 3.4 Percentage Increase of Electricity Consumption due to Temperature Rise	50
Table 3.5 Summary of Economic Impact of Electricity Consumption due to Climate Change.....	51
Table 3.6 Relationship Between Gas Consumption and Ambient Temperature	55
Table 3.7 Percentage Increase of Gas Consumption due to Temperature Rise	55
Table 3.8 Summary of Economic Impact of Gas Consumption due to Climate Change.....	55
Table 3.9 Relationship Between Electricity Consumption of A/C Units and Ambient Temperature	56
Table 3.10 Percentage Increase of Electricity Consumption of A/C Units due to Temperature Rise ..	56

Table 4.1 Mean, Standard Deviation, Minimum, Maximum and 1, 5, 95, 99 Percentile Values of the Daily Number of Total Deaths and Temperature Variables in Hong Kong between 1995 and 2001...	64
Table 4.2 Number of Reported Heat Stroke in Hong Kong (source: Department of Health)	66
Table 4.3 Number of Notified Dengue Fever Cases (source: Department of Health).....	67
Table 4.4 The Monthly Averaged Temperature, Monthly EP, Hypothetical EP at T+1, T+2 and T+3 for the Year 2003.....	70
Table 4.5 Ten Years Averaged $\Delta EPT+1$, $\Delta EPT+2$, and $\Delta EPT+3$ Averages and Their Standard Deviations	70
Table 4.6 Calculated Relative Percentage Change of the Epidemic Potential (ΔEP) in Hong Kong, Compared to the Baseline (1994-2003 monthly mean temperature)	71
Table 4.7 Number of Notified Malaria Cases (source: Department of Health).....	72
Table 4.8 The Monthly Averaged Temperature, Monthly EP for <i>P. vivax</i> , Hypothetical EP at T+1, T+2 and T+3 for the Year 2003.....	75
Table 4.9 The Monthly Averaged Temperature, Monthly EP for <i>P. falciparum</i> , Hypothetical EP at T+1, T+2 and T+3 for the Year 2003.	75
Table 4.10 Ten Years Averaged $\Delta EPT+1$, $\Delta EPT+2$, and $\Delta EPT+3$ of <i>P. falciparum</i> and their Standard Deviations.....	76
Table 4.11 Estimated Relative Percentage Change of the Epidemic Potential (ΔEP) of Malaria in Hong Kong, Compared to the Baseline (1994-2003 monthly mean temperature)	75
Table 5.1 Hourly Percentage of Ozone Exceed Standard ($240\mu\text{g}/\text{m}^3$) in the First Three Stations	82
Table 5.2 Correlation Coefficients of the Entire Data Set in the Tung Chung Station a: statistically significant (significance of t value < 0.05)	85
Table 5.3 Linear Equations of Ozone Generated from the Entire Data Set in the Tung Chung Station.....	85
Table 5.4 Correlation Coefficients when $O_3 > 240\mu\text{g}/\text{m}^3$ in the Tung Chung Station.....	85
Table 5.5 Linear Equations of Ozone when $O_3 > 240\mu\text{g}/\text{m}^3$ in the Tung Chung Station.....	85
Table 5.6 Correlation Coefficients when the Temperature is Greater than 32°C	86

<i>Table 5.7 Linear Equations of Ozone when the Temperature is Greater than 32°C in the Tung Chung Station.....</i>	<i>86</i>
<i>Table 6.1 Special Interest Activities of Visitors in Hong Kong in 2001 (source: Hong Kong Tourism Board)</i>	<i>88</i>
<i>Table 7.1 Production of Local Agricultural Food.....</i>	<i>92</i>
<i>Table 7.2 GDP by Economic Activity at Current Prices (Hong Kong Yearbook, 2002).....</i>	<i>93</i>
<i>Table 7.3 Capacity of Hong Kong reservoirs (Water Supplies Department, HKSAR).....</i>	<i>93</i>
<i>Table 7.4 Average Recurrence Interval of Flooding Prevention in Hong Kong Drainage Systems.....</i>	<i>100</i>
<i>Table 8.1 Category of Ecological Species in Hong Kong.....</i>	<i>102</i>
<i>Table 8.2 Numbers of 24 Migration Birds in Hong Kong</i>	<i>103</i>
<i>Table 8.3 Numbers of Saunders' Gulls in Past Ten Years.....</i>	<i>104</i>
<i>Table 8.4 Number of hill Fires Between 1991 and 2002</i>	<i>105</i>
<i>Table 8.5 Linear Regression Between the Number of Hill Fires, Temperature and Relative Humidity</i>	<i>106</i>
<i>Table10.1 Current Storm Tide Increment Δh_p (in meter) in Hong Kong at Different Frequencies.....</i>	<i>118</i>
<i>Table10.2 Predicted Change in Return Period of StormTide due to Sea LevelRise.....</i>	<i>118</i>
<i>Table10.3 Standards of Dams and Seawalsl in the GuangdongProvince (1995)</i>	<i>119</i>
<i>Table10.4 Design Standards of Drainage in Hong Kong.....</i>	<i>120</i>
<i>Table10.5 Change in Design of ReturnPperiod of Storm in the Pearl River Estuary Stations (0.3m sea level rise).....</i>	<i>120</i>
<i>Table10.6 Impact on the Storm Tide Level of the Pearl River Delta according to a 0.3m Rise in Sea Level.....</i>	<i>121</i>
<i>Table10.7 Design Standards of Tide WaveHeight at Present and in 2030.....</i>	<i>122</i>
<i>Table10.8 Reduction of Beach and Shore Area due to Sea Level Rise in 2030 (unit of area : km²)</i>	<i>125</i>
<i>Table10.9 Horizontal Erosion Distance of Beaches due to Sea Level Rise in 2030.....</i>	<i>128</i>

Content of Figures

<i>Figure 1.1 Routes for Air Temperature Measurement</i>	<i>13</i>
<i>Figure 1.2 Measurement Equipment and Setting.....</i>	<i>15</i>
<i>Figure 1.3 Temperature Distributions Along the Routes</i>	<i>16</i>
<i>Figure 1.4 Linear Relationship Between Normalized and Original Temperature.....</i>	<i>17</i>

<i>Figure 1.5 Diurnal Temperature Variation and the Polynomial Fitted Curve [a: on 2nd June 2004; b: on 24th September 2004; c: on 9th January 2004]</i>	19
<i>Figure 1.6 The UHI Values in Different Periods</i>	21
<i>Figure 1.7 Specific UHI Values in All Periods</i>	23
<i>Figure 1.8 Temperature Anomalies Distributions in Summer Weekday at 0300 (upper side), 1500 (middle side) and 2200 (lower side) respectively</i>	27
<i>Figure 1.9 Temperature Anomalies Distributions in Summer Weekend at 0300 (upper side), 1500 (middle side) and 2200 (lower side) respectively</i>	28
<i>Figure 1.10 Temperature Anomalies Distributions in Autumn Weekday at 0300 (upper side), 1500 (middle side) and 2200 (lower side) respectively</i>	29
<i>Figure 1.11 Temperature Anomalies Distributions in Autumn Weekend at 0300 (upper side), 1500 (middle side) and 2200 (lower side) respectively</i>	30
<i>Figure 1.12 Temperature Anomalies Distributions in Winter Weekday at 0300 (upper side), 1500 (middle side) and 2200 (lower side) respectively</i>	31
<i>Figure 1.13 Temperature Anomalies Distributions in Winter Weekend at 0300 (upper side), 1500 (middle side) and 2200 (lower side) respectively</i>	32
<i>Figure 2.1 Annual Mean Temperature Recorded at the Hong Kong Observatory Headquarters (1885-2002). Data are not available from 1940 to 1946</i>	35
<i>Figure 2.2 Annual Mean Daily Diurnal Range Recorded at the Hong Kong Observatory Headquarters (1947-2002)</i>	35
<i>Figure 2.3 Annual Mean Daily Maximum and Minimum Temperatures Recorded at the Hong Kong Observatory Headquarters (1947-2002)</i>	36
<i>Figure 2.4 Percentage of Occurrence of Reduced Visibility Below 8 km (cases due to fog, mist or rain excluded) Observed at the Hong Kong Observatory Headquarters (1968-2002)</i>	36
<i>Figure 2.5 Cloud Amount Recorded at the Hong Kong Observatory Headquarters (1961-2002)</i>	37
<i>Figure 2.6 Annual Mean Daily Total Global Solar Radiation at King's Park (1964-2002)</i>	38
<i>Figure 2.7 Annual Total Evaporation at King's Park (1964-2002)</i>	38

<i>Figure 2.8 Number of Days with Hourly Rainfall Greater than 30 mm, 50mm and 70mm Respectively Recorded at the Hong Kong Observatory Headquarters (1947-2002)</i>	39
<i>Figure 2.9 Annual Number of Days with Thunderstorm (1947-2002)</i>	39
<i>Figure 2.10 Annual Number of Tropical Cyclones Landing Over the south China Coast Within 300 km of Hong Kong (1961-2002)</i>	40
<i>Figure 2.11 Annual Mean Sea Level Recorded at North Point/Quarry Bay (1954-2003)</i>	40
<i>Figure 2.12 Annual Mean Sea Level Recorded at Tai Po Kau (1963-2003)</i>	40
<i>Figure 2.13 Projected Annual Mean Temperature for Hong Kong in the 21st century</i>	42
<i>Figure 3.1 Global Temperature Trend Under Different Scenarios (source:IPCC, 2001)</i>	44
<i>Figure 3.2 Hong Kong's Electricity Consumption from 1990 to 2002</i>	46
<i>Figure 3.3 Temperature Dependence of Electricity Consumption</i>	47
<i>Figure 3.4 Hong Kong's Gas Consumption from 1990 to 2000</i>	53
<i>Figure 3.5 Temperature Dependence of Gas Consumption</i>	54
<i>Figure 3.6 Hong Kong's Oil Product Consumption from 1997 to 2003</i>	56
<i>Figure 3.7 Normalized Electricity Consumption of A/C units in Government Buildings</i>	57
<i>Figure 3.8 Electricity Consumption of Buildings with Air Cooled and Sea Cooled A/C Units</i>	58
<i>Figure 4.1 Causal Pathways of Public Health Impacts from Climate Change</i>	61
<i>Figure 4.2 Conceptual Representation of the Health Impact of the MIASMA Model</i>	63
<i>Figure 4.3 Time series of the Total Number of Daily Deaths and the Daily Average Temperature in Hong Kong between 1995 and 2001</i> ..	65
<i>Figure 4.4 Mortality-Temperature Relation for Temperatures of 14.8°C or less (left) and of 29.8°C or over (right) between 1995 and 2001</i>	65
<i>Figure 4.5 Epidemic Potential for Dengue Fever</i>	68
<i>Figure 4.6 Relationship between Temperature and Factors of Dengue Transmission. (A): Incubation Period n of Dengue Virus in the Mosquito; (B): Mosquito Biting Frequency a; (C): Survival Probability of Adult Mosquito p</i>	69
<i>Figure 4.7 Monthly Average Percentage Change in Epidemic Potential of Dengue Fever in 1994-2003. The error bars denote the maximum and minimum values</i>	71
<i>Figure 4.8 Epidemic Potential for <i>P. vivax</i> (right side) and <i>P. falciparum</i> (left side)</i>	71

<i>Figure 4.9 Monthly Average Percentage Change in Epidemic Potential of Malaria in 1994-2003. The error bars denote the maximum and minimum values.</i>	<i>76</i>
<i>Figure 4.10 Average of Monthly Ovitrap Index (2000-2003) against Mean Temperature.....</i>	<i>78</i>
<i>Figure 4.11 Average of Monthly Ovitrap Index (2000-2003) against Mean Rainfall.....</i>	<i>78</i>
<i>Figure 5.1 Percentage of O₃ Exceedance in EPD Air Monitoring Stations (CW states for Central/Western, KC states for Kwai Chung, KT states for Kwun Tong, SP states for Sham Shui Po, ST states for Sha Tin, TC states for Tung Chung, TM states for Tap Mum, TP states for Tai Po, TW states for Tsuen Wan, YL states for Yuen Long).</i>	<i>82</i>
<i>Figure 5.2 Seasonal Trends of O₃ exceedance, Ambient Temperature and Global Solar Radiation in the Tung Chung Station.</i>	<i>83</i>
<i>Figure 5.3 Hourly Ozone Concentration Against Ambient Temperature in the Tung Chung Station</i>	<i>84</i>
<i>Figure 7.1 Daily Average Water Consumption.....</i>	<i>94</i>
<i>Figure 7.2 Fresh Water Demand in the Future.....</i>	<i>95</i>
<i>Figure 7.3 The Number of Rainstorm Warning in Hong Kong Between 1995 and 2003</i>	<i>97</i>
<i>Figure 7.4 The Number of Flooding Announcements in the Northern Territories in Hong Kong Between 1995 and 2003.....</i>	<i>98</i>
<i>Figure 7.5 A Time Series of Annual Rainfall and Number of Flooding Complaints in Between 1989 and 2002</i>	<i>98</i>
<i>Figure 7.6 The Number of Flooding Complaints in Different Districts in the Northern Part of Hong Kong Between 1997 and 2002</i>	<i>99</i>
<i>Figure 7.7 Extensive Flooding in Shenzhen River and Ma Tso Lung areas, Sheung Shui, during Typhoon Dot in 1993 (left) and The Completed Shenzhen River Regulation Project Stages I & II (right)</i>	<i>100</i>
<i>Figure 8.1 Relationship Between Hill Fires and Relative Humidity.....</i>	<i>105</i>
<i>Figure 8.2 Relationship Between Hill Fires and Rainfall.....</i>	<i>106</i>
<i>Figure 8.3 Approximate Number of Trees Planted Against the Number of Hill Fires Between 1997 and 2001</i>	<i>107</i>
<i>Figure 8.4 Approximate Number of Trees Planted And its Unit Cost in Tree-Planting Program Between 1997 and 2001.....</i>	<i>108</i>
<i>Figure 9.1 Healthy (left and middle sides) and Bleached (right side) Corals in Hong Kong Waters</i>	<i>109</i>
<i>Figure 10.1 Four Influence Zones of Flooding/Tidal Level due to Sea Level Rise in the Pearl River Delta.....</i>	<i>121</i>

*Figure 10.2 Distribution of Tide, Mixed and Flooding Zones in the Pearl
River Delta..... 127*

Figure 10.3 Shoreline Retreat of Beaches and Sea Level Rise 128

Objectives

The aim of this consultancy project is to characterize the impacts of Urban Heat Island and global warming on the climatic, social-economic and ecological systems of Hong Kong.

Work Specifications:

I. Quantify the UHI

- Field measurement on cross-city ambient temperature
- Impact of UHI on A/C power consumption

II. Evaluate Global Warming Indicators

- Annual Surface Temperature Trends
- Sea Level Change in Hong Kong
- Tropical cyclone Trends
- Precipitation Trends

III. Delineate the Potential Impacts of Local and Global Climate Change on Hong Kong

- Impact on natural environment: Estimate the potential impacts on local marine resources, local terrestrial and avian species and ecological habitats.
- Impact on Socio-Economics: Based on the published literature and data collected in this project, comment on the relationship between climate change in Hong Kong and the following issues as far as possible.
- Heat related illness and epidemic diseases such as Malaria and Dengue disease.
- Hill fire outbreaks.
- Agricultural returns in terms of crop yields and livestock productivity.
- Health of forest and wild plants.
- Cost of infrastructure such as drainage system and coastal works.
- Quality of building structure.
- Potential damage to local tourism.

IV. Take stock of the existing and potential adaptive strategies related to coastal areas, water resources, fisheries, agriculture and public health.

Part One: Urban Heat Island in the HKSAR

This report on the urban heat island (UHI) confirms the existence of UHI phenomenon, especially in the Kowloon Peninsular and northern part of Hong Kong Island. The UHI values are defined by the difference between air temperature measured in the urban areas and the air temperature at the Cheung Chau Station (Fixed Station). The UHI value was about 2.17°C in Hong Kong. The largest UHI occurred in the mixed commercial urban area of Causeway Bay, Yau Ma Tei and Mongkok. The averaged UHI values were 2.12°C in summer, 3.04°C in autumn and 1.35°C in winter respectively.

Chapter1: Hong Kong's Urban Heat Island

1.1 Introduction

Global warming has many implications to the environment with significant impacts on economic development and sustainability of the ecosystem. The increase in temperature induces global warming and consequently ice melting and the rise in sea level over decades. Global warming is a consequence of emissions of green house gases in the urbanization process. Microscopically, urbanization may give rise to urban heat island (UHI) in which the heat generated from fuel combustion in vehicles and power usage from air conditioning is trapped by high-rise buildings. As a result, the temperatures in the urban areas are substantially higher than the rural areas. There is evidence of the existence of UHI as the land air temperature in urban areas has been increasing over the last few decades.

Hong Kong is a typical example of urban city in Asia. The rate of urbanization has been very fast as it develops into a world city. It is interesting to study the existence and impacts of UHI. Hong Kong Observatory (HKO) reported that the surface temperature in urban areas of Hong Kong is rising and it might be due to UHI effects. The HKO had conducted a study about the regional temperature variation in winter (December to February) between 1991 and 1995. The study reported that the average difference in minimum temperature variation among nine fixed stations was only one or two degrees and the greatest average difference of around three degrees was recorded between Ta Kwu Ling and the HKO. It showed that there may be an existence of heat island effect in winter of Hong Kong. (The HKO Technical Note (Local) No. 72) It is also suspected that UHI effect would increase energy demand for air conditioning. Power consumption statistics show that electricity used for space conditioning has increased by 4159 GWh since 1990. (Hong Kong Energy End-use Data 1990-2000).

UHI is not unique in Hong Kong, it exists elsewhere. A research on the impact of anthropogenic heat on urban climate in Japan revealed that the space cooling energy in winter and heating energy in summer were significant and the energy demand at hotels was as high as 170W/m² in the morning for heating water. (Toshiake Ichinose,1999). Another study on UHI in Singapore confirmed the existence of UHI there. Subsequently, the Singapore government implemented mitigation measures to reduce the accumulation

of heat energy in urban areas. Rooftop garden, as one of the measures, was employed to reduce the energy demand for cooling and provide a creative green urban outlook. (Nyuk Hien Wong, 2003)

To sustain the development of Hong Kong, it is necessary, as an initial step, to characterize the UHI in Hong Kong and its impacts on the ecological, social and economic systems. The first objective of this study is therefore to verify the existence of UHI. Temperature profiles across the urban areas were established using instrumented cars running from North to South and East to West of the Territory in summer, autumn and winter seasons. The diurnal temperature range in urban and rural areas and the temperature difference between urban and rural areas were observed in daytime and nighttime from June of 2003 to January 2004.

1.2 Methodology

Two cars equipped with Global Positioning System (GPS) instruments and a set of temperature sensors were driven along fixed routes across the urban areas. Two typical routes are shown in Figure 1.1 below.

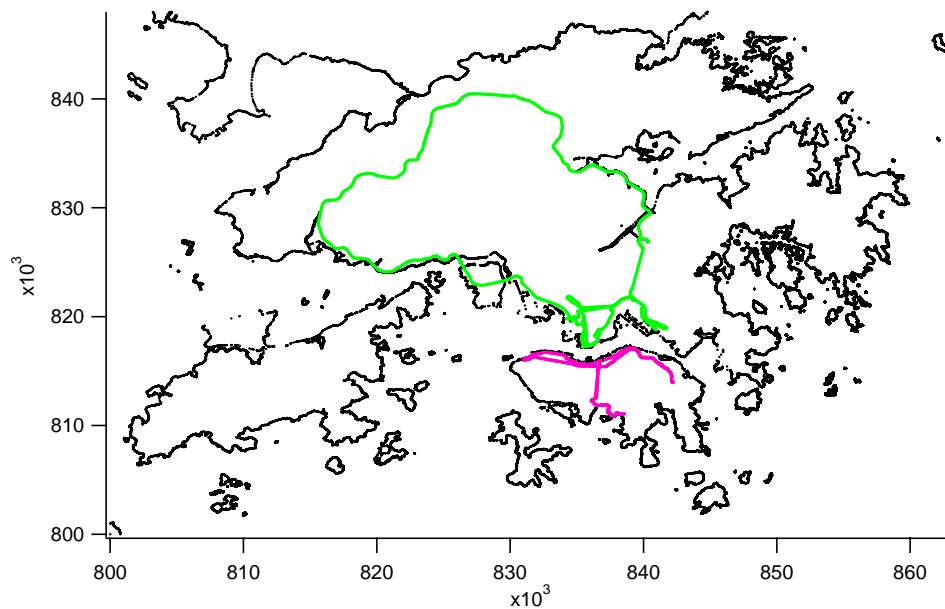


Figure 1.1 Routes for Air Temperature Measurement

The routes cover both the urban and rural areas, passing through mixed residential and commercial urban areas in the Kowloon peninsular and the northern part of Hong Kong Island. The routes also pass through the mixed residential and industrial zones of Kwun Tong, as well as the rural areas of Sai Kung and Shek O.

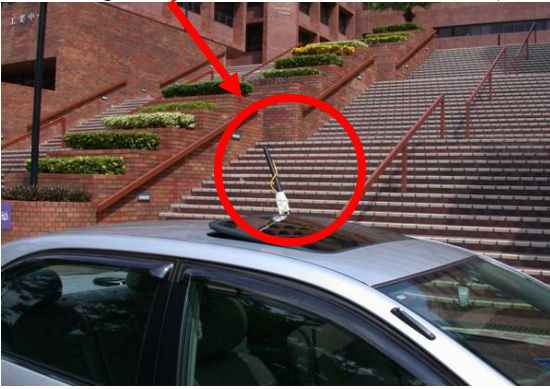
Two vehicles were driven along selected routes on Hong Kong Island and the Kowloon peninsular to collect field data three times a day, i.e., morning, afternoon and night in

order to capture the biggest daily temperature difference. The experiment was carried out on one weekday and one holiday in the summer, autumn of 2003 as well as January 2004 (i.e. winter).

UHI is defined as the temperature difference between rural and urban locations measured at the same time. It took more than two hours to complete one trip. The diurnal temperature cycle may introduce a significant error in the UHI between two different locations due to a time lag in measurement. It was necessary to convert all measurements to unified times. All temperatures measured in the morning trips were adjusted to 03:00, the afternoon trips were adjusted to 15:00 and the night trips were adjusted to 22:00. In order to determine the temperature adjustment due to diurnal variation, the daily temperature records were obtained from the HKO Headquarter on the measurement days. Results indicated that the temperature adjustment was necessary, especially in the afternoon.

The GPS instruments which record the vehicle locations and the temperature sensors which measure the air temperature were linked to the computers on board of the cars for realtime data recording. The two GPS receivers (Global Map@100 and i-Finder®) showed the location of the vehicle every second. Two set of temperature sensors (IAQ Calc thermister and one thermocouple) were fixed onto the rooftop of each vehicle. These sensors provided readings in degree Celsius every 2 seconds. The temperature sensors were enclosed by a screen box similar to the Stevenson screen to abate solar radiation heating and wind chill. The equipment settings and the experiment instruments are displayed in Figure 1.2.

Two temperature sensors
(Thermocouple in yellow and thermistor in black)



Screen Box

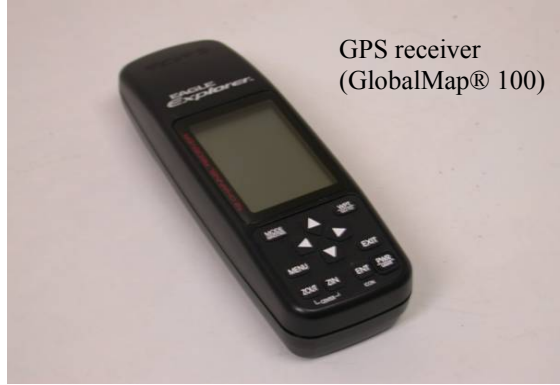


Data captured
in computer

Temperature
(IAQ Calc)



GPS receiver
(GlobalMap® 100)



Temperature Sensor
(Thermocouple)

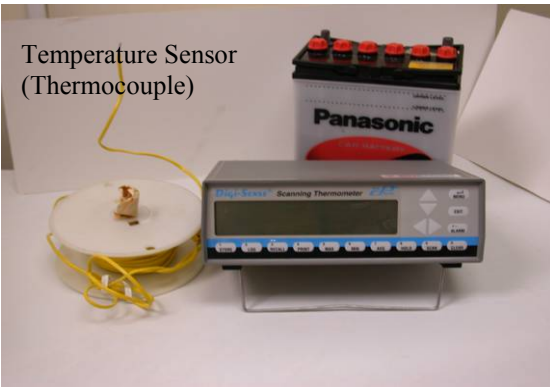


Figure 1.2 Measurement Equipment and Setting

Temperature profiles of the corresponding time periods were then constructed. The seasonal measurements were performed on 2 June (weekday), 6 July (weekend), in 24 September (weekday), 28 September (weekend) of 2003 and 9 January (weekday), and 11 January (weekend) of 2004 respectively. A typical spatial temperature distribution recorded is displayed in Figure 1.3 below.

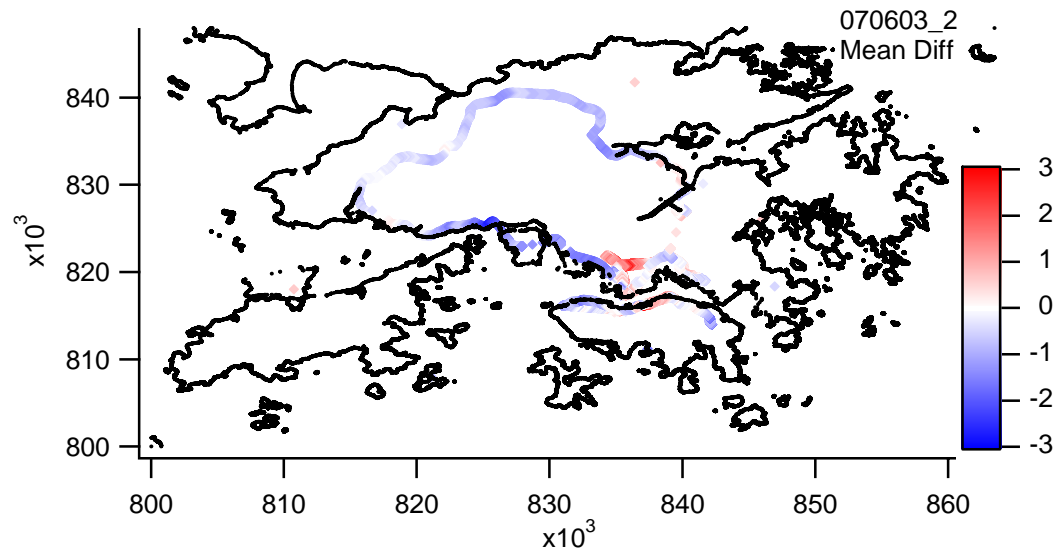


Figure 1.3 Temperature Distributions Along the Routes

Quality Control and Quantity Assurance

Before sampling, all temperature sensors were placed in the same room to measure the same temperature for 24 hours. The temperature measured was compared with a certified mercury thermometer. The most accurate sensor was taken as the reference. The correlation of readings between each sensor and the reference sensor were obtained. The temperature outputs of all sensors were normalized according to the correlation. Two temperature sensors of different principles were used for real time inter-comparison. The models of iFinder and Global Map@100 are approved by the US Government and their horizontal accuracy in tropical region is about 20 meters.

Data Analysis

UHI values are determined from the differences between averaged temperatures in the urban center of Hong Kong, mainly in the Kowloon peninsular and the northern part of Hong Kong Island, and the relative rural areas, Cheung Chau (HKO provided), Sai Kung and Shek O.

Temperature Adjustment:

Temperature was adjusted by two steps and the empirical formula is described as below:

$$T_i = T_{ni} + T_{di}$$

where T_i is the adjusted temperature in specific time i , T_{ni} is the adjusted temperature due to normalization between different thermometers in specific time i and T_{di} is the adjusted temperature due to the diurnal change based upon the HKO Headquarter records respectively.

First, all temperatures were normalized according to the procedures as described in the quality control session earlier in the chapter. The correlation formulae between each thermister and the reference sensor are shown in Table 1.1. The correlation between one thermister and the reference thermocouple is plotted in Figure 1.4.

sensor (S/N)	Correlation Formula	Linear correlation coefficient, R
IAQ (01110374)	$T' = 1.012(T) - 0.821$	0.954
IAQ (03030470)	$T' = 1.0131(T) - 0.673$	0.952

T' and T are the normalized and original temperatures respectively

Table 1.1 Correlation Formula for Each Temperature Sensor

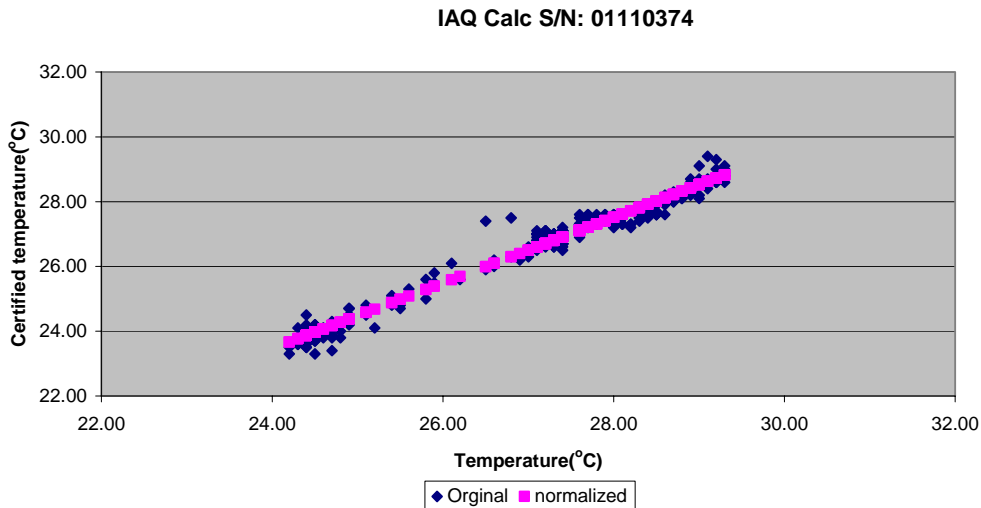


Figure 1.4 Linear Regression Between One Thermocouple and One Thermister

The first survey trip started at 13:00 on a clear sunny day and completed by 16:00 hours. Another two survey trips were made between 20:00 to 23:00 hours and 2:00 to 5:00 hours respectively. All temperatures were adjusted to the reference times at 15:00, 22:00 and 3:00 hours of the day. The first and third periods covered the highest and lowest temperatures of the day.

The diurnal temperature variations of the day were obtained from the HKO Headquarter to assess regional variations. The hourly temperature was plotted against the time and a fitted polynomial

curve with 14 powers was obtained as shown in Figure 1.5. The temperature adjustments of two field days are listed in Tables 1.2-1.4.

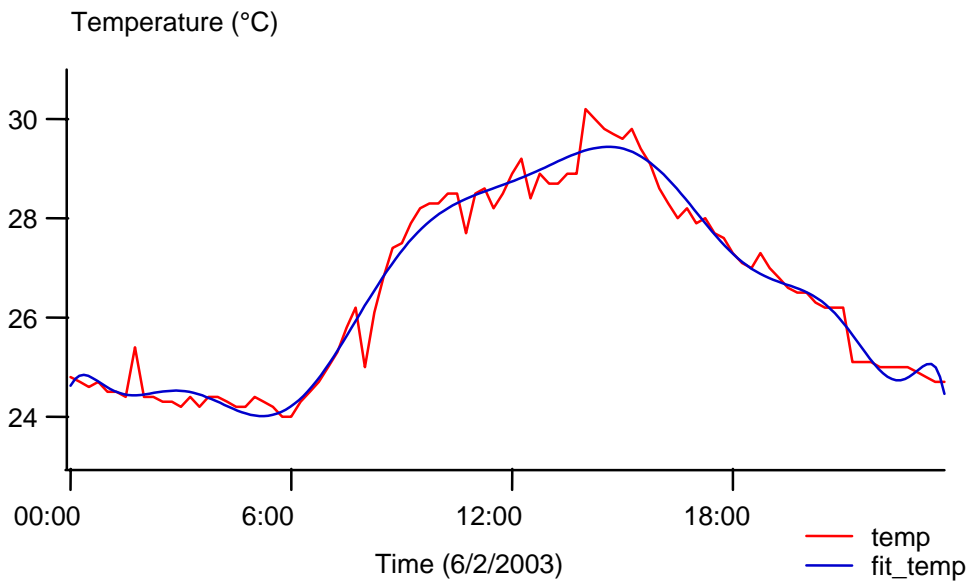


Figure 1.5(a) Diurnal Temperature Variation and the Polynomial Fitted Curve on 2 June 2003

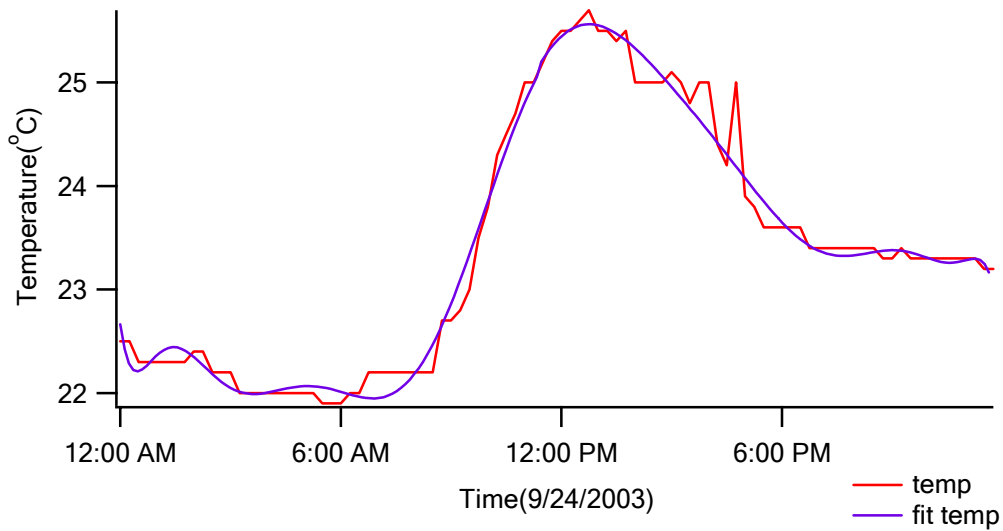


Figure 1.5 (b) Diurnal Temperature Variation and the Polynomial Fitted Curve on 24 September 2003

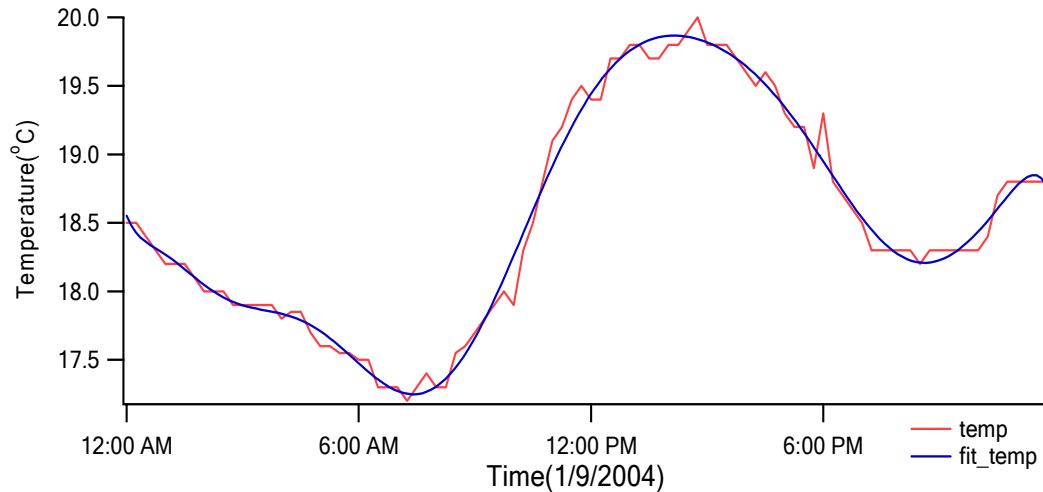


Figure 1.5(c) Diurnal Temperature Variation and the Polynomial Fitted Curve on 9 January 2004

The records from the HKO Headquarter showed that the diurnal temperature variation in June increased gradually in the morning due to sunlight, it reached the peak in the afternoon, then started to drop from 16:00 and fell to the minimum temperature at the mid-night. The surface temperature was sensitive to solar intensity, cloud amount and wind chill.

Diurnal temperature adjustment, T_{di} , was determined from the temperature difference between the reference time and the measurement time as below. It may be negative or positive. The diurnal adjustment were between -0.3°C and $+0.6^{\circ}\text{C}$, between -0.4°C and $+0.2^{\circ}\text{C}$ and -0.6°C and $+0.4^{\circ}\text{C}$ in summer, autumn and winter respectively.

$$T_{di} = T_{hko} - T_{sp}$$

where T_{hko} is the temperature measured at the HKO Headquarter in time i , and T_{sp} is the temperature measured at the HKO at specific time (0300 in morning, 1500 in afternoon, 2200 in night) respectively

Data	Time period	Diurnal Temperature adjustment ($^{\circ}\text{C}$), T_{di}
2 June 03 (weekday/afternoon)	14:01 to 16:20	-0.08 ~ +0.597
2 June 03 (weekday/evening)	21:25 to 23:41	-0.277 ~ +0.105
6 June 03 (weekday/morning)	02:36 to 04:47	-0.224 ~ +0.266
6 July 03 (weekend/afternoon)	13:50 to 16:55	+0.287 ~ +0.174
6 July 03 (weekend/evening)	20:37 to 00:15(7 July)	-0.198 ~ +0.163
6 July 03 (weekend/morning)	02:09 to 05:01	-0.308 ~ +0.217

Table 1.2 Temperature Adjustment for Diurnal Variation in Each Period in Summer

Data	Time period	Diurnal Temperature adjustment (°C), T_{di}
24 Sept 03 (weekday/afternoon)	14:01 to 15:35	-0.3744 ~ +0.2326
24 Sept 03 (weekday/evening)	21:01 to 23:15	-0.0632 ~ +0.0485
25 Sept 03 (weekday/morning)	02:10 to 04:15	-0.1835 ~ +0.0582
28 Sept 03 (weekend/afternoon)	12:50 to 15:30	-0.290 ~ +0.179
28 Sept 03 (weekend/evening)	21:01 to 23:10	-0.1899 ~ +0.026
28 Sept 03 (weekend/morning)	02:01 to 04:00	-0.0084 ~ +0.006

Table 1.3 Temperature Adjustment for Diurnal Variation in Each Period in Autumn

Data	Time period	Diurnal Temperature adjustment (°C), T_{di}
9 Jan 04 (weekday/afternoon)	13:22 to 15:35	-0.0492 ~ +0.0876
9 Jan 04 (weekday/evening)	20:34 to 22:06	-0.1009 ~ +0.2290
9 Jan 04 (weekday/morning)	02:38 to 04:56	-0.0338 ~ +0.3561
11 Jan 04 (weekend/afternoon)	13:53 to 15:37	-0.0094 ~ +0.1529
11 Jan 04 (weekend/evening)	19:41 to 21:15	-0.5890 ~ -0.2600
11 Jan 04 (weekend/morning)	01:29 to 03:04	-0.1339 ~ +0.001

Table 1.4 Temperature Adjustment for Diurnal Variation in Each Period in Winter

Air temperature gradually decreases with altitude. The selected routes for this study were relatively flat and most of the time near sea level. The influence of altitude is considered insignificant.

1.3 Results and Discussion

Table 1.5 below summarizes the UHI values in summer and autumn. Each region has at least 200 samples which fulfill the sample size requirement for significance test.

The detailed temperature records of each type of land use areas (i.e. residential, commercial and rural) are shown in Appendix A. In this study, Causeway Bay, Wan Chai and Central, and North Point are classified as mixed commercial urban areas. Tsim Sha Tsui, Yau Ma Tei, Mongkok, Shum Shui Po, Tai Po, Sha Tin, Chai Wan, Sai Wan, Tseung Kwan O, Amoy Gardens, Olympic MTR Station, Yuen Long, Ho Man Tin and To Kwa Wan are classified as residential urban areas. Kwun Tong is classified as the industrial urban areas. Sai Kung, Stanley, Red Hill and Shek O are classified as rural areas. The temperature at Cheung Chau Station has been taken as the reference rural temperature.

UHI values were determined by the difference between averaged temperatures in the urban areas and the temperature at Cheung Chau at a particular time. The general formula is illustrated as below:

$$UHI(\text{avg}) = T_{uj} - T_r$$

where T_{uj} denotes the average urban temperature in specific regions j ,
 T_r denotes reference rural temperature in Cheung Chau Station

General Observation

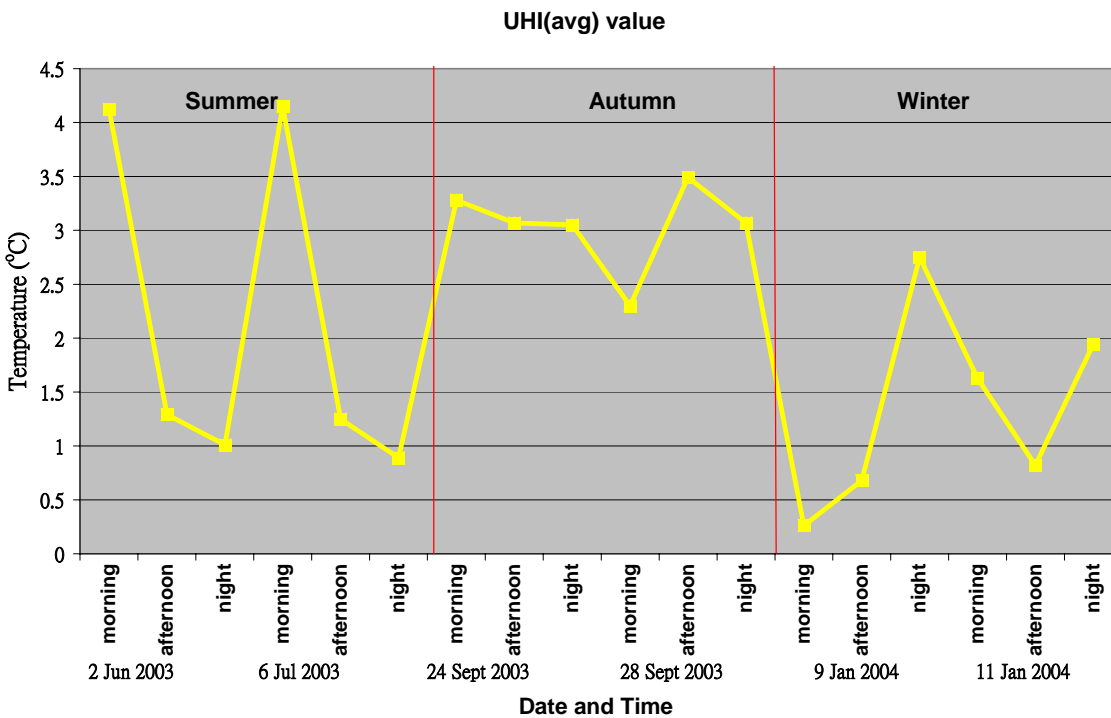


Figure 1.6 The UHI Values in Different Periods

In summer, the averaged UHI value ranged from 1.01°C to 4.12°C on weekday and from 0.89°C to 4.15°C on weekend respectively. In autumn, the averaged UHI value ranged from 3.05°C to 3.28°C on weekday and from 2.30°C to 3.49°C on weekend. In winter the averaged UHI value ranged from 0.26°C to 2.75°C on weekday and from 0.82°C to 1.94°C on weekend. The maximum UHI values in summer occurred in the morning while in winter it occurred at night

(Figure 1.6). It appears that the Urban Heat Island effect could be best observed in the early morning of clear summer days or within a few hours after sunset in winter.

The urban temperature depends mainly on the air temperature and the heat budget of the concrete surface. It is difficult to comment on the strength of UHI in different seasons without operating an UHI model. Solar radiation and urban heat emissions are important heat sources. The UHI values recorded were stronger in fall and weaker in winter. UHI is a relative figure; it is the difference between rural and urban temperature. Although solar radiation is much stronger in summer, summer UHI was low both in the afternoon and evening but high in small hours. In fall, though solar radiation is not as strong as it is in summer, UHI was high. In general Hong Kong has more clear sky days in fall. Radiation loss and cloud amount might be important factors.

Compare to Singapore, the UHI values between urban Orchard Road and rural Paya Lebar measured in early 1990 were 1 - 2°C at 22:00, and 2.4°C at mid-night,. (C.P.Tso, 1996). Whereas in this study, the averaged UHI values were 2.12°C at night (22:00), 2.62°C in the morning (03:00) and 1.77°C in the afternoon (15:00). The UHI values observed in Hong Kong were slightly higher than that in Singapore. The heat island effect is probably caused by topography and dense population of Hong Kong. Dense development in the form of high rise buildings impedes heat dissipation.

UHI Values in Specific Regions

The UHI values in three different representative regions were also compiled: Chai Wan (residential urban area), Wan Chai and Central (mixed commercial urban areas) and Kwun Tong (industrial area). These regions represent the main land use pattern in urban areas and the specific UHI values are illustrated in Figure 1.7 and Table 1.5.

In general, the UHI values in Wan Chai and Central (commercial areas) are the highest, with the exceptions of weekends of summer nights, weekdays and weekends of winter mornings. In commercial areas, all buildings adopt the central conditioning system for space cooling and ventilation. Cooling load is maximum in summer time. The system pumps the indoor heat energy into the atmosphere and warms up the urban atmosphere during the day. Together with the strong solar radiation, the heat gain of urban atmosphere in summer time is enormous. In the evening, hot buildings and road surfaces keep the air warm until mid-night. At the same time summer is a growth season. In rural areas, the plants absorb solar energy and use it for photosynthesis in daytime and much of the solar energy is consumed by the plants. There is not much energy source to warm the rural areas at night. Therefore, these two phenomena would induce large temperature difference between commercial and rural areas in the early morning in summer time. The explanation for small UHI in the summer afternoon could be attributed to local meteorology. The summer field trip was carried out on a sunny day with blue sky where land and sea breeze was the typical meteorology. The wind speed was more turbulent in the afternoon under sea breeze condition. Better ventilation induces better mixing. Thus the air temperature in Hong Kong is quite uniform in the afternoon. On the other hand, nocturnal inversion layers suppress mixing in the morning hours. When advection and turbulence die down, radiation loss becomes dominant. This is one of the possible explanations for the small UHI during summer afternoon and high UHI in the morning. This is a subject of scientific interest. It warrants further investigations.

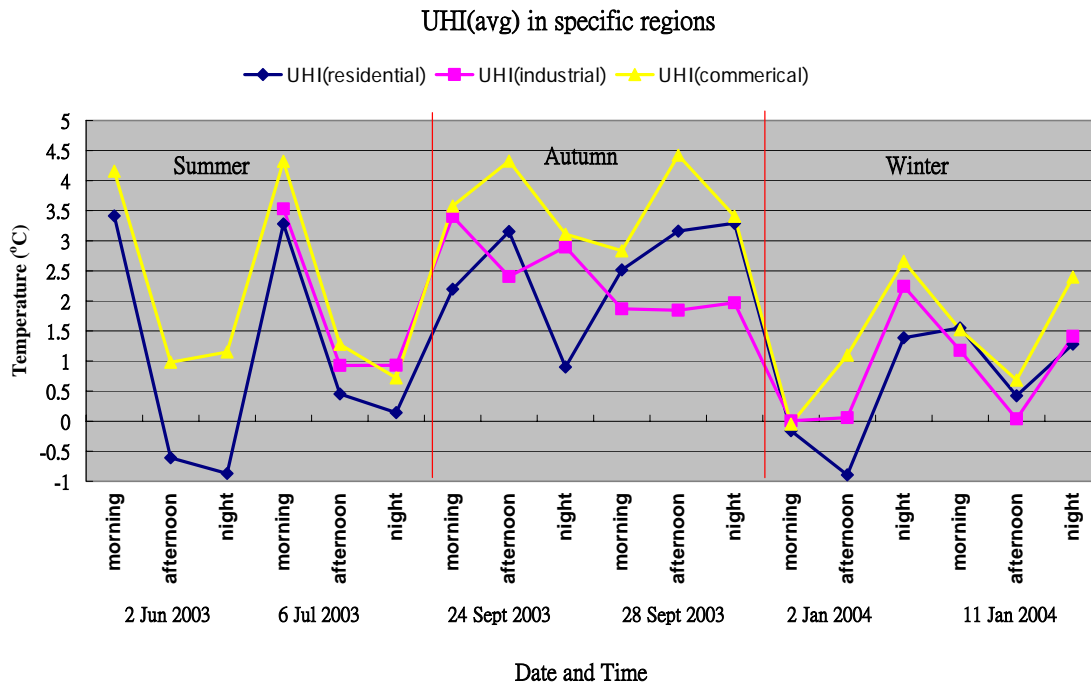


Figure 1.7 Specific UHI Values in All Periods

The results showed that negative UHI values occurred in summer and winter. This implies that the rural temperature was higher than urban temperature during those times. Chow Shu Zhen also pointed out that western countryside temperature is 1.7°C higher than the roadside of He Fei (合肥), an urban area in Shanghai. (Chow Shu Zhen, 1989) This phenomenon appears due to less activity in residential areas in daytime. Most people go to work during the daytime and the energy consumption is lower in residential area. The energy dissipation rate varies between rural and urban areas. Therefore, the ambient temperature at certain times could be higher in rural areas than urban area.

In winter, the UHI values in another industrial area, Kwai Chung, were measured during the weekdays and weekends. Compared with the values in Kwun Tong, the UHI values were similar to each other. Apart from this, the UHI values in residential areas were similar to that in industrial areas. Industrial development has rapidly shifted to China since 1997. Only a few manufacturing industries remained in Hong Kong. Thus the UHI characteristics of industrial and residential areas did not have much difference.

Season/ Period	Summer						Autumn					
	Weekday (6/2/2003)			Weekend (7/6/2003)			Weekday (9/24/2003)			Weekend (9/28/2003)		
	Morning	Afternoon	Night	Morning	Afternoon	Night	Morning	Afternoon	Night	Morning	Afternoon	Night
Daily averaged UHI	2.14			2.10			3.13			2.95		
UHI(avg.) value*	4.12	1.29	1.01	4.15	1.25	0.89	3.28	3.07	3.05	2.30	3.49	3.07
For specific Regions												
Maximum UHI(avg.) (Location)**	4.69 (YMT & MK)	2.56 (YMT & MK)	2.86 (YMT & MK)	6.13 (CB)	2.42 (SSP)	2.19 (YMT & MK)	3.92 (YMT & MK)	4.47 (CB)	4.03 (CB)	2.83 (Wan Chai + Central)	4.57 (Sai Wan)	3.86 (CB)
Minimum UHI(avg.) (Location)**	3.41 (Chai Wan)	-0.61 (Chai Wan)	-0.87 (Chai Wan)	2.42 (Sha Tin)	0.45 (Chai Wan)	0.06 (Sha Tin)	2.19 (Chai Wan)	1.40 (SSP)	0.90 (Chai Wan)	1.79 (Amoy Garden)	1.85 (Kwun Tong)	1.97 (Kwun Tong)
Chai Wan (residential)	3.41	-0.61	-0.87	3.28	0.45	0.14	2.19	3.16	0.90	2.52	3.16	3.29
Kwun Tong (Industrial)	---	---	---	3.53	0.93	0.93	3.40	2.41	2.90	1.87	1.85	1.97
Central & Wanchai (Commercial)	4.16	0.98	1.15	4.32	1.28	0.72	3.58	4.32	3.11	2.83	4.42	3.41

continued

continued

Season/ Period	Winter					
	Weekday (1/9/2004)			Weekend (1/11/2004)		
	Morning	Afternoon	Night	Morning	Afternoon	Night
Daily averaged UHI	1.23			1.46		
UHI(avg.) value*	0.26	0.68	2.75	1.63	0.82	1.94
For specific Regions						
Maximum UHI(avg.) (Location)**	1.00 (YMT)	1.71 (Wan Chai)	3.53 (YMT)	2.26 (MK)	1.66 (TST)	2.71 (Sai Wan)
Minimum UHI(avg.) (Location)**	-0.16 (Chai Wan)	-0.89 (Chai Wan)	1.31 (Sai Wan)	1.06 (Sai Wan)	-0.39 (Sai Wan)	1.03 (Kwai Chung)
Chai Wan (residential)	-0.16	-0.89	1.39	1.55	0.42	1.28
Kwun Tong (Industrial)	0.01	0.06	2.24	1.18	0.04	1.41
Central & Wanchai (Commercial)	-0.05	1.10	2.66	1.52	0.68	2.39

* UHI value represents the whole urban areas traveled in the field

** SSP states for Shum Shui Po, YMT states for Yau Ma Tei, MK states for MongKok, CB states for Causeway Bay

Table 1.5 Summary of Field Sampling

Heat Island Temperature Distribution

The UHI of all three urban areas are illustrated in Figure 1.7. The temperature anomalies distributions in the morning period of two seasons are shown in Figures 1.8-1.13. The hottest regions are the Kowloon Peninsular and the northern part of Hong Kong Island (mixed urban areas) while the coldest regions are Sai Kung, and the eastern and southern parts of Hong Kong Island (residential urban areas). It appears that the surface air temperatures along most of the highways in Hong Kong are similar.

1.4 Limitations of Temperature Scanning using Motor Cars

The limitations of this experiment are listed as follows:

1. Mobile transport is rather slow for cross-city travel. The traveling time is limited to about two hours per trip. Prolonged traveling time undermines the credit of the results due to diurnal variation in temperature. Temperature shift is rather large in the afternoon session. Unfortunately, this is the period of frequent traffic congestion.
2. Hong Kong has a complex terrain. It is meaningless to take a low temperature at high elevation as rural temperature. On the other hand, it is difficult to find a rural temperature near sea level elevation. After a thorough search, it is found that the eastern coastal region of Hong Kong can represent rural temperature of Hong Kong.
3. It is difficult to define industrial, commercial and residential district in Hong Kong. Most of the industrial buildings are mixed with residential buildings.
4. Industrial, commercial and residential areas involved in this study share similar urban characteristics. Thus, it is expected that their UHI effects are similar.
5. Mobile transport is constrained by the road system. It cannot reveal the entire temperature distribution of Hong Kong. It is impossible to draw an accurate temperature field of Hong Kong using isothermal contours.

A much better methodology for the study of UHI is to use airborne scanning. Satellite IR thermal imaging is a good and low cost alternative. Unfortunately, this methodology is plagued by the blockage of clouds and air pollution. On average, only one legible image is available per year. It is proposed to carry out a thermal scanning using small aircraft to study heat island effect.

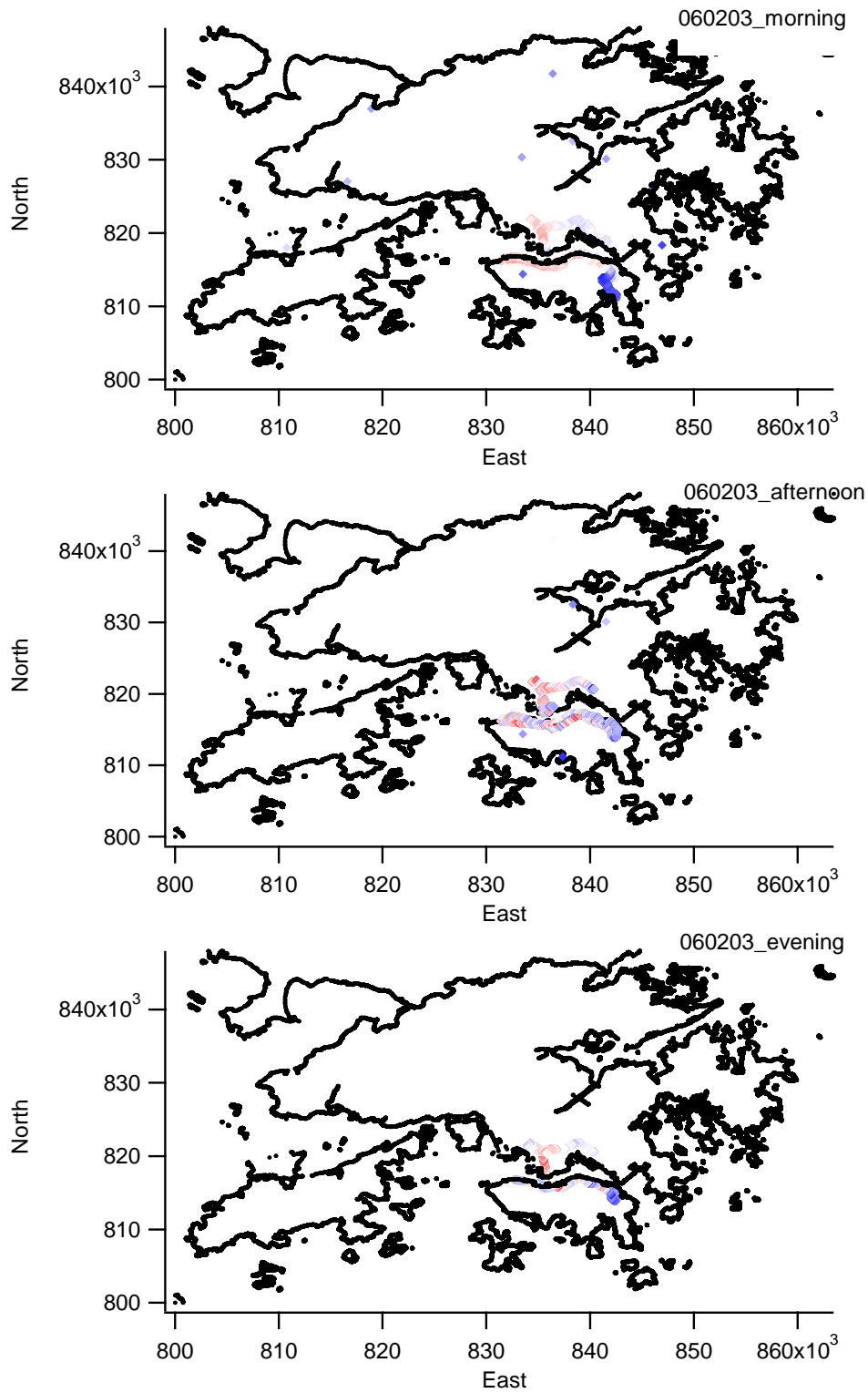


Figure 1.8 Temperature Anomalies Distributions in Summer Weekday at 0300 (upper side), 1500 (middle side) and 2200 (lower side) respectively

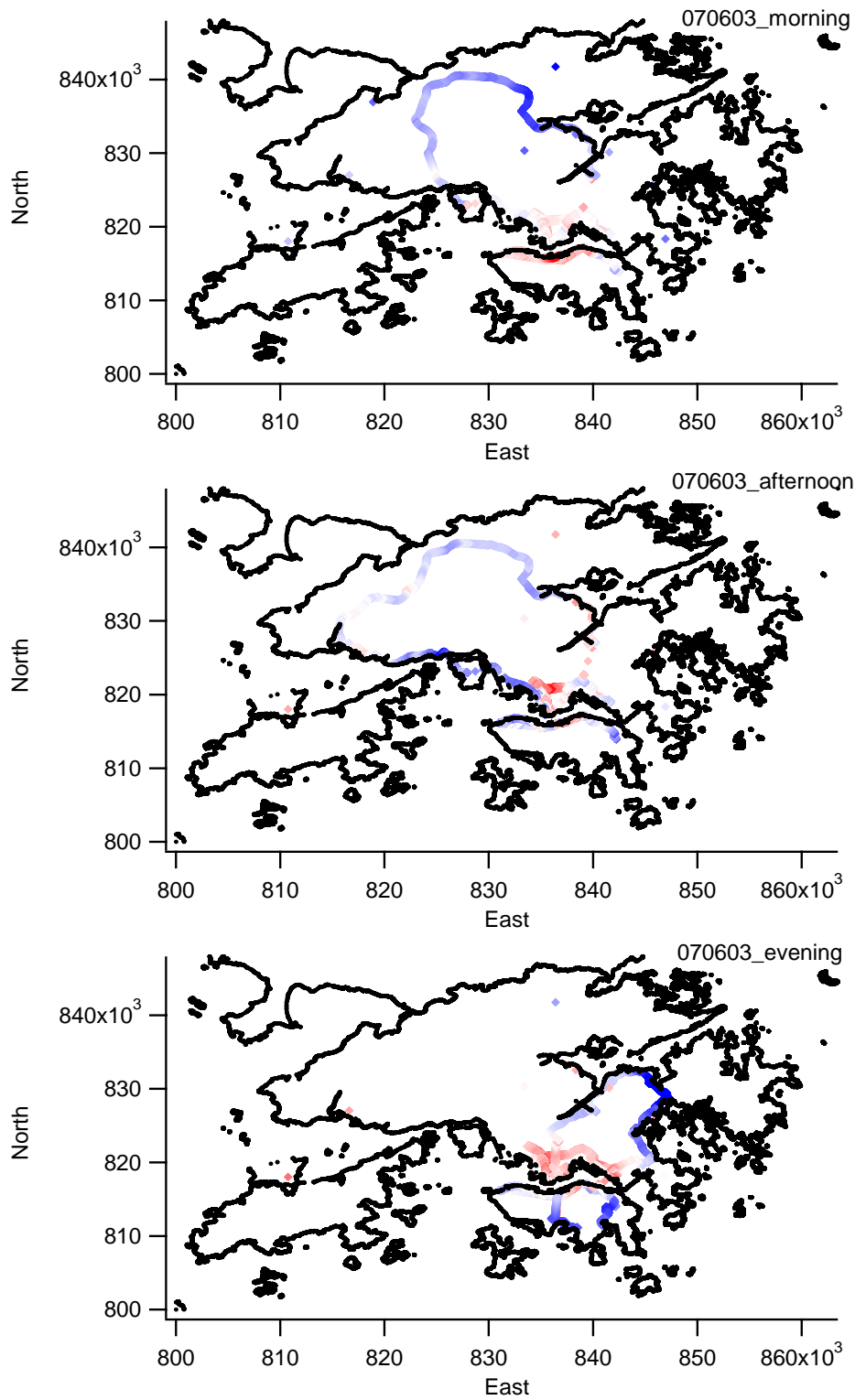


Figure 1.9 Temperature Anomalies Distributions in Summer Weekend at 0300 (upper side), 1500 (middle side) and 2200 (lower side) respectively

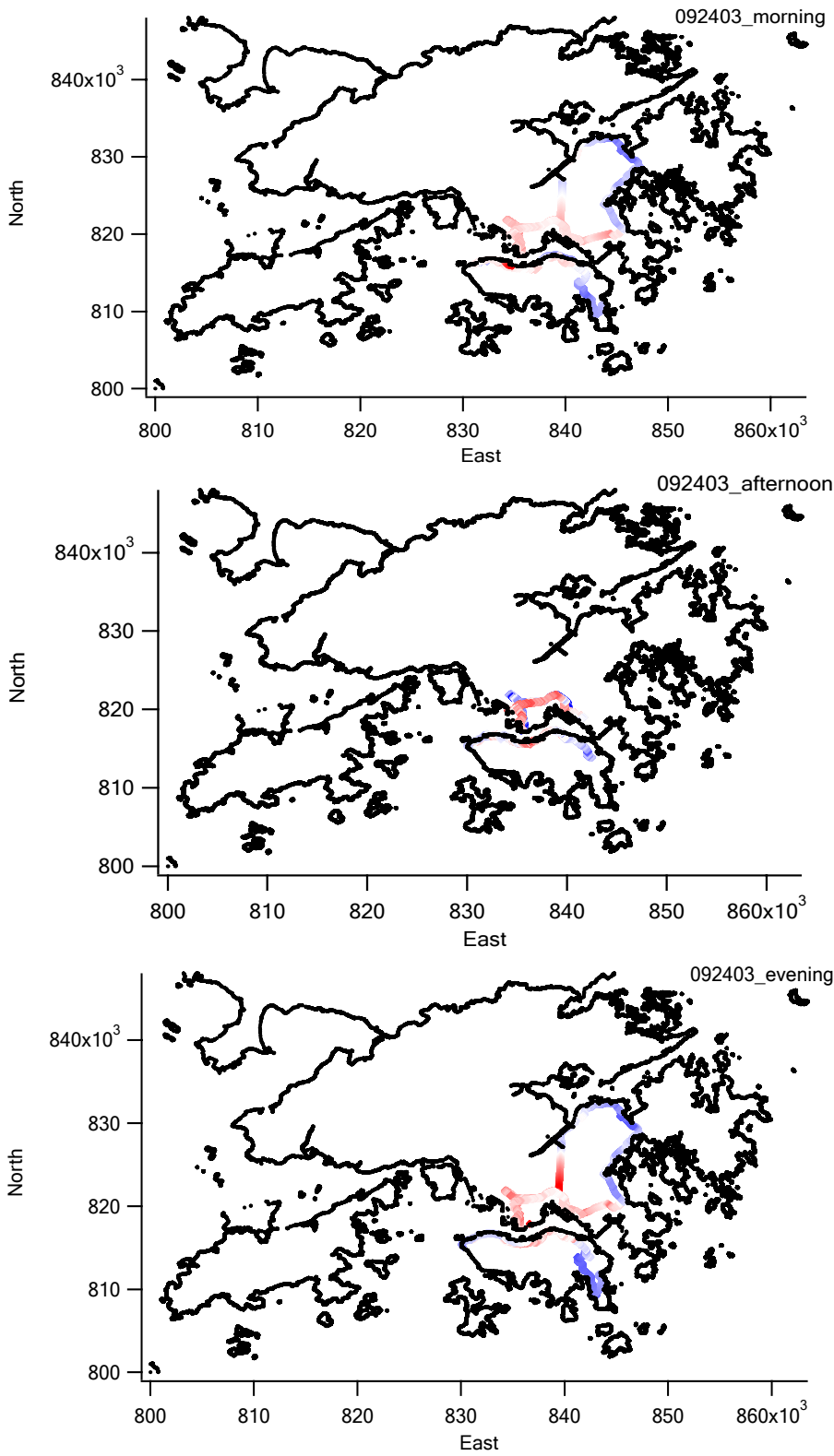


Figure 1.10 Temperature Anomalies Distributions in Autumn Weekday at 0300 (upper side), 1500 (middle side) and 2200 (lower side) respectively

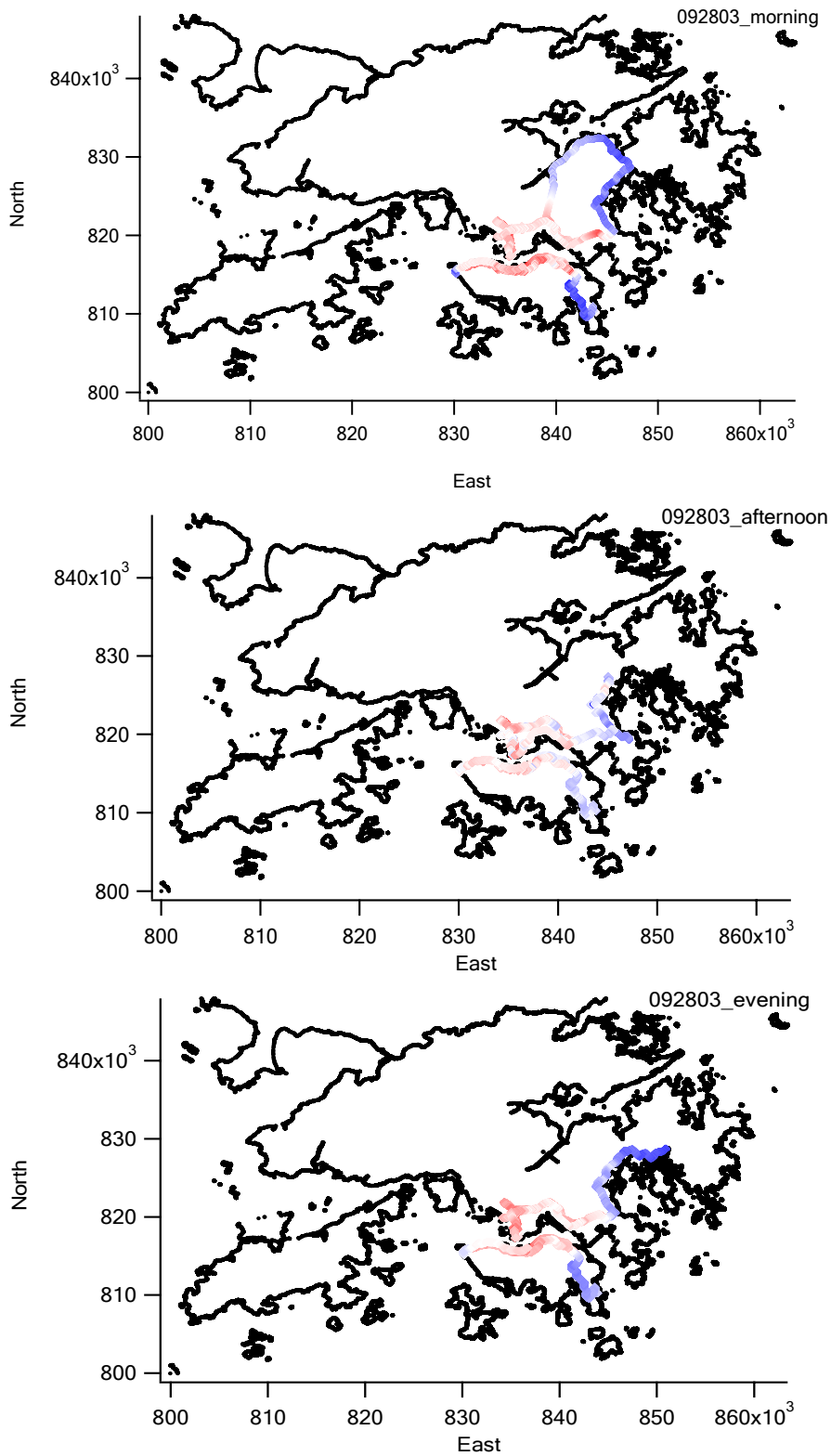


Figure 1.11 Temperature Anomalies Distributions in Autumn Weekend at 0300 (upper side), 1500 (middle side) and 2200 (lower side) respectively

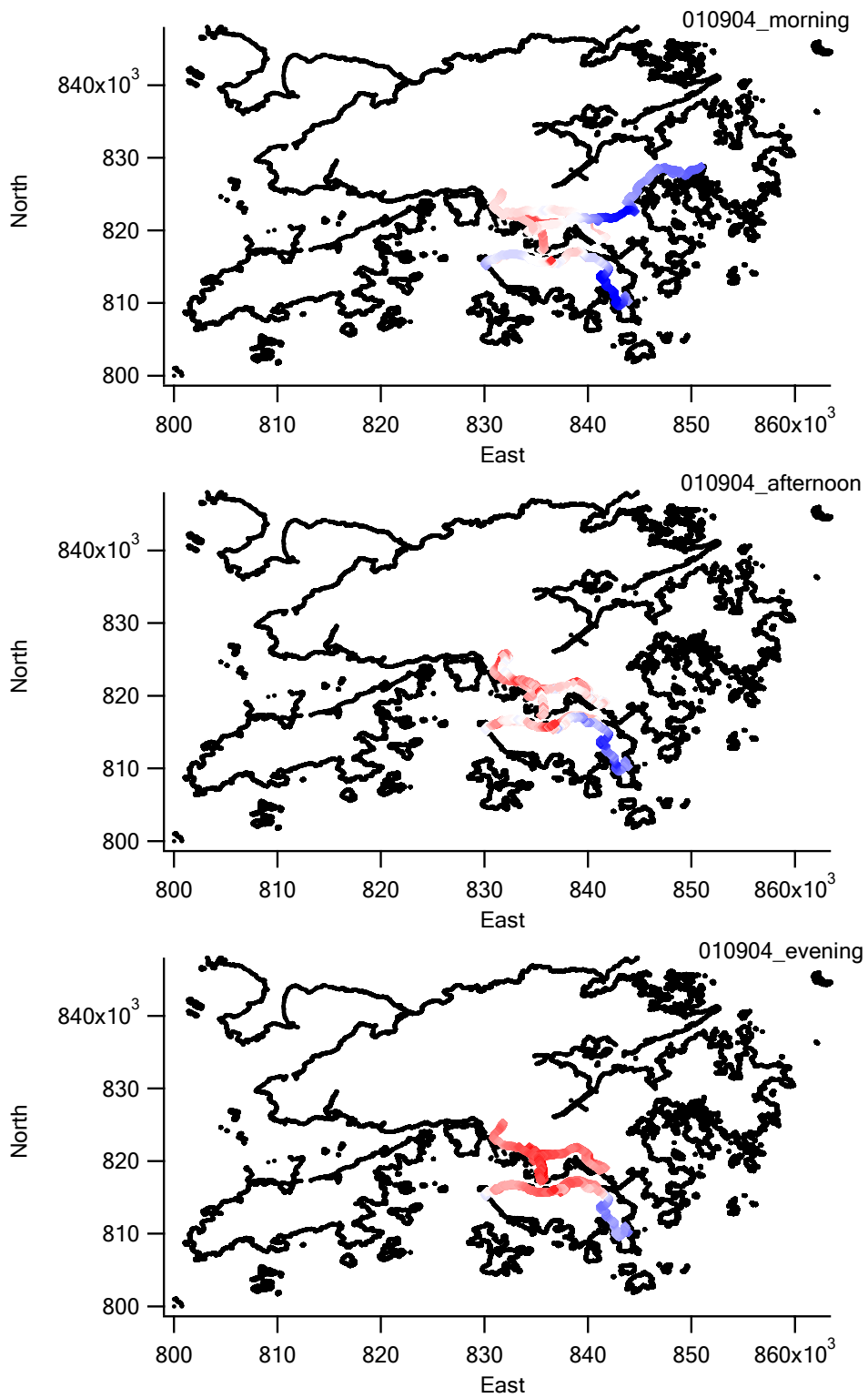


Figure 1.12 Temperature Anomalies Distributions in Winter Weekday at 0300 (upper side), 1500 (middle side) and 2200 (lower side) respectively

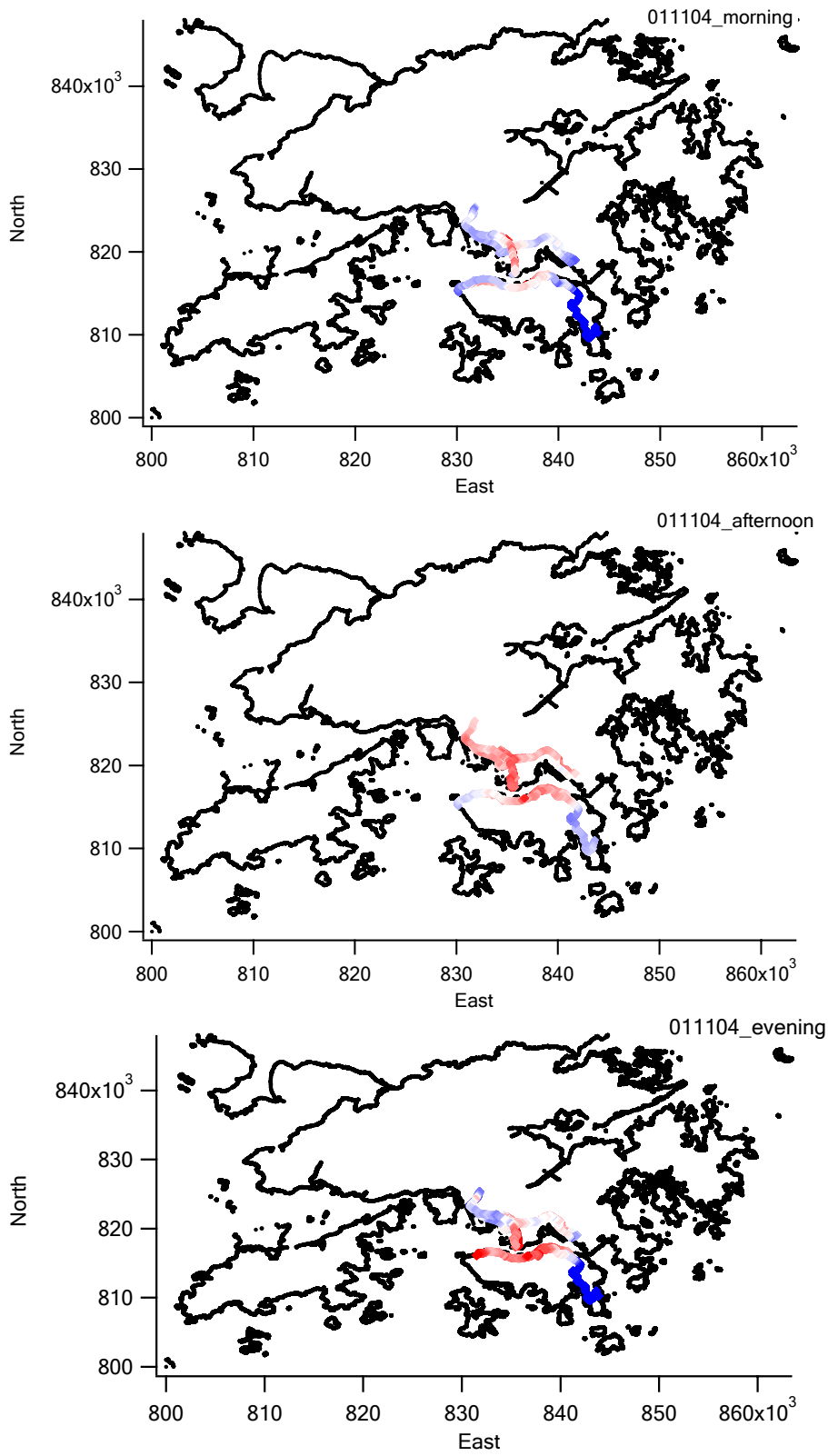


Figure 1.13 Temperature Anomalies Distributions in Winter Weekend at 0300 (upper side), 1500 (middle side) and 2200 (lower side) respectively

1.5 Conclusion

This study confirms the existence of urban heat island (UHI) phenomenon, especially in the Kowloon Peninsular and northern part of the Hong Kong Island. The UHI value is about 2.17°C in Hong Kong. The largest UHI occurs in the mixed commercial urban areas of Causeway Bay, Yau Ma Tei and Mongkok. The average UHI value is 2.12°C in summer, 3.04°C in autumn, and 1.35°C in winter respectively. The maximum UHI value appears in the early morning of clear cloudy days in urbanized Hong Kong.

1.6 References

1. Hong Kong Energy End-use Data (1990-2000) Electrical and Mechanical Services Department, HKSAR.
2. Hong Kong Observatory Technical Note (Local) No. 72: Regional Temperature Variation in winter of Hong Kong, The Hong Kong Observatory, HKSAR, 1997.
3. Toshiaki Ichinose, 1999, Impact of anthropogenic heat on urban climate in Tokyo, *Atmospheric Environment* 33, 3897-3909, 1999.
4. Nyuk Nien Wong, 2003, Life cycle cost analysis of rooftop gardens in Singapore, *Building and Environment* 38, 499-509, 2003.
5. C.P. Tso, 1996, A Survey of Urban Heat Island Studies in Two Tropical Cities, *Atmospheric Environment* Vol. 30, No.3, 507-519, 1996.
6. Zhou Shu Zhen, Zhang Chao, Zheng Jing Chuen, 1989, Urban Climate and Regional Climate with special regard to the urban climate of Shanghai.

Part Two: Present and Future Climate in the HKSAR

Chapter 2. Climatology for Hong Kong from The Hong Kong Observatory

Global temperature is increasing due to the anthropogenic emission of carbon dioxide into the atmosphere. Temperature increasing, ice melting and sea level rising are the consequences of global warming. Rainstorm or disasters occur more frequently in this century. Storms and heavy precipitations destroy seawalls, farm productions and inundate coastal areas. Extreme weather events would incur enormous economic loss.

According to the IPCC Third Assessment Report (2001), the global mean surface temperature, discounting the effects of localized temperature rises due to urbanization, has increased by $0.6 \pm 0.2^{\circ}\text{C}$ in the 20th century. The IPCC Third Assessment Report also concluded that over the past 50 years, the estimated rate and magnitude of warming due to the increase in greenhouse gas alone are comparable with, or larger than, the observed warming.

Hong Kong is located in the subtropical region. Urbanization would exacerbate the climate change impact in Hong Kong. According to The HKO, long term meteorological trends have been detected in Hong Kong (The HKO Technical Note No. 107). A summary of meteorological change in Hong Kong is listed in Table 2.1. The following sections extracted key results from this report.

Meteorological Characters	Changes due to Climate (in the past)
Rural temperature	Increased $0.2^{\circ}\text{C}/\text{decade}$
Urban temperature	Increased $0.6^{\circ}\text{C}/\text{decade}$
Daily diurnal range	Decreased $0.28^{\circ}\text{C}/\text{decade}$
Percent of time of reduced visibility	Increased $1.9\%/\text{decade}$
Cloud amount	Increased $1.8\%/\text{decade}$
Global solar radiation	Decreased $1 \text{ MJ}/\text{m}^2$ per decade
Evaporation	Decreased $184 \text{ mm}/\text{decade}$
Frequency of heavy rain	Increased $0.4 \text{ days}/\text{decade}$
Frequency of thunderstorms	Increased $1.7 \text{ days}/\text{decade}$
Number of tropical cyclones	Decreased $0.17/\text{decade}$
Sea level rise	Increased $2.3 \text{ mm}/\text{year}$

Table 2.1 Summary of Climate Change in the HKSAR

2.1 Past Climate Change in the HKSAR

2.1.1 Surface Temperature

In the last ten years (1989 to 2002), the urban temperature (HKO Headquarters) rose about 0.6°C per decade, the rural areas have been warming up about 0.2°C per decade. And the annual mean daily diurnal range also decreased at a rate of 0.28°C per

decade. The decrease in diurnal range is mainly due to the significant increase in the annual mean daily minimum temperature, which shows a rising trend of 0.28°C per decade during the 56-year period after World War II recorded at the HKO Headquarters (Figure 2.3). The trend of mean temperatures and diurnal range are plotted in Figures 2.1 and 2.2 respectively.

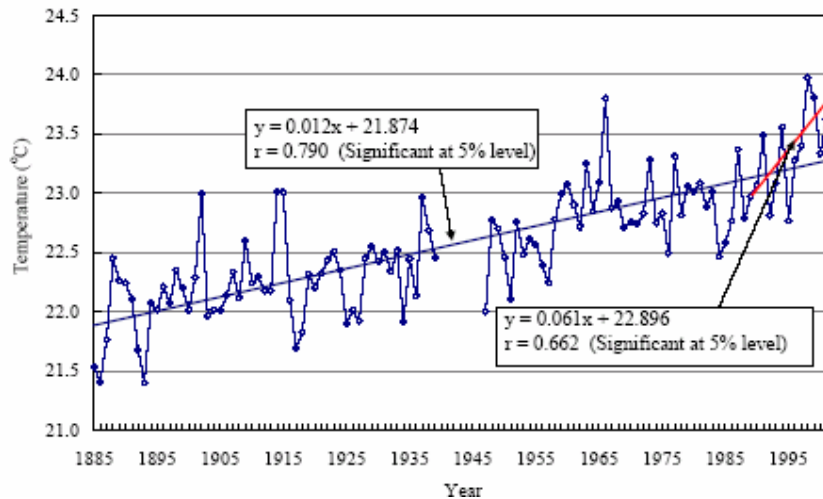


Figure 2.1 Annual Mean Temperature Recorded at the Hong Kong Observatory Headquarters (1885-2002). Data are not available from 1940 to 1946

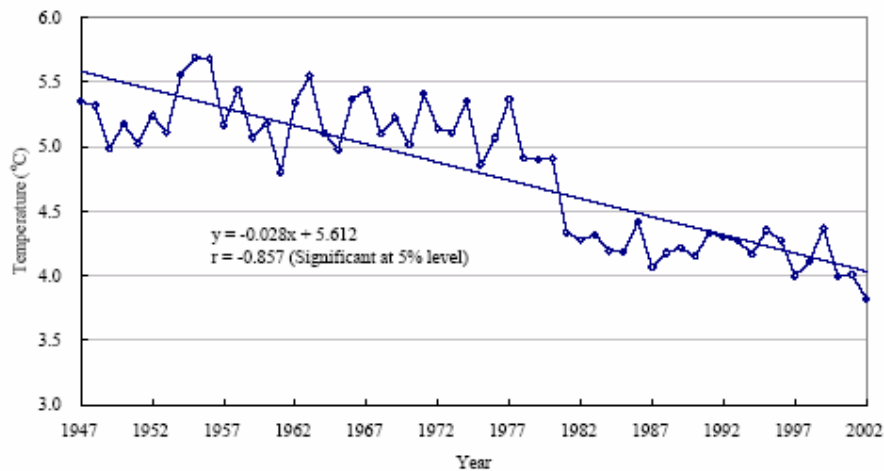


Figure 2.2 Annual Mean Daily Diurnal Range Recorded at the Hong Kong Observatory Headquarters (1947-2002)

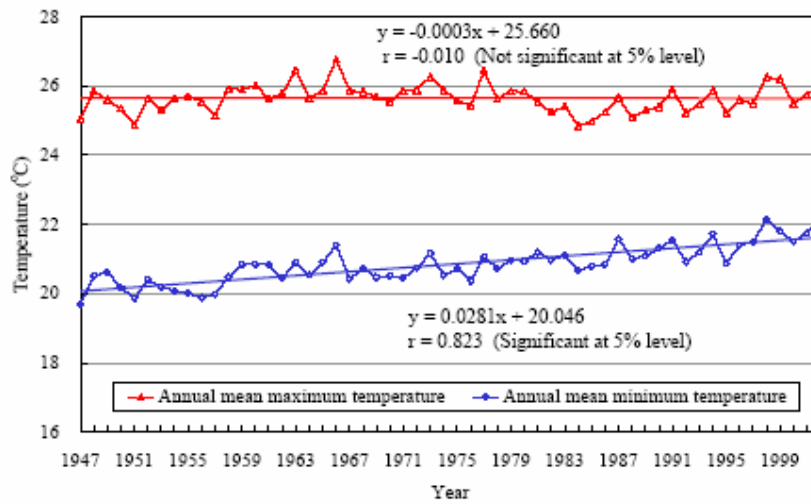


Figure 2.3 Annual Mean Daily Maximum and Minimum Temperatures Recorded at the Hong Kong Observatory Headquarters (1947-2002)

2.1.2 Visibility

Urbanization causes an increase in suspended particulates in the atmosphere and thus a decrease in visibility. At the HKO Headquarters, the visibility of 8 km or less was at about 2% in the early 1970s. And it was increased to some 9% by 2002, around 4 times that of the early 1970s. Figure 2.4 below also shows that reduced visibility was increasing at an average rate of about 1.9% per decade over the 35-year period.

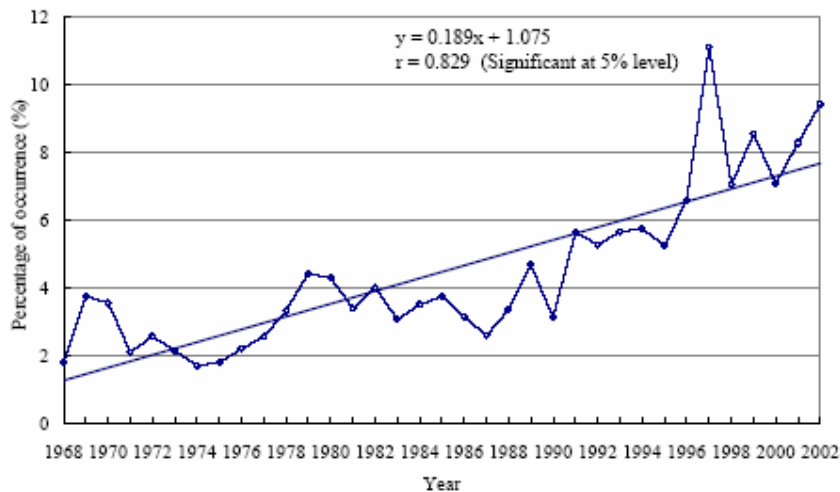


Figure 2.4 Percentage of Occurrence of Reduced Visibility Below 8 km (cases due to fog, mist or rain excluded) Observed at the Hong Kong Observatory Headquarters (1968-2002)

2.1.3 Cloud Amount

Decrease in diurnal temperature range is a consequence of increase in cloud amount. Cloud in the sky reduce the incoming solar radiation during daytime and traps the long-wave radiation at night. In Hong Kong, cloud amount data has been collected at the HKO Headquarters since 1961. Figure 2.5 shows that the annual mean cloud amount has been increasing at an average rate of 1.8% per decade in the past 40 years. The cloud amount is in an overall increasing trend but with many fluctuations from year to year.

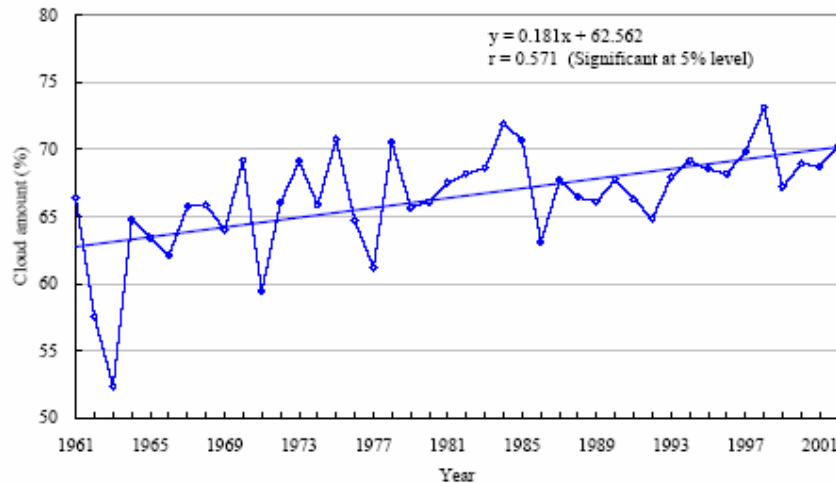


Figure 2.5 Cloud Amount Recorded at the Hong Kong Observatory Headquarters (1961-2002)

2.1.4 Global Solar Radiation

Reducing the amount of solar radiation reaching the surface is probably caused by the increase in the concentration of suspended particulates and cloud amount. The decreasing trend of global solar radiation has been observed at King's Park since mid-1960s. It has decreased by 26%, at a rate of $1\text{MJ}/\text{m}^2$ per decade (Figure 2.6).

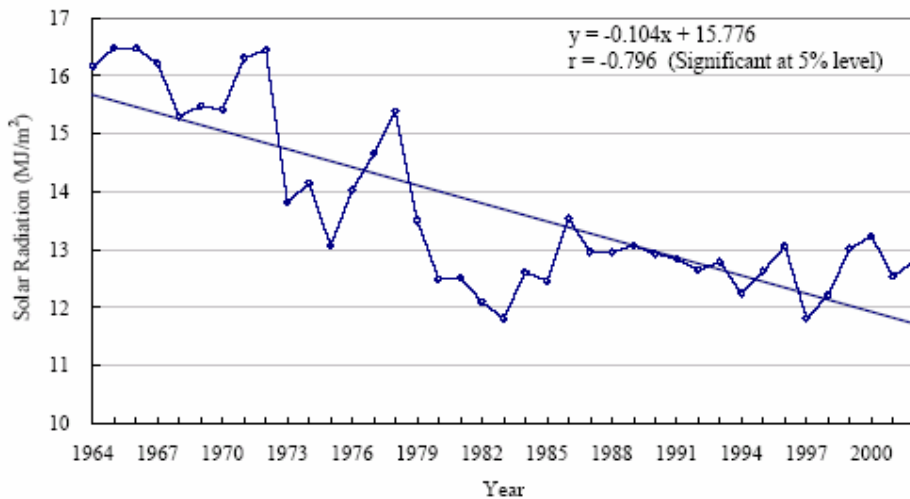


Figure 2.6 Annual Mean Daily Total Global Solar Radiation at King's Park (1964-2002)

2.1.5 Evaporation

Evaporation depends mainly on the amount of solar radiation received, the relative humidity of the atmosphere and wind speed. Decrease in global solar radiation reduced the annual total evaporation by 40% from the 1960s to 2002 (Figure 2.7).

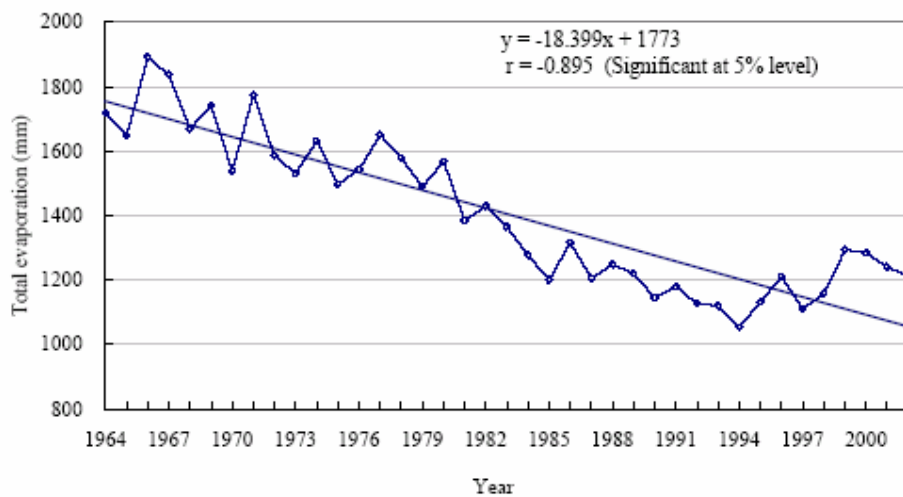


Figure 2.7 Annual Total Evaporation at King's Park (1964-2002)

2.1.6 Rainfall / Thunderstorms / Tropical Cyclones

Increasing trend in rainfall and thunderstorms, and decreasing trend in tropical cyclones are not statistically significant at 5% level. The annual number of heavy

rain days with hourly rainfall greater than 30mm and thunderstorms has been increasing at an average rate of 0.4 days per decade and 1.7 days per decade respectively, as shown in Figures 2.8 and 2.9.

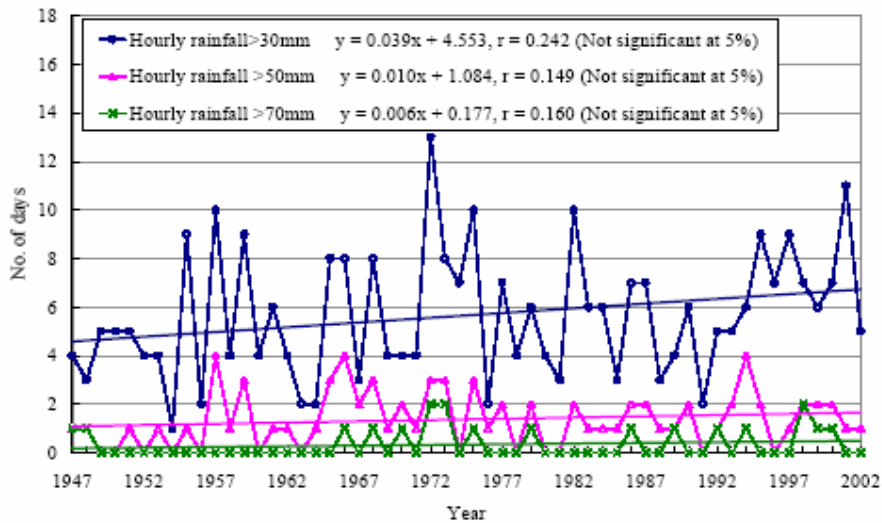


Figure 2.8 Number of Days with Hourly Rainfall Greater than 30 mm, 50mm and 70mm Respectively Recorded at the Hong Kong Observatory Headquarters (1947-2002)

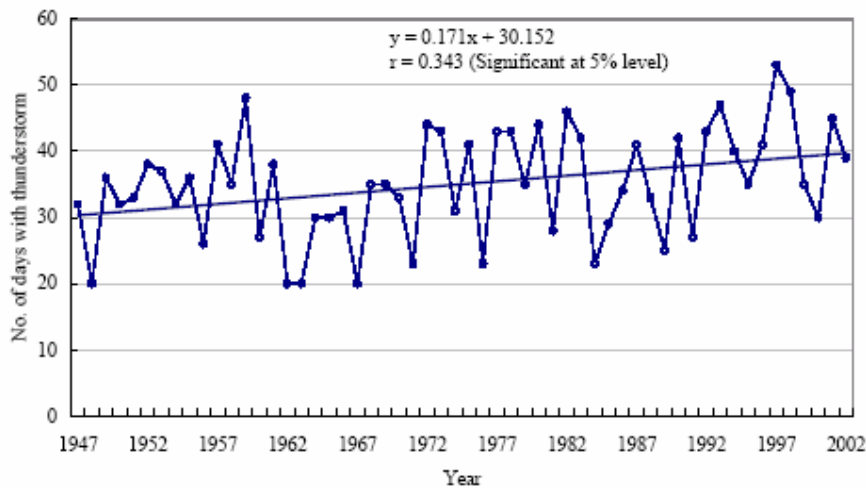


Figure 2.9 Annual Number of Days with Thunderstorm (1947-2002)

Tropical cyclone is defined as a cyclone landing over the south China coast within 300 km of Hong Kong. A decreasing trend was recorded since 1960s, at a rate of about 0.17 per decade, see Figure 2.10.

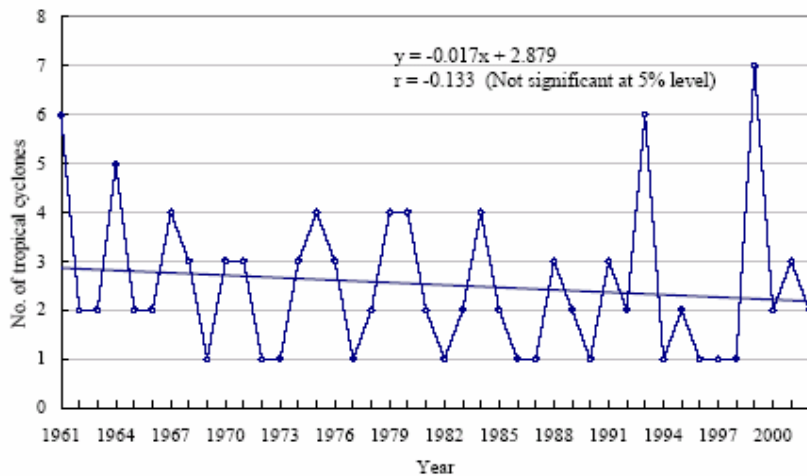


Figure 2.10 Annual Number of Tropical Cyclones Landing Over the south China Coast Within 300 km of Hong Kong (1961-2002)

2.1.7 Mean Sea Level

Sea level is related to global warming due to the melting of mountain glaciers and ice caps. In Hong Kong, mean sea level has been measured and was found to be rising at the average rate of 2.3 millimeter per year for the past 50 years at North Point/Quarry Bay station and of 3.0 millimeter per year at Tolo Harbour respectively. Figures 2.11 and 2.12 show the annual sea level recorded at North Point/Quarry Bay and Tolo Harbour respectively.

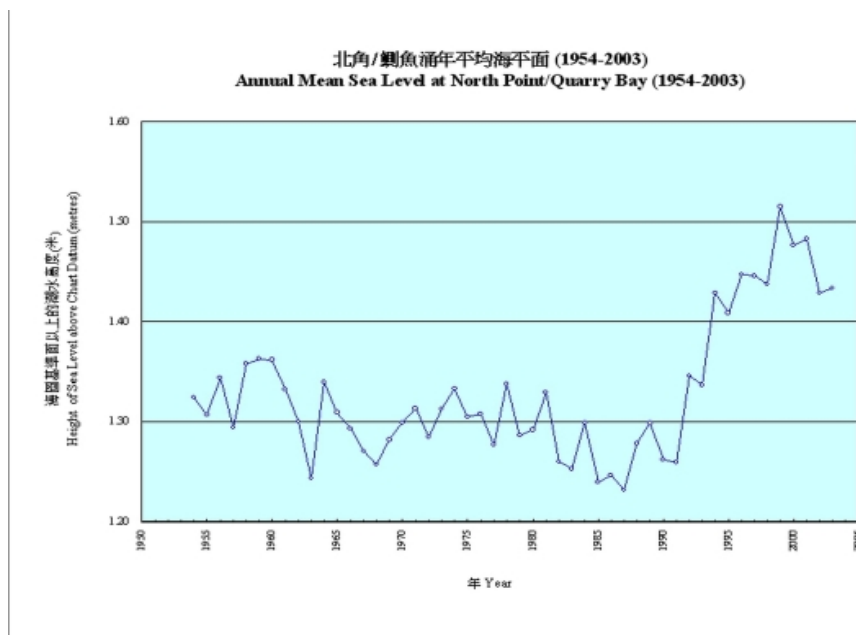


Figure 2.11 Annual Mean Sea Level Recorded at North Point/Quarry Bay (1954-2003) [Sources: The Hong Kong Observatory]

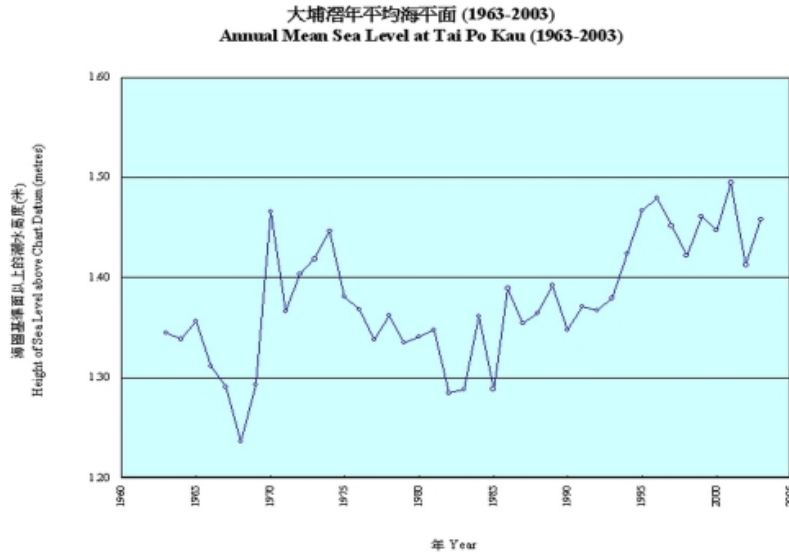


Figure 2.12 Annual Mean Sea Level Recorded at Tai Po Kau (1963-2003)
[Sources: The Hong Kong Observatory]

2.2 Projected temperature in the 21st century

According to the HKO, temperature projected for Hong Kong was conducted. (Leung et al, 2004) In that study, statistical downscaling technique is employed for obtaining local scale meteorological information from large scale information. The large scale (global climate) models include GSIRO-Mk2, WCHAM4/OPYC3, HadCM3, NCAR DOE-PCM, GFDL (consisting of the low resolution GFDL-R15 and the high resolution GFED-R30, CCCma (consisting of CGCM1 & CGCM2) and CCSR/NIES. There are three methods to project temperature in this downscaling technique. One of these is linear regression, which downscaling the temperature from seven models above. Another two methods are the single grid point method and extrapolation, which projecting the temperature from past temperature trend.

That report showed that the annual ensemble mean temperature in Hong Kong could be expected to rise about 3.5°C, and the range was between 1.7°C and 5.6°C, as shown in Figure 2.13. The single grid point method generally gave higher prediction. By 2090-2099, the single grid point method gave an ensemble mean of 4.0°C, 0.5°C higher the 3.5°C given by the regression method. Extrapolation (from the trend line between 1947 and 2002) yielded the lowest projection, with an ensemble mean of 2.0°C.

Past and projected annual mean temperature for Hong Kong

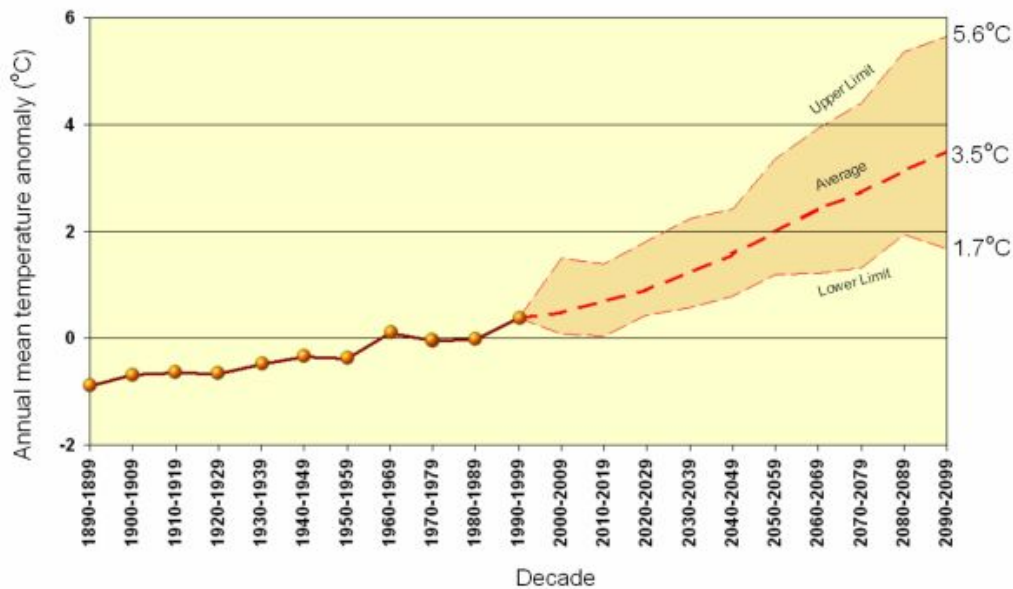


Figure 2.13 Projected Annual Mean Temperature for Hong Kong in the 21st century
[Source : The Hong Kong Observatory]

The above analysis indicates that it is likely that Hong Kong will be warmer in the coming century. In the next section, we shall analyze the potential impacts of global warming. The discussion includes:

- Chapter 3. — Energy Industry
- Chapter 4. — Human Health
- Chapter 5. — Air Pollution and Secondary Pollutant
- Chapter 6. — Tourism Industry
- Chapter 7. — Agricultures and Water Resources
- Chapter 8. — Ecosystems
- Chapter 9. — Coastal Zones and Marine Life

2.3 References

1. The Hong Kong Observatory Technical Note No. 107: Climate Change in Hong Kong, The Hong Kong Observatory, HKSAR, 2004
2. HKO announces findings on long-term sea level change in HK (14 June 2004), Hong Kong Observatory, HKSAR.
(<http://gb.weather.gov.hk/wxinfo/news/2004/pre0614e.htm>)
3. Leung Y.K., Cinn E.W.L., Wu M.C., Yeung K.H. and Chang W.L., Temperature Projects for Hong Kong In the 21st Century. Bulletin of the Hong Kong Meteorological Society for publication. (in press), 2004

Part Three: The impacts of Climate Change and Adaptation Strategies in the HKSAR

It is believed that global climate change would result in both sea level and temperature rise. Global climate change influences sea level, coastal resources, water resources and land resources. Sea level rise would inundate the coastal areas and cause more sea water surges. Temperature rise might be conducive to extreme events like heavy precipitation and flooding. Exacerbated flooding would affect economy, public works and promote growth of disease. The impacts on land and sea ecosystems in turn affect wild life and marine species, human health, standard of living and eco-tourism. This part of the report consists of eight chapters discussing the impacts of global climate change on Hong Kong and their adaptation strategies. The topics discussed are: Chapter 3 – Energy Industries, Chapter 4 – Human Health, Chapter 5 – Air Pollutions, Chapter 6 – Tourism Industry, Chapter 7 –, Agricultures and Water Resources, Chapter 8 – Ecosystems, Chapter 9 – Coastal Zones and Marine Life, and Chapter 10 – Sea Level Rise Impact.

Chapter3: Energy Industry

3.1 Introduction

Global warming is caused by emission and accumulation of greenhouse gases. Accumulation of greenhouse in the atmosphere is mainly due to the use of energy. Energy consumption plays a significant role in climate change. The per capita energy consumption of Hong Kong is high. In year 2002, Hong Kong's electricity consumption was 144,942 tera-joule. The gas consumption was 26,641 tera-joule and the retained imports of oil product was 17 giga-liter. The GDP of Hong Kong in 2002 was HK\$1,247 billion (Census and Statistics Department, HKSAR). The average electricity tariff in the same year was about \$1 per kWhr. The annual electric bill of Hong Kong was about HK\$38,087 million. This represented 3% of GDP. Together with other energy products including gas and oil, the energy sector is one of the major components of our economy.

IPCC forecasts that the temperature of the world will be rising in the next 100 years (Figure 3.1). The rise in temperature would range from 1.4°C to 5.8°C under different adaptation scenarios by 2100. As energy consumption in Hong Kong amounts to tenths of billion, it is important to estimate the impact of climate change on energy usage. The economic impact of energy consumption is calculated based on the data in year 2002.

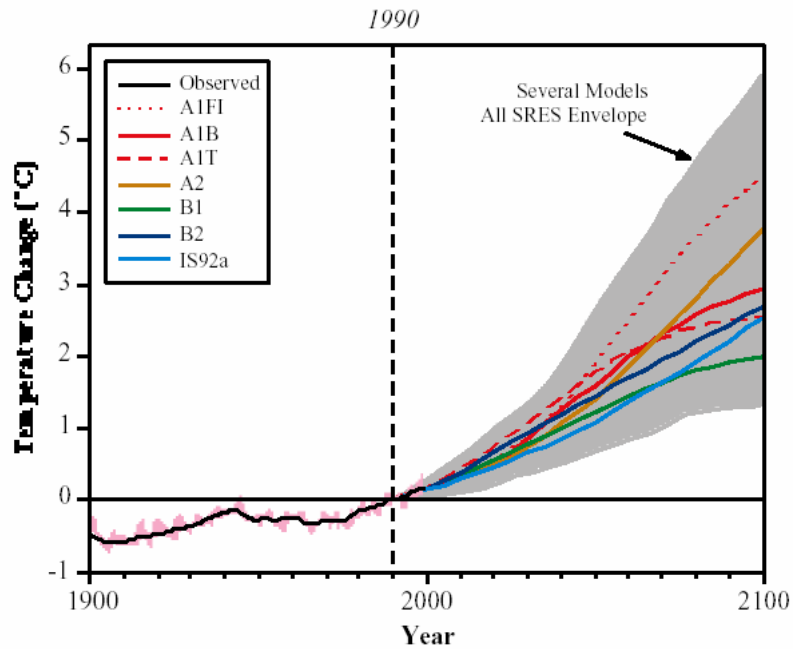


Figure 3.1 Global Temperature Trend Under Different Scenarios (source: IPCC, 2001)

3.2 Methodology

The methodology is empirical. The monthly energy consumption records between 1990 and 2002 of different energy products i.e., electricity, gas and oil, were acquired from the Census and Statistics Department. Three major power consumption sectors, i.e., domestic, commercial and industry were examined. The monthly average temperature was acquired from the HKO. The temperature was measured at the Hong Kong Observatory Headquarter located in Tsim Sha Tsui (fully commercial urban area).

It assumes that the energy consumption E in each sector is a function of ambient temperature T : $E = A + BT + CT^2$ where A , B and C are constants. The relationship between energy consumption of one specific type of energy statistics and ambient temperature was explored by plotting the monthly energy consumption against monthly averaged temperature. When the energy consumption of one energy product was found temperature dependent, the function for that energy sector was constructed using least-square linear or polynomial regression analysis. The function then allow E to be modelled at different temperature. Assuming the ambient temperature increased by 1°C in each month, let $E(\text{month}, T)$ be the historical record of one month energy consumption, the hypothetical energy consumption at the same month at $T + 1$ can be computed using the function $A + B(T+1) + C(T+1)^2$. The difference $E(\text{month}, T+1) - E(\text{month}, T) = \delta E(\text{month}, 1^\circ\text{C})$ is the extra energy consumed due to 1°C temperature rise in that month. Summing δE over 12 months, we got the δE for one year. The work was then repeated for 2°C and 3°C temperature increase. To tackle the problem

of population growth, the methodologies of population normalization or population trend removal were not adopted. Instead, the δE was computed year by year. The percentage of δE over “one year total energy consumption” was computed. If this $\delta E/E$ ratio remains invariant for different years, it is not necessary to carry out further analysis. It turns out that this simple method worked perfectly well for Hong Kong’s statistics.

It is understood that the demand for air conditioning is most temperature dependent. To supplement our analysis, the relationship of electricity consumption for air-conditioning alone will be explored using the power consumption records of 3 air-cooled and 3 water-cooled air conditioning systems in 6 government buildings.

3.3 Results and Discussions

3.3.1 Electricity Consumption

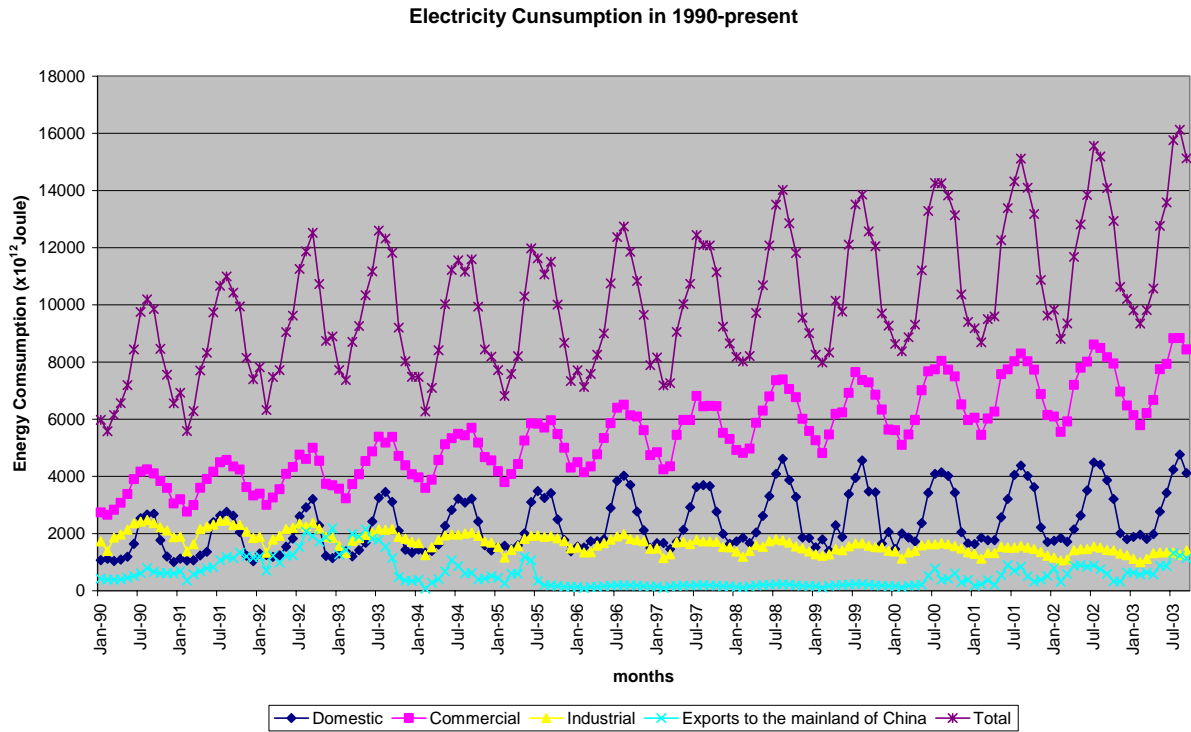


Figure 3.2 Hong Kong's Electricity Consumption from 1990 to 2002

The electricity consumption in Hong Kong from 1990 to 2002 is shown in Figure 3.2 above. The commercial sector was the largest consumer. There was a rising trend of commercial electricity consumption that had increased by more than 100% from 1990 to 2002. The domestic electricity consumption was about half of the commercial consumption and had remained steady since 1998. The consumption of the industrial sector had been decreasing in recent years due to migration of factories to the mainland. The electricity consumption in both the commercial and domestic sectors showed a strong seasonal cycle, demonstrating a temperature dependent characteristic.

There was a rising trend in the time series. To avoid complication owing to time effects in the analysis, we chose to look into the temperature effects within each year. The domestic, commercial and industrial electricity consumption on a monthly basis in 1990, 1996 and 2002 are plotted against the monthly average ambient temperature. The results are shown in Figure 3.3. The electricity consumption in all 3 sectors was clearly temperature dependent.

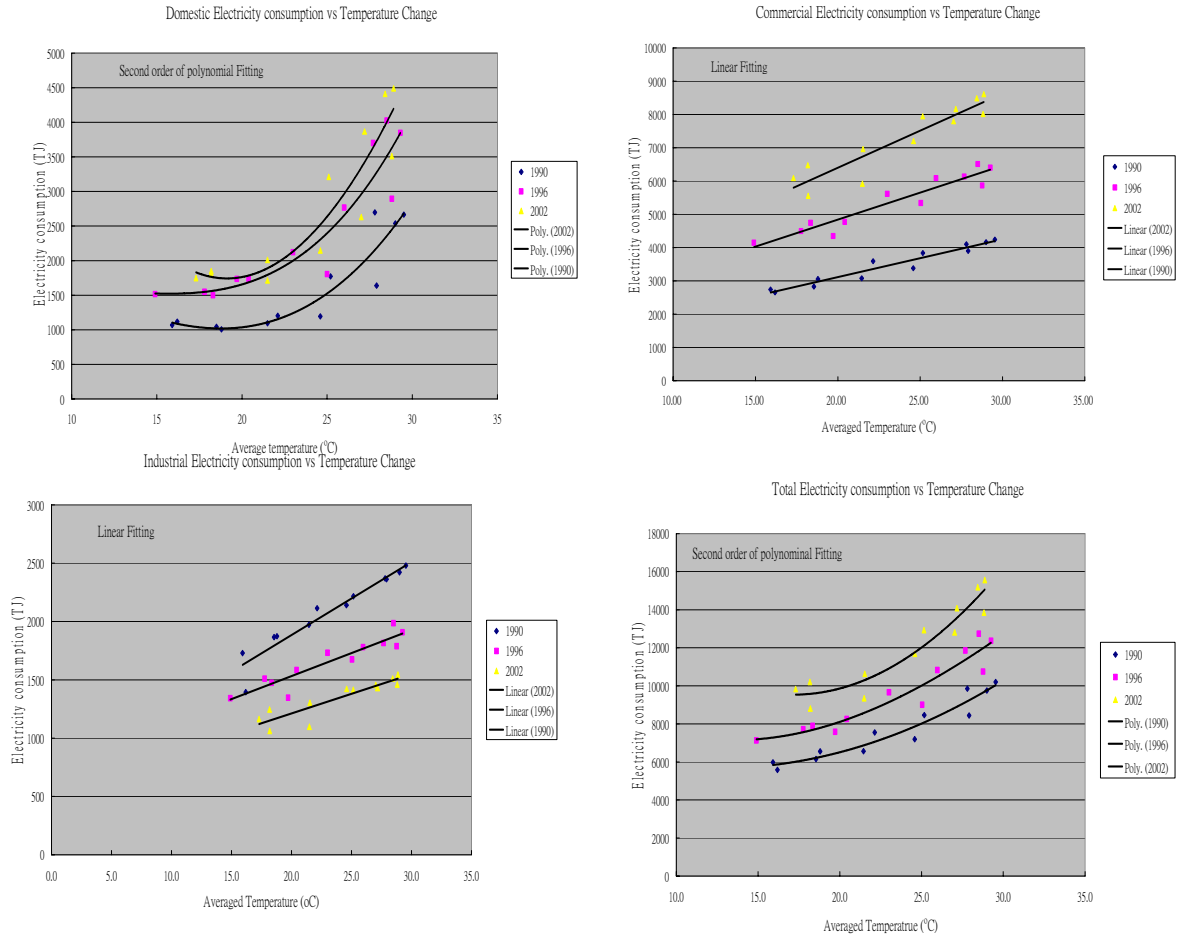


Figure 3.3 Temperature Dependence of Electricity Consumption

The temperature function of the domestic sector was best fit by a power 2 polynomial, while that of the commercial sector and industrial sector by a straight line. All the regressions satisfied the 0.05 level of significance. The polynomial functions and their statistical confidence are listed in Table 3.1. The analysis of variance was carried out using SPSS ver 11.0.

Year	Domestic consumption related with temperature equations (with 95% confidence interval)	Correlation coefficient, r	Coefficient of Determination, R ²	t value
1990	$C=(6166.305\pm5425.829)+(-548.860\pm492.723)T+(14.567\pm10.786)*T^2$	0.926	0.857	3.055
1996	$C=(6266.148\pm7602.450)+(-551.299\pm692.338)T+(15.950\pm15.430)*T^2$	0.926	0.858	2.373
2002	$C=(11052.200\pm12945.351)+(-974.781\pm1144.830)T+(25.524\pm24.589)*T^2$	0.921	0.848	2.348
Commercial consumption related with temperature equations				
1990	$C=(831.904\pm487.686)+(114.065\pm20.694)T$	0.968	0.937	12.281
1996	$C=(1598.776\pm900.901)+(162.095\pm37.905)T$	0.950	0.902	9.528
2002	$C=(1941.102\pm1539.164)+(223.041\pm63.449)T$	0.927	0.860	7.832
Industrial consumption related with temperature equations				
1990	$C=(630.031\pm309.504)+(62.711\pm13.134)T$	0.959	0.918	10.639
1996	$C=(740.168\pm267.996)+(39.568\pm11.282)T$	0.927	0.859	7.814
2002	$C=(537.651\pm277.684)+(33.694\pm11.447)T$	0.901	0.811	6.558
Overall consumption related with temperature equations				
1990	$C=(8056.874\pm9584.876)+(-380.591\pm870.409)T+(15.158\pm19.054)*T^2$	0.961	0.923	1.800
1996	$C=(9777.934\pm12963.399)+(-447.254\pm1180.548)T+(18.223\pm25.970)*T^2$	0.950	0.902	1.590
2002	$C=(21381.019\pm21640.915)+(-1381.672\pm1913.827)T+(40.288\pm41.106)*T^2$	0.954	0.910	2.217

Table 3.1 Polynomial and Linear Regression Results Between Electricity Consumption C and Ambient Temperature T.

Monthly Averaged Temperature (T) in 2002	Actual consumed Electricity (TJ) = a	When temperature increased by 1°C		When temperature increased by 2°C		When temperature increased by 3°C		
		Predicted consumed energy at T+1 = b1	Extra electricity consumed = b1-a	Predicted consumed energy at T+2 = b2	Extra electricity consumed = b2-a	Predicted consumed energy (TJ) T+3 = b3	Extra electricity consumed = b3-a	
Jan	17.30	1747	1761.478	14.47801	1746.404	-0.59585	1782.379	35.37857
Feb	18.19	1849	1745.614	-103.386	1776.484	-72.516	1858.402	9.40182
Mar	21.49	1714	2041.212	327.2122	2240.541	526.5411	2490.918	776.9183
Apr	24.60	2147	2825.294	678.2939	3182.872	1035.872	3591.499	1444.499
May	27.02	2630	3769.244	1139.244	4249.338	1619.338	4780.481	2150.481
Jun	28.82	3510	4670.168	1160.168	5242.149	1732.149	5865.179	2355.179
Jul	28.87	4489	4725.069	236.0692	5302.155	813.1553	5930.29	1441.29
Aug	28.44	4412	4455.669	43.6692	5007.231	595.2312	5609.841	1197.841
Sept	27.17	3868	3861.179	-6.82146	4351.483	483.4826	4892.835	1024.835
Oct	25.15	3210	2997.702	-212.298	3380.805	170.8048	3814.956	604.9558
Nov	21.52	2011	2041.212	30.21221	2240.541	229.5411	2490.918	479.9183
Dec	18.17	1808	1745.614	-62.3856	1776.484	-31.516	1858.402	50.40182
		Yearly consumed		3244.5		7101.9		11571.1
		% of change		9.72		21.3		34.6
1996								
Jan	17.77	1549	1539.224	-9.7761	1603.609	54.6094	1699.896	150.8957
Feb	14.90	1516	1532.905	16.90481	1504.778	-11.2219	1508.552	-7.44789
Mar	19.72	1734	1688.832	-45.1685	1813.828	79.82848	1970.726	236.7262
Apr	20.42	1737	1772.98	35.97981	1920.307	183.3073	2099.536	362.5356
May	25.04	1805	2714.825	909.8247	3008.896	1203.896	3334.868	1529.868
Jun	28.77	2893	4002.007	1109.007	4417.301	1524.301	4864.496	1971.496
Jul	29.25	3847	4205.666	358.6663	4636.911	789.9106	5100.056	1253.056
Aug	28.50	4025	3883.639	-141.361	4289.363	264.3631	4726.988	701.9876
Sept	27.67	3700	3582.029	-117.971	3962.232	262.232	4374.336	674.3359
Oct	25.96	2767	3008.896	241.8958	3334.868	567.8676	3692.74	925.7402
Nov	23.00	2122	2222.385	100.3849	2452.654	330.6544	2714.825	592.8247
Dec	18.34	1500	1567.429	67.42905	1647.765	147.7649	1760.002	260.0016
		Yearly consumed		2525.8		5397.5		8652.0
		% of change		8.7		18.5		29.6

Table 3.2 Computation of Increased Electricity Consumption of Domestic Sector due to 1°C, 2°C, and 3°C Increase in Ambient Temperature (2002 and 1996).

Monthly Averaged Temperature (T) in 1990	Actual consumed Electricity (TJ) = a	When temperature increased by 1°C		When temperature increased by 2°C		When temperature increased by 3°C		
		Predicted consumed energy at T+1 = b1	Extra electricity consumed = b1-a	Predicted consumed energy at T+2 = b2	Extra electricity consumed = b2-a	Predicted consumed energy (TJ) T+3 = b3	Extra electricity consumed = b3-a	
Jan	15.91	1069	1050.923	-18.0772	1008.979	-60.0211	996.1682	-72.8318
Feb	16.19	1117	1035.281	-81.7193	1002.077	-114.923	998.0059	-118.994
Mar	18.55	1045	1002.466	-42.5344	1036.268	-8.73217	1099.203	54.20318
Apr	21.45	1093	1191.272	98.27166	1312.473	219.4733	1462.808	369.808
May	24.58	1194	1661.825	467.8249	1873.339	679.3392	2113.987	919.9866
Jun	27.91	1640	2470.382	830.3823	2778.036	1138.036	3114.823	1474.823
Jul	29.00	2537	2810.404	273.4036	3150.104	613.1036	3518.937	981.9368
Aug	29.53	2665	2976.612	311.6119	3330.879	665.8785	3714.278	1049.278
Sept	27.80	2697	2441.219	-255.781	2745.96	48.95954	3079.833	382.8329
Oct	25.16	1772	1785.238	13.23754	2014.232	242.2317	2272.359	500.359
Nov	22.14	1202	1260.497	58.49664	1399.178	197.1781	1566.993	364.9927
Dec	18.79	1007	1009.547	2.547286	1052.089	45.08945	1123.765	116.7647
		Yearly consumed		1657.664		3665.613		6023.159
		% of change		8.707134		19.25419		31.63756

Table 3.3 Computation of Increased Electricity Consumption of Domestic Sector due to 1°C, 2°C, and 3°C Increase in Ambient Temperature (1990).

Using these equations, the computed results of the average increases in electricity consumption due to 1°C, 2°C, and 3°C increases in ambient temperature for the three years of 1990, 1996 and 2002 are shown in Table 3.2 and Table 3.3. The average increase in electricity consumptions for all sectors is listed in Table 3.4.

Increasing electricity demand percentage per year	Temperature increase by		
	1°C	2°C	3°C
Domestic	9.02%	16.15%	30.97%
Commercial	3.13%	6.26%	9.38%
Industrial	2.64%	5.28%	7.91%
Total	4.53%	9.52%	14.98%

Table 3.4 Percentage Increase of Electricity Consumption due to Temperature Rise

The results show that the increase of ambient temperature has a significant impact on electricity consumption in Hong Kong. To express the impact in monetary terms, we took the electricity tariff as HK\$1.00 per kWh. 1kWh is equivalent to 3.6×10^6 joules. In 2002, the total electricity consumption was 3.8×10^{10} kWh. If the ambient temperature of 2002 is increased in all months by T+1, the total sum of the domestic/commercial/industrial electricity impact is 1.72×10^9 kWh. For 1°C temperature rise, the economic impact is HK\$1.72 billion, see Figure 3.5. For 2°C

rise, the estimated impact is HK\$3.26 billion. For 3°C rise, the estimated impact is HK\$5.50 billion.

		Economic impact of electricity consumption			
		Domestic	Commercial	Industrial	Total
Electricity consumption in 2002		33,394 TJ	87,606 TJ	16,112 TJ	
Temperature increased by	1°C	HK\$0.84 billion	HK\$0.76 billion	HK\$0.12 billion	HK\$1.72 billion
	2°C	HK\$1.50 billion	HK\$1.52 billion	HK\$0.24 billion	HK\$3.26 billion
	3°C	HK\$2.87 billion	HK\$2.28 billion	HK\$0.35 billion	HK\$5.50 billion

Table 3.5 Summary of Economic Impact of Electricity Consumption due to Climate Change

A case study, in Los Angeles, reported that the demand for electric power in the warm afternoons increased nearly 3.6% for every degree Celsius increases in daily maximum temperature (Heat Island Group). The demand for electricity could rise by 4.53% per Celsius increase in Hong Kong. The energy impact of temperature rise in Hong Kong is similar to that in LA.

It is rather surprising that the above simple methodology yield consistent results. Energy consumption depends on social and economic cultures, standard of living, population and weather. Hong Kong has experienced two major changes within the period. First, there was a major political turnover in the year 1997 when it became a special administrative region. Second, Hong Kong suffered a rather long term economic recession between 1998 and 2003. Despite major political and economic changes, the energy consumption trends (Figure 3.1) remain unchanged. There are two probable explanations: (1) The city has maintained its lifestyle throughout these years and (2) the industrial sector is a small electricity consumer (about 10%). Population is another prime factor that needs to be accounted for. The influence of population growth on energy consumption was avoided by analyzing the energy consumption data year by year. The temperature range between 17°C in winter and 28°C in summer is wide enough to allow the E(month, T) function and the $\delta E/E$ to be computed using only one year data. Repeating the analysis for 13 different years was to check the precision of this methodology. The above results have shown that the population growth affects only the absolute energy consumption amount but not the relative ratio of $\delta E/E$. The small population growth rate of about 1.1% per year in Hong Kong is probably an explanation. Taking a closer look at the arithmetic, the temperature in January 2002 was 17.3°C, the electricity consumption was 1747 TJ. The exercise was to estimate the consumption when January's temperature increased to 18.3°C. It would be a full scale modeling exercise if we start from basic principles. However, we knew that in the year 2002, at 18.2°C (in February) the consumption was 1849 TJ and at 21.5°C (in March) the consumption was 1714 TJ. The fictitious energy consumption should be somewhere between 1714 TJ and 1849 TJ. Thus it became a simple interpolation exercise. Furthermore, the extra-energy estimation was based on the data somewhere between February and March which is only about one

month away from January. The population change in one month was less than 0.1% and it explains how population growth was tackled by this methodology.

Weather variables are important parameters. In practice, the regression analysis should be carried out by incorporating temperature, relative humidity (RH), wind speed and visibility. Furthermore, the summer and winter energy consumption should be analyzed separately. It has also been published that replacing the temperature parameter by heating/cooling degree days improved the level of significance. Previous studies have reported that the temperature variable explains more than 80% of the energy consumptions in United States, RH explains less than 15% and wind speed is not correlated at all, so most of the recent studies on energy impact were carried out using temperature only. Regarding the seasonal variations, the energy consumption pattern in most countries in mid-latitudes is dominated by space heating in winter and cooling in summer. The space heating and cooling hardware are very different and thus the energy analysis has to deal with summer and winter separately. Hong Kong has a sub-tropical climate and is different in this aspect. Figure 3.3 does not exhibit the common U shape energy versus temperature curve. Apart from the domestic electricity consumption which shows a little bit of winter heating requirements, basically the commercial and industrial electricity did not consume electricity for space heating in cold weather. It has been reported that in Hong Kong 59.1% of the electricity consumed in summer was spent on air conditioning units whereas 23.5% of the electricity consumed in winter was spent on air conditioning units. Only 2.6% of the electricity consumed in winter was spent on space heating. Therefore, it is not necessary to carry out winter analysis in Hong Kong. It follows that it is not necessary to consider the heating degree days. As a matter of fact, most of the air conditioning systems in Hong Kong do not have heating device. There is also no benefit to replace the temperature variable by population weighted cooling degree days Unlike large countries such as China or United States, the spatial variation of population is negligible because the area of Hong Kong is very small, only about 1000 km².

Considering the energy consumption breakdown, for domestic electrical consumption, the main appliances are air conditioners, lighting, lift, water pumps, refrigerator, computers, AV equipment, kitchen/bathroom appliances. Some electrical appliances are temperature dependent (air conditioner and refrigerator) but others are not (lighting, TV, pumps and lift). The consistency of this methodology relies upon the fact that non-temperature dependent appliances should consume a relatively constant amount of energy throughout the year. In this case, this portion of the energy consumption will be contained in the constant term A in the polynomial function $A+BT+CT^2$. When δE is computed, the constant A will cancel out itself. Therefore constant energy consumers will not affect the accuracy of this analysis. Other cities in the world may not have this consumer behavior.

3.3.2 Gas Consumption:

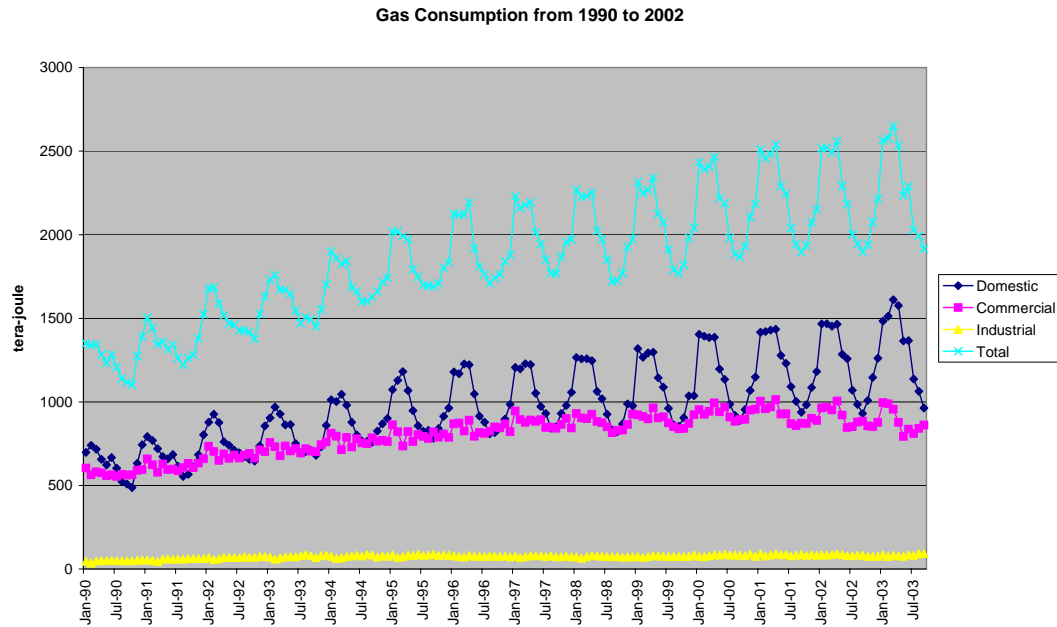


Figure 3.4 Hong Kong's Gas Consumption from 1990 to 2000

The gas consumption in Hong Kong from 1990 to 2002 is shown in Figure 3.4. The consumption of domestic sector occupied the largest share and exhibited a rising trend. The domestic gas consumption had increased by more than 100% from 1990 to 2002. The commercial gas consumption was always less than the domestic consumption and had remained steady since 1998. Furthermore, the domestic gas consumption had a strong seasonal cycle whereas the commercial gas consumption exhibited only a small seasonal variation. The industrial sector was a small gas consumer in Hong Kong and had been insignificant over the years. The domestic gas consumption catered for cooking and boiling hot water. Unlike electricity, more gas was consumed in winter than summer. When temperature increased, gas consumption decreased.

Similar to the electricity consumption analysis, the change in gas consumption due to T+1, T+2 and T+3 was studied year by year. The domestic, commercial and industrial gas consumption in 1990, 1996 and 2002 were plotted against the monthly average ambient temperature. The results are shown in Figure 3.5. The gas consumption in the domestic sector was clearly temperature dependent whereas the commercial or industrial gas consumptions were not. By statistical analysis, the relationship between the industrial/commercial gas consumption and the ambient temperature was not significant at 5% level. Therefore, temperature impact analysis was carried out on the domestic sector only.

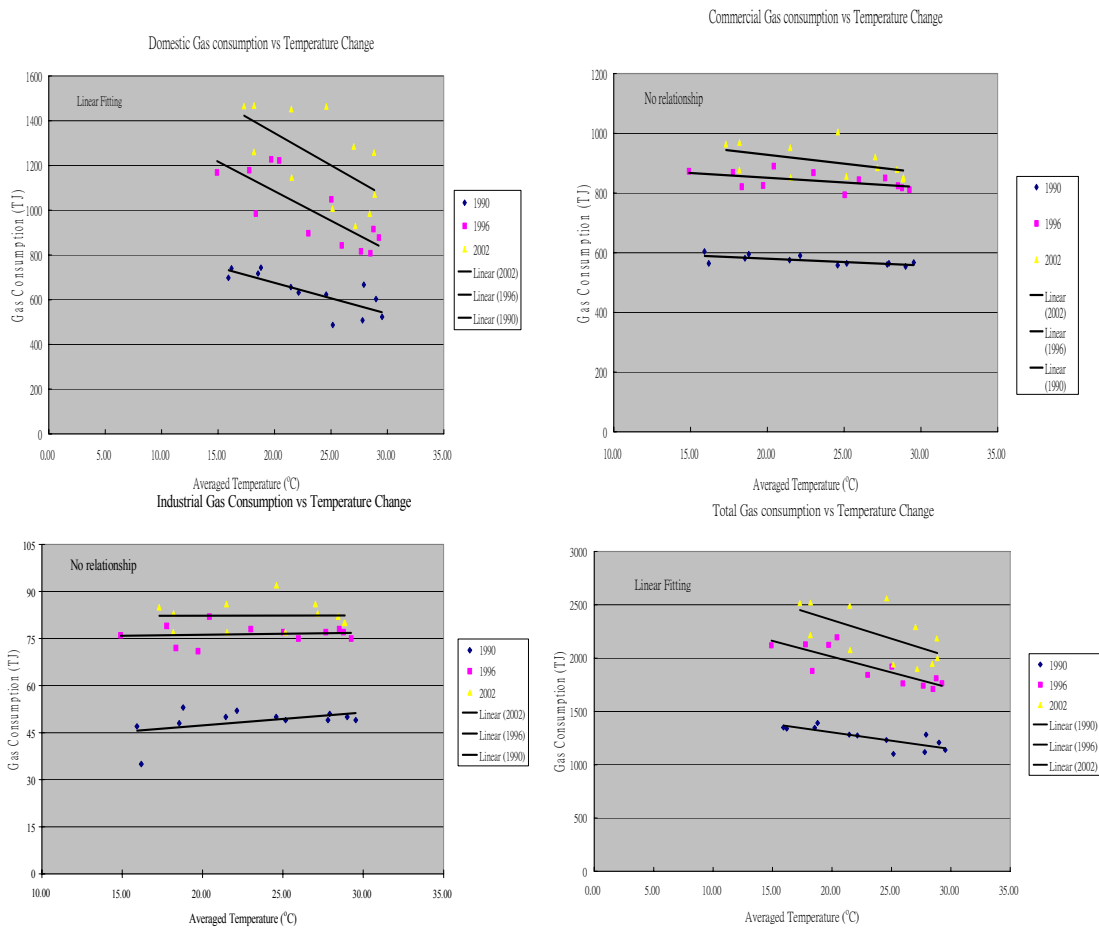


Figure 3.5 Temperature Dependence of Gas Consumption

The temperature function of the domestic sector was best fit by a straight line. The functions and their statistical confidence are listed in Table 3.6.

Year	Domestic consumption related with temperature equations (with 95% confidence interval)	Correlation of Coefficient, r	Coefficient of Determination, R^2	t value
1990	$C = (951.247 \pm 189.619) + (-13.783 \pm 8.046)T$	0.770	0.563	-3.817
1996	$C = (1613.072 \pm 331.166) + (-26.383 \pm 13.941)T$	0.800	0.640	-4.217
2002	$C = (1922.407 \pm 618.264) + (-28.863 \pm 25.487)T$	0.624	0.389	-2.523

Table 3.6 Relationship Between Gas Consumption and Ambient Temperature

Reduction of gas demand % per year	Temperature increase by		
	1°C	2°C	3°C
Domestic sector	-2.39%	-4.78%	-7.16%

Table 3.7 Percentage Increase of Gas Consumption due to Temperature Rise

The decrease in average gas consumption if the temperature of all months increases by 1°C, 2°C, and 3°C is listed in Table 3.7. The results show that the impact is beneficial. The higher the ambient temperature, the lower will be the gas consumption. To express the impact in monetary terms, we take the gas tariff as HK\$0.21 per MJ. In 2002 the gas consumption of domestic users was 14794 TJ. If the ambient temperature of 2002 had increased in every month by 1°C, the economic saving would have HK\$0.074 billion. For 2°C rise, the estimated saving would be HK\$0.149 billion. For 3°C rise, the estimated saving would be HK\$0.222 billion, as shown in Table 3.8.

	Temperature increase by		
	1°C	2°C	3°C
Economic impact of gas consumption in domestic sector	HK\$-74.25 million	HK\$-148.50 million	HK\$-222.44 million

Table 3.8 Summary of Economic Impact of Gas Consumption due to Climate Change

3.3.3 Oil Product Consumption:

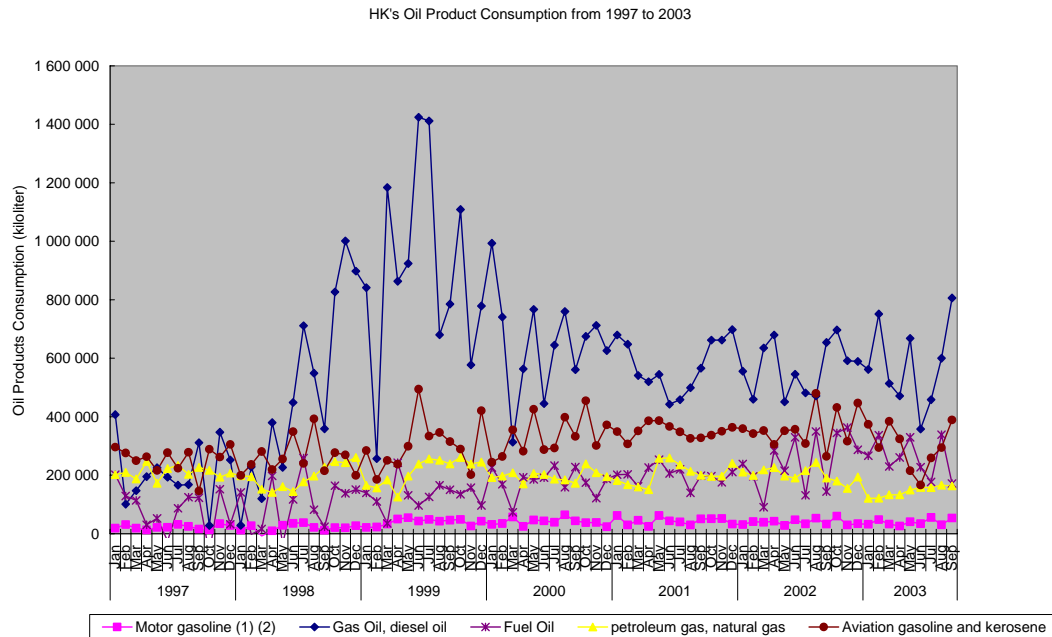


Figure 3.6 Hong Kong's Oil Product Consumption from 1997 to 2003

The monthly consumption of oil products in Hong Kong from 1997 to 2003 is shown in Figure 3.6. Unlike the electricity and gas consumption, no seasonal cycle could be discerned. It is concluded that oil product consumption has no correlation with temperature.

The Census & Statistics Department does not breakdown oil consumption by types of users. The Energy End Use Data (EMSD, 2002, December) provided annual oil consumption by types of user but no monthly breakdown figures are available. It was not possible to carry out similar analysis as in the case of electricity and gas.

3.3.4 Electricity Consumption for Government Office Buildings

(Commercial Sector)

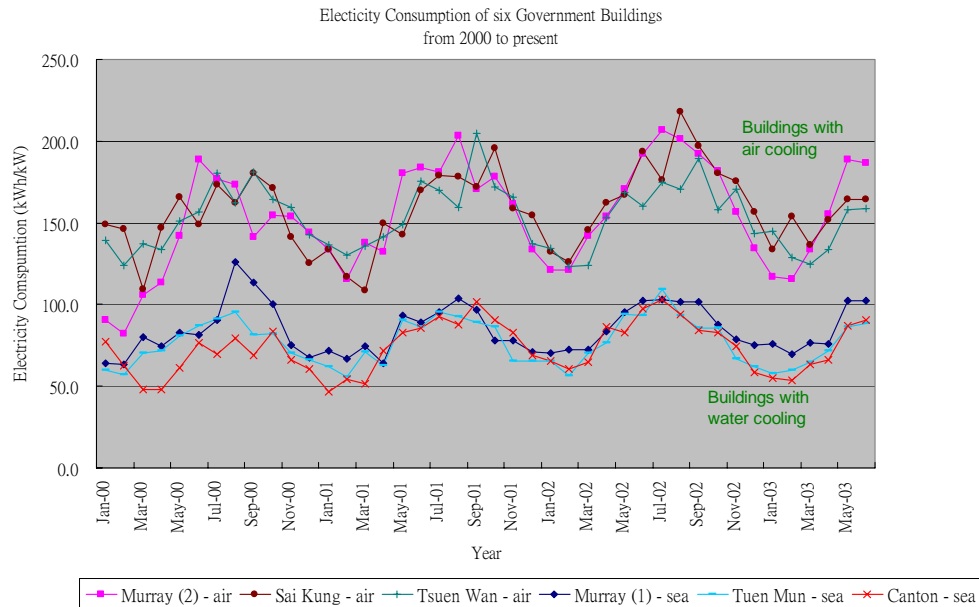


Figure 3.7 Normalized Electricity Consumption of A/C units in Government Buildings.

Presumably power consumption of air conditioning was most sensitive to ambient temperature, especially in the hot tropical summer of Hong Kong. Six government office buildings were selected to assess this temperature sensitivity. The normalized electricity consumptions from 2000 to 2003 in six government office buildings are shown in Figure 3.7. The electricity consumption was normalized by the total cooling capacity (kW) of each government buildings.

The major electrical appliances in the buildings were A/C, lighting, lift and pump. The power consumption of lightings, lifts and pumps were more or less constant throughout a year. Only the A/C plants had to work against temperature gradient and their energy consumption was highly dependent on ambient temperature. It is reasonable to assume that electricity consumption of facilities, other than air-conditioner, of an office building should be relatively non-temperature dependent; the temperature effect was largely due to the response of the air-conditioning to the ambient temperature.

Unlike the commercial electricity consumption analysis, the energy dependence of A/C units can be studied by combining the data in all three years because there was no trend in the time series. The electricity consumption in buildings with both air and water cooled A/C systems was confirmed temperature dependent. The monthly electricity consumption of buildings with air and water cooled systems were plotted against the monthly average ambient temperature. The results are shown in Figure 3.8.

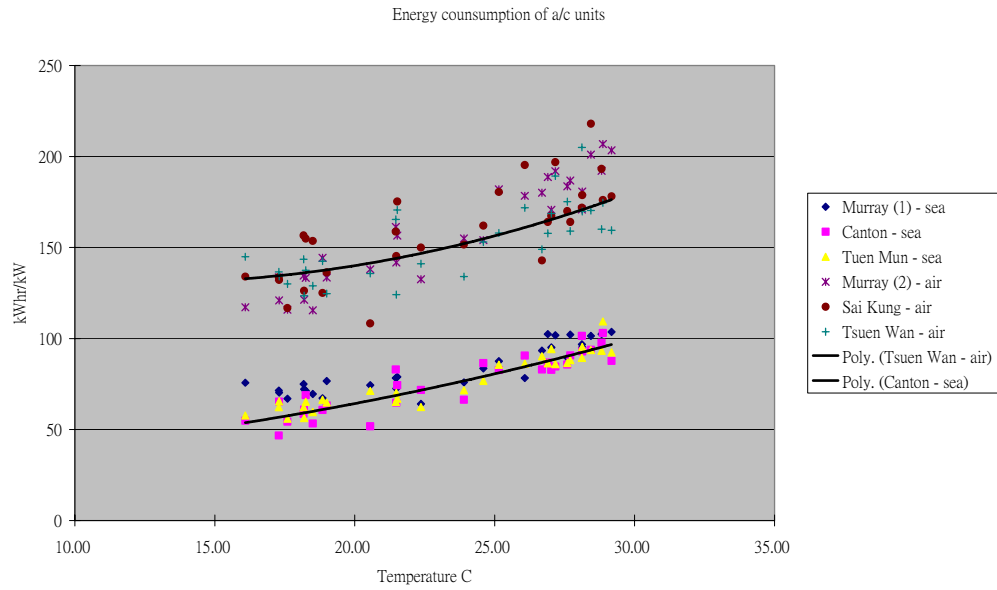


Figure 3.8 Electricity Consumption of Buildings with Air Cooled and Sea Cooled A/C Units

	Temperature functions	Correlation of coefficient, r	Coefficient of Determination, R ²	T value
Buildings with Air Cooled system	$C_a = (53.291 \pm 29.683) + (4.636 \pm 1.244) * T$	0.792	0.628	7.573
Buildings with Water Cooled System	$C_w = (127.156 \pm 92.844) - (-7.846 \pm 8.399) * T + (0.241 \pm 0.184) * T^2$	0.903	0.816	2.668

Table 3.9 Relationship Between Electricity Consumption of A/C Units and Ambient Temperature

The electricity consumption in buildings with the A/C units if the temperature of all months is increased by 1°C, 2°C, and 3°C are computed. The results are listed in Table 3.10.

Temperature increase by	Percentage increase in electricity demand	
	Air Cooling system	Water Cooling system
1°C	2.86%	4.61%
2°C	5.72%	9.81%
3°C	8.59%	15.62%

Table 3.10 Percentage Increase of Electricity Consumption of A/C Units due to Temperature Rise

The results show that the increase of ambient temperature has a significant impact on A/C energy consumption in Hong Kong. If the energy consumption in buildings can be broken down in different categories like A/C system, lighting and office equipment, the impact due to temperature rise in each item can be estimated. If the total A/C unit capacity of Hong Kong is known, we can estimate the related socio-economic impact. For 1°C temperature rise, the air cooled and water cooled electricity consumption in government buildings will be increased by 2.86% and 4.61% respectively. This figure is very close to the 3.13% increase computed from the commercial electricity consumption (Table 3.4).

It is interesting to compare the consumption between the air cooled system against the water cooled system. “Territory-wide Implementation Study For Water-Cooled Air Conditioning Systems in Hong Kong, Final Executive Summary, EMSD (August 2002)” reported that the Water-Cooled Air Conditioning Systems were generally more energy efficient than Air-Cooled Air Conditioning System by 20 to 40%. Figure 3.8 shows that the ‘electricity consumption per kW cooling capacity’ of the water cooled systems was 50% more energy efficient than that of the air cooled systems. To obtain a more accurate figure, an energy audit should be carried out in each government building.

3.4 Conclusion:

Temperature change has significant impact on the energy sector of Hong Kong. Raising the ambient temperature by 1°C will increase electricity consumption by 9.02%, 3.13%, and 2.64% in the domestic, commercial and industrial sectors respectively. In contrast, gas consumption will be reduced in the domestic sector. For 1°C temperature rise, the gas demand will be reduced by 2.39% in the domestic sector. However, the gas consumption in the commercial or industrial sector does not appear to be affected by change in ambient temperature. Oil consumption is not sensitive to temperature change and is unaffected by temperature change.

For 1°C temperature rise, the economic impact on the total electricity consumption is HK\$1.72 billion (data in year 2002 was used as reference). For 2°C rise, the estimated impact is HK\$3.26 billion. For 3°C rise, the estimated impact is HK\$5.50 billion. On the other hand, the savings in the gas consumption on the domestic sector is HK\$0.074 billion, HK\$0.149 billion and HK\$0.222 billion for 1°C, 2°C and 3°C temperature rise. Summing up, for 1°C temperature rise, the total energy cost of Hong Kong will increase by HK\$1.65 billion.

3.5 References

1. Census and Statistics Department, HKSAR
(<http://www.info.gov.hk/censtatd/home.html>)
2. Climate Change 2001, The Scientific Basis, International Panel on Climate Change
3. EMSD's Energy End Use Data (1990-2000)
(http://www.emsd.gov.hk/emsd/c_download/pee/hkeeu db_sim_90.pdf)
4. Hong Kong Energy Statistics 2002
5. Heat Island Group, Lawrence Berkeley National Laboratory, Berkeley
(<http://eetd.lbl.gov/HeatIsland/EnergyUse/>)
6. Raw Data of gas consumption in Hong Kong since 1990
(http://www.info.gov.hk/censtatd/eng/hkstat/fas/energy/gas_consum_index.html)
7. Raw Data of electricity consumption in Hong Kong since 1990
(http://www.info.gov.hk/censtatd/eng/hkstat/fas/energy/electricity_consum_index.html)
8. Raw Data of oil consumption in Hong Kong since 1990
(http://www.info.gov.hk/censtatd/eng/hkstat/fas/energy/ri_oil_index.html)
9. Territory-wide Implementation Study For Water-Cooled Air Conditioning Systems in Hong Kong, Final Executive Summary, EMSD (August 2002)

Chapter 4. Human Health

4.1 Introduction

Global climate change causes direct and indirect impacts on human health. The direct impacts include sea-level rise, more frequent heat waves, more weather disasters such as flooding and drought. More frequent droughts, floods and storms will increase infectious diarrhea. The rise in sea-level rise may lead to overcrowding, poor sanitation and an increase in infectious diseases. Other impacts of sea-level rise in the Pearl River Delta Region will be discussed separately in more detail in Chapter 11. The increase in temperature will cause more heat related diseases such as cardiovascular and respiratory illnesses. Hotter climate will lead to more energy consumption. Poorer air quality will enhance morbidity in asthma and respiratory illnesses. Natural disasters threaten food supply and may lead to malnutrition. An important impact of climate change encompasses induction of vector-borne, air-borne and marine-borne diseases. Diseases that are spread by mosquitoes and other insects will become more prevalent if warmer temperature enables those insects to become established farther north. Such "vector-borne" diseases include malaria, dengue fever, yellow fever and encephalitis. The sensitivity of vector-borne diseases to climate change depends on preceding and coexistent circumstances, such as socio-economic development, local environmental conditions, human behavior and immunity, and the effectiveness of control measures. The casual pathways of impacts on public health due to climate change are shown in Figure 4.1.

In the past two decades, to predict the impact of climate change on human health, many developed countries have used different approaches. Most methodologies rely on retrieving long term data that are collected, catalogued and analyzed by intergovernmental departments and non-governmental organizations. The most common methodology is to evaluate different factors and to establish empirical formulae for estimating the impacts.

In the North America (the U.S.A. and Canada), GIS is commonly used, in an environmental contemplating approach, to evaluate and predict the impacts of climate changes on human health. It involves geographical and time-scale considerations that integrate: 1.) climate changes, 2.) subsequent ecological change, 3.) human disease activity, and 4.) human habitation. The response time of human disease systems to climate change varies by disease or location. Difference in response time may be resulted from different life spans of intermediate hosts, as well as from differences in interactions and feedback loops at various ecosystem levels (Patz & Balbus, 1996).

In the Netherlands, an integrated modeling approach is used to assess the potential impacts of global climate change on human health. The model they use is called "Model for the health Impact Assessment of Man-induced Atmospheric changes" (MIASMA). An outline of the prototype of MIASMA in conceptual terms is illustrated in Figure 4.2 (Martens, 1996). This integrated approach is the most

comprehensive treatment of the interactions between atmospheric changes and the society.

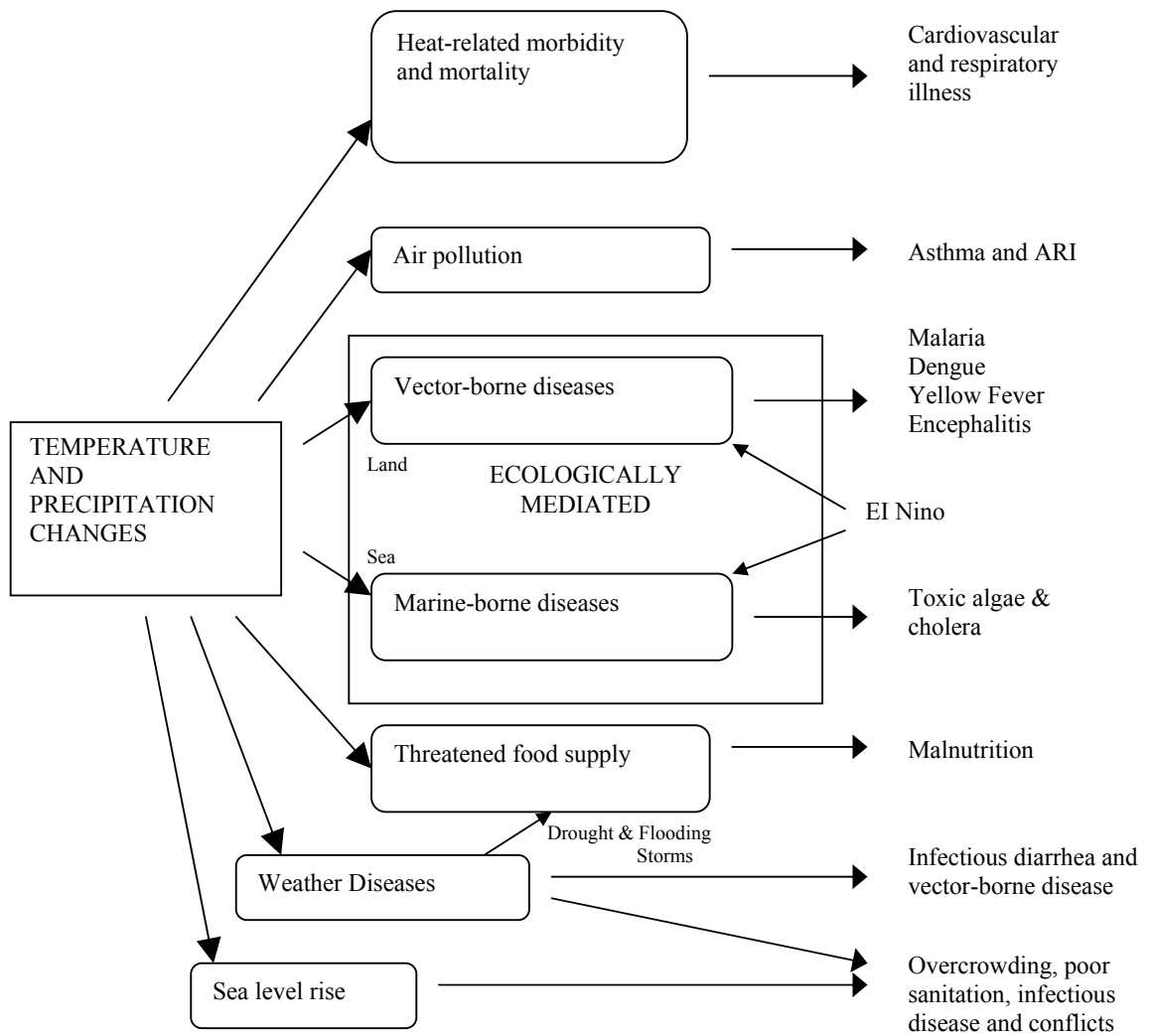


Figure 4.1 Causal Pathways of Public Health Impacts from Climate Change

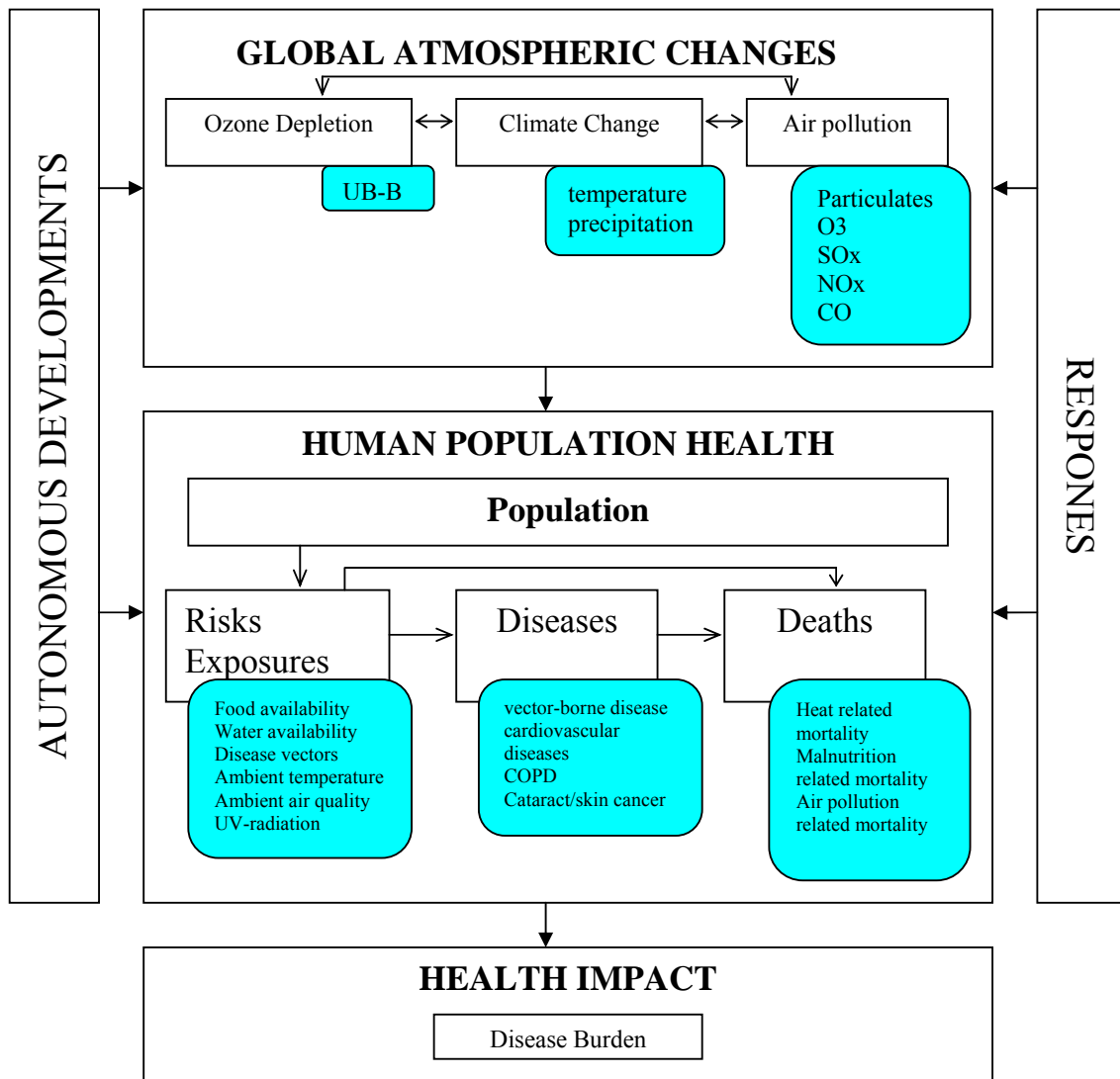


Figure 4.2 Conceptual Representation of the Health Impact of the MIASMA Model

MIASMA has been developed on a global scale. It has a time horizon of 130 years starting from 1970, and runs in time steps of 1 year till the year 2100. It is part of the modeling framework of ‘Global Dynamics and Sustainable Development’ of Public Health and Environmental Protection in the Netherlands and is commonly used by developed countries in Europe. It contemplates for interregional variations in the magnitude of effects. MIASMA also considers other relevant environmental aspects. Important issues of model developing are flexible integrated methodology to allow for flexible inclusion of various sets of determinants and disease specific sub-models as well as the collection of global and regional data for validation. MIASMA is composed of seven individual models. These include ozone depletion, climate change, air pollution, population, risk exposures, diseases and mortality (Rotmans & Vries, 1997).

Hong Kong does not have the infrastructure to run this kind of model. To begin with, the consultants focused on the impact of temperature rise. Regression analysis was carried out to explore whether Hong Kong's mortality rate was temperature dependant. The consultants then worked on three important areas covered in this chapter: the heat-related diseases, dengue fever and malaria.

4.2 Correlation between Mortality and Ambient Temperature

in Hong Kong

A direct approach is adopted in this section to observe whether the mortality rate in Hong Kong depends on the ambient temperature. Daily mortality records between 1995 and 2001 were acquired from the Hospital Authority, the HKSAR. Some records were deleted due to missing information on date. The time series of the daily mortality rate and daily ambient temperature in Hong Kong between 1995 and 2001 are shown in Figure 4.3. Hot days and cold days were identified by taking the values of average temperature on those days that were greater than the 99% percentile and less than the 1% percentile value respectively from "smoothed" temperature series (Hajat et al., 2002). Linear regressions were carried out independently for hot days and cold days.

Statistical Results

Table 4.1 lists the mean, standard deviation, minimum, maximum and 1, 5, 95, 99 percentile values of the daily mortality rate and temperature parameters in Hong Kong between 1995 and 2001. Totally, 2557 samples were collected within this period. Figure 4.3 shows that there was a strong seasonal pattern in the mortality series with more deaths occurring in the winter months of each year. Also, the number of deaths seemed to be lower at moderate temperatures, with an increase in deaths as the temperature dropped and and also when the temperature was extremely low or high.

	Mean	Std. Deviation	Minimum	Maximum	Percentiles			
					1	5	95	99
Daily Mortality	85.7	12.9	46	138	59	66	109	119
Average Daily temperature	23.5°C	5.0°C	6.9°C	31.3°C	11.9	14.8	29.8	30.3
Maximum Daily Temperature	25.7°C	5.2°C	8.4°C	35.1°C	13.5	16.5	32.5	33.3
Minimum Daily temperature	21.6°C	5.0°C	5.8°C	29.5°C	10.0	12.8	28.0	28.9

Table 4.1 Mean, Standard Deviation, Minimum, Maximum and 1, 5, 95, 99 Percentile Values of the Daily Number of Total Deaths and Temperature Variables in Hong Kong between 1995 and 2001

A time series of total daily mortality and daily average temperature in period of 1995-2001

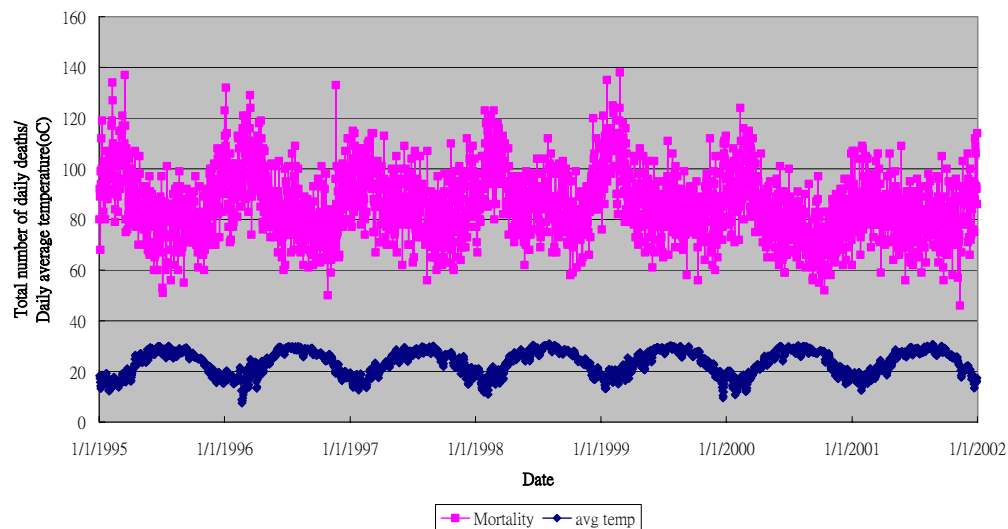


Figure 4.3 Time series of the Total Number of Daily Deaths and the Daily Average Temperature in Hong Kong between 1995 and 2001.

Within these 7 years, only 17 cold days and 15 hot days occurred in Hong Kong. The number of samples was inadequate to carry out a statistically significant analysis. As a result, the definition of hot and cold were relaxed using 95% and 5% percentiles. Figure 4.4 depicts linear regression between both hot or cold days and mortality. Both regressions indicate that mortality rate increased as the temperature got hotter or colder. It is noted that, assume 95% confidence and 0.5 permitted error of daily mortality, a sample of 2032 daily mortality record for cold days or hot days should be needed.

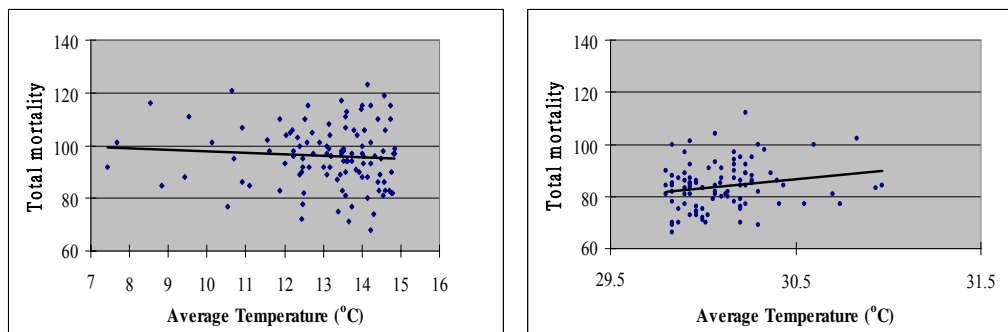


Figure 4.4 Mortality-Temperature Relation for Temperatures of 14.8°C or less (left) and of 29.8°C or over (right) between 1995 and 2001

Regression Results

Two meteorological parameters, average temperature and relative humidity, were input into the model. The regression showed that the correlation between relative humidity and mortality rate was not significant, whereas the correlation between

temperature and mortality rate was significant. A hot day was defined as having temperature $> 29.8^{\circ}\text{C}$ and a cold day as having temperature $< 14.8^{\circ}\text{C}$. Increase in 1°C in hot days was associated with 6.82 increase in deaths (95% CI -0.38 to 14.02) while increase in 1°C in cold days was associated with 0.61 decrease in deaths (95% CI -0.2 to 0.82). The result is interesting because cold months had higher mortality rate than hot months, yet the change in mortality rate per $^{\circ}\text{C}$ decrease in cold months was lower than that in hot months. Although it is well known that absolute value and slope are different parameters, caution should be exercised in interpreting regression results. Nevertheless, visual inspection of Figure 4.4 indicates that the mortality rate would increase when the temperature was very cold or very hot.

Limitation

Owing to the lack of a comprehensive health database, more in-depth regression analysis could not be carried out. A better analysis can be performed in the future if the health database includes additional information such as the cause of death, age and hospital consultation records.

4.3 Heat Stroke

The number of reported heat stroke between 1998 and 2002 in Hong Kong is listed in Table 4.2.

Year	1998	1999	2000	2001	2002
No. of Heat Stroke	23	19	22	19	13

Table 4.2 Number of Reported Heat Stroke in Hong Kong
(source: Department of Health)

The most direct impact of heat stress on the human body is the onset of heat exhaustion or heat-stroke. It is a tropical heat-related disease due to prolonged period of excessive heat and humidity. The three stages of heat stress include heat cramps, heat exhaustion and finally heat stroke. Heat stroke, the most severe of these conditions, can be fatal. If the body temperature reaches 40°C or above, it may result in damages to the kidneys, muscles, heart and blood cells. Sweating will stop altogether. Death due to complications such as kidney failure may occur immediately or may be delayed up to several weeks. In general, climate change, including high temperature together with high humidity and low wind speed, will increase the chance of heat stroke in summer. Urbanization helps keep more warmth in the city at night and urban residents are at greater risks of heat stroke and other heat-related causes of mortality. Owing to the small number of health records on heat stroke in Hong Kong, it is difficult to carry out further analysis.

In Europe, North America, and Australia, the recorded mortality rates of heat stroke have been increasing. In 2000, more than 2.45 million people older than 65 living in the state of New York, suffered from heat-related diseases - about 12% of the population. By 2025, the number is expected to increase to 3.3 million and will make up more than 16% of the state population.

Based upon the data of the Shanghai population aged over 65 years (between the period of 1980-1989), the IPCC Technical Summary of Climate Change reported that the threshold temperature for heat-related mortality in summer was 34°C. Days with high afternoon temperature, low wind speed and high humidity were associated with the biggest increase in mortality rate. The transient models (GFDL-X2 and UKMO-X6) estimated that heat-related deaths in Shanghai would increase by 3.6 – 7.1 times of the present figure by the year 2050. Since global warming is a gradual process, this increase in mortality rate could drop to 2.5 – 2.6 times of the present figure if acclimatization of population was taken into consideration (IPCC, Climate Change 2001).

4.4 Dengue Fever (DEN)

The morbidity of dengue fever between 1997 and 2003 in Hong Kong is listed in Table 4.3.

Year	1997	1998	1999	2000	2001	2002	2003
Notifiable Dengue	10	15	5	11	17	44	49

Table 4.3 Number of Notified Dengue Fever Cases (source: Department of Health)

Although the number of dengue fever is small in Hong Kong, there has been a rising trend since 1999. The number of notifiable dengue fever is the total sum of local and oversea cases. Nearly all cases of dengue fever cases were imported. This figure therefore did not reflect the case of dengue fever in Hong Kong.

In general, dengue fever is endemic in Southeast Asian countries whose hot and humid climates are highly favorable to mosquito breeding. In Hong Kong, *Aedes aegypti* is the principle vectors of dengue transmission. This dengue virus belongs to the family of *Flaviviridae* and the genus *Flavivirus*. A parameter called epidemic potential, EP, is introduced to calculate the vector population in an endemic area. EP is defined as the reciprocal of the host density threshold m_c . EP is a key summary parameter which is used as a comparative index in estimating the effect on the risk of vector diseases. Figure 4.5 depicts the relationship between EP and temperature for dengue (*Flavivirus*) fever. The EP of dengue transmission was estimated to increase by 31- 47% globally (Martens, 1997).

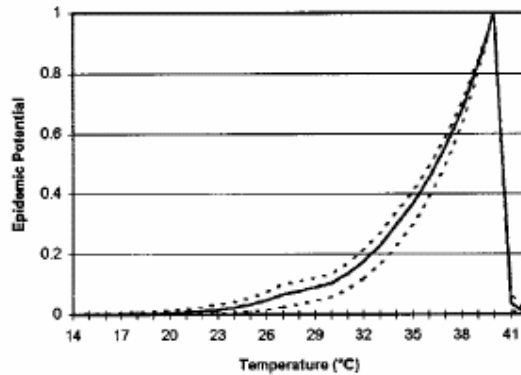


Figure 4.5 Epidemic Potential for Dengue Fever

Figure 4.5 shows that the maximum EP occurs at 40°C for dengue fever. By 2030, the maximum average temperature in Hong Kong would increase by 1°C to 31°C. The EP of dengue fever in Figure 4.5 is on a positive slope at 31°C. Thus the potential risk of dengue fever is anticipated to increase in the next 30 years. The computation of the increase of EP of dengue fever in Hong Kong is shown in the following section.

Methodology

First of all, population growth is ignored. The transmission of dengue was estimated by considering temperature-dependent parameters in the EP formula. The potential is the reciprocal of the host density. The mosquito/man ratio (critical host density) for dengue transmission is expressed as below:

$$m_c = \frac{1}{EP} = k_1 * \frac{-\log(p)}{a^2 p^n}$$

where:

- p denotes the survival probability of the mosquito;
- a is the biting frequency of taking meals on human blood;
- n represents the incubation period of the parasite in the vector;
- k_1 is a constant = 30.011 (derived from Figure 5.6),

k_1 incorporates variables that are assumed to be independent of temperature (including the efficiency with which an infector mosquito infects a susceptible human and vice-versa, as well as the propensity of the mosquito population to feed on human beings and the ability of infected human beings to recover).

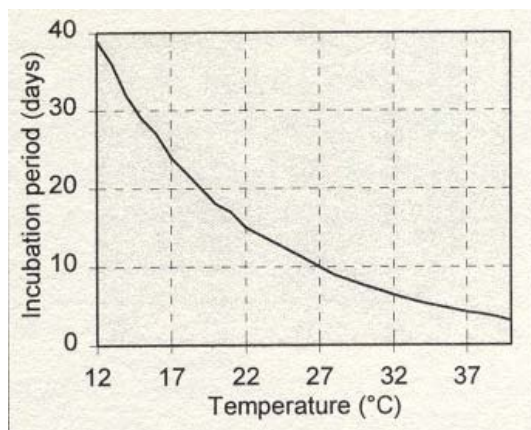
The incubation period n depends on the development rate of dengue virus, digestion of blood meal and virus titer in infecting blood meal. These development rates are highly correlated to temperature changes, as $n = f(T)$. The temperature dependence of n is shown in Figure 4.6 (Focks et al., 1995).

The biting frequency of mosquito a depends on the female weight (temperature dependant), the feeding habit of Aedes mosquito and human blood meals. Some of these parameters are temperature dependant and some are not. The biting frequency cannot be represented by an analytical equation. The temperature dependence of a is shown in Figure 4.6.

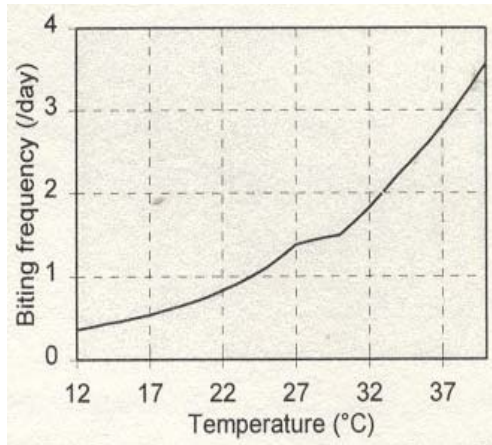
The survival probability of mosquito p is set at 0.89 per day at temperature ranged between 6°C and 40°C. Below or above this temperatures range, the survival rate declines linearly.

The impact of temperature rise on the EP of dengue is estimated on a monthly basis. EP_T is the EP at monthly temperature T (given in Figure 4.5). Similar to the technique used in the energy impact estimation in chapter 4, assuming the global temperature is increased by 1°C due to climate change, the predicted EP at a new temperature $T+1$ in all twelve months are computed one by one by looking up the factors a , p and n in Figure 4.6. The increase in EP (ΔEP) at a certain month is obtained by $\Delta EP = EP_{T+1} - EP_T$.

(A) Incubation Period of Dengue Virus



(B) Mosquito Biting Frequency



(C) Survival Probability of Adult Mosquito

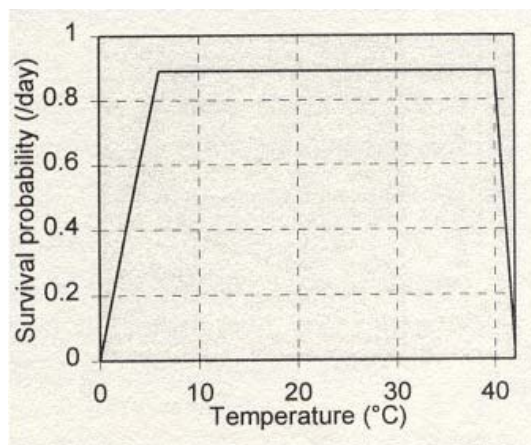


Figure 4.6 Relationship between Temperature and Factors of Dengue Transmission.

(A): Incubation Period n of Dengue Virus in the Mosquito; (B): Mosquito Biting Frequency a ; (C): Survival Probability of Adult Mosquito p

Findings

2003	avg. temp °C	EP _T	T+1 °C	EP _{T+1}	ΔEP (%)	T+2	EP _{T+2}	ΔEP (%)	T+3	EP _{T+3}	ΔEP (%)
Jan	16.1	0.0031	17.1	0.0042	0.11	18.1	0.0062	0.31	19.1	0.0082	0.51
Feb	18.5	0.007	19.5	0.009	0.2	20.5	0.0105	0.35	21.5	0.012	0.5
Mar	19.0	0.008	20.0	0.01	0.2	21.0	0.011	0.3	22.0	0.013	0.5
Apr	23.9	0.033	24.9	0.045	1.2	25.9	0.055	2.2	26.9	0.065	3.2
May	26.9	0.07	27.9	0.09	2	28.9	0.106	3.6	29.9	0.138	6.8
June	27.7	0.08	28.7	0.105	2.5	29.7	0.135	5.5	30.7	0.15	7
July	29.6	0.13	30.6	0.15	2	31.6	0.175	4.5	32.6	0.238	10.8
Aug	28.8	0.11	29.8	0.14	3	30.8	0.16	5	31.8	0.18	7
Sept	27.6	0.08	28.6	0.105	2.5	29.6	0.135	5.5	30.6	0.14	6
Oct	25.3	0.05	26.3	0.065	1.5	27.3	0.075	2.5	28.3	0.097	4.7
Nov	22.2	0.025	23.2	0.035	1	24.2	0.04	1.5	25.2	0.05	2.5
Dec	17.6	0.0052	18.6	0.0072	0.2	19.6	0.0092	0.4	20.6	0.0108	0.56

Table 4.4 The Monthly Averaged Temperature, Monthly EP, Hypothetical EP at T+1, T+2 and T+3 for the Year 2003.

1994-2003	Average temp °C	Average ΔEP			Standard Deviation		
		T+1	T+2	T+3	T+1	T+2	T+3
January	16.62	0.18	0.37	0.56	0.04	0.05	0.05
February	16.87	0.16	0.32	0.49	0.05	0.08	0.07
March	19.39	0.18	0.72	1.52	0.13	0.69	0.96
April	23.11	0.95	2.07	3.29	0.54	0.69	0.85
May	25.78	1.36	3.24	5.53	0.61	1.08	1.61
June	28.15	2.66	4.89	7.27	0.38	0.36	0.32
July	28.71	2.30	4.93	7.85	0.61	0.57	1.18
August	28.57	2.49	5.05	7.59	0.49	0.39	0.93
September	27.61	2.39	5.00	7.08	0.52	0.72	0.58
October	25.51	1.12	2.99	4.91	0.36	0.55	0.27
November	21.99	0.83	1.89	2.86	0.45	0.25	0.34
December	18.30	0.19	0.36	0.68	0.03	0.05	0.41

Table 4.5 Ten Years Averaged ΔEP_{T+1}, ΔEP_{T+2}, and ΔEP_{T+3} Averages and Their Standard Deviations

The monthly average temperature T, EP_T, ΔEP_{T+1}, ΔEP_{T+2}, and ΔEP_{T+3}, for the year 2003 are shown in Table 4.4. The analysis was repeated for ten years. The ten years average values of ΔEP_{T+1}, ΔEP_{T+2}, and ΔEP_{T+3} and their standard deviations are shown in Table 4.5.

The seasonal variations of the ten years averaged ΔEP_{T+1}, ΔEP_{T+2}, and ΔEP_{T+3} listed in Table 4.5 are shown in Figure 4.7. The impact of global climate change on the dengue fever's transmission was the greatest in summer months and almost negligible in winter months.

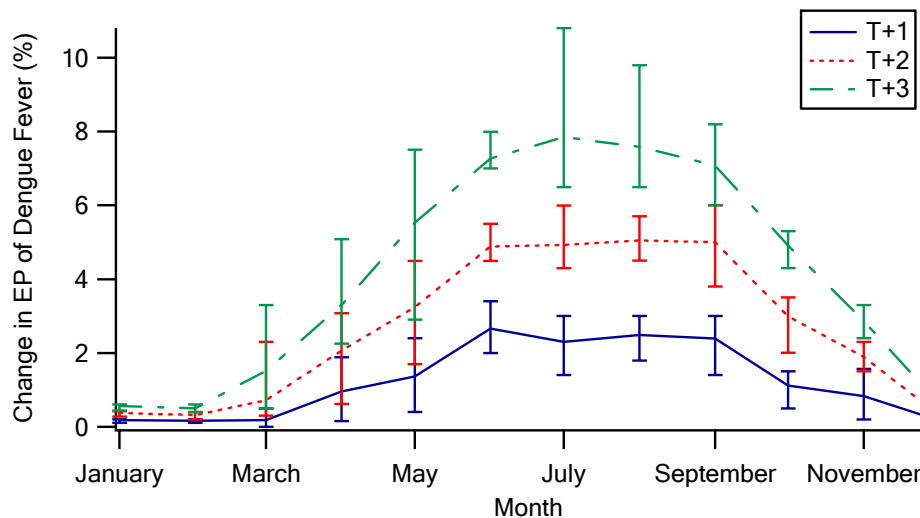


Figure 4.7 Monthly Average Percentage Change in Epidemic Potential of Dengue Fever in 1994-2003. The error bars denote the maximum and minimum values.

The yearly average ΔEP of dengue is summarized in Table 4.6. The ΔEP of dengue fever was estimated at 1.24%, 2.62% and 4.12% for 1°C, 2°C and 3°C temperature rise in Hong Kong. The results showed that the risk of dengue would increase due to global temperature rise but the impact was not significant. The increase was only a few percents.

Temperature Increase	Increase of Epidemic Potential (Dengue Fever)
1°C	1.24% (0%-3.4%)
2°C	2.62% (0.2%-6.0%)
3°C	4.12% (0.39%-10.8%)

Table 4.6 Calculated Relative Percentage Change of the Epidemic Potential (ΔEP) in Hong Kong, Compared to the Baseline (1994-2003 monthly mean temperature)

This analysis is rather sensitive to temperature rise. Figure 4.5 shows that the relationship between EP and temperature is non-linear. The EP of dengue fever shows a critical temperature at about 32°C. The curve rises gently at low temperatures. When the temperature exceeds 32°C, EP increases at a much faster rate. At present, the maximum average monthly temperature is about 30°C which is quite close to the critical temperature. When the temperature rises by 2°C, ΔEP is not very significant but when the temperature rises by 5°C, ΔEP can be very significant. If global warming increases the frequency and magnitude of El Niño Southern Oscillation (ENSO) events, it is likely to trigger outbreaks of dengue fever in Southeast Asia.

Based upon the output of the global circulation model HADCM2 (0.5°x0.5° grid size), the baseline probability of an epidemic in Hong Kong was estimated to be 0.67 in the 1990s. The model output also projected the probability of transmission of dengue in Hong Kong to increase by 0.76, 0.82 and 0.88 in the 2020s, 2050s and 2080s respectively. Since it is greater than 0.5, the whole population of Hong Kong is

currently “at risk” (Hales, 2002). The results of the preceding section are consistent with the HADCM2 model output. Both anticipated that climate change would increase the probability of transmission of dengue fever in Hong Kong.

4.5 Malaria

The morbidity rate of malaria between 1997 and 2003 in Hong Kong is listed in Table 4.7

	1997	1998	1999	2000	2001	2002	2003
Notifiable Malaria Record	101	54	55	35	47	23	21

Table 4.7 Number of Notified Malaria Cases (source: Department of Health).

Malaria is transmitted by the *Anopheline* mosquito. The optimum temperature for survival of *Anopheline* mosquitoes lies in the range of 20°C-25°C. Malaria is caused by the species of parasites which belong to the genus *Plasmodium*. There are four species of the malaria parasite: (1) *P. vivax*, (2) *P. falciparum*, (3) *P. ovale*, (4) *P. malariae*. *P. vivax* has the most extensive geographic range; *P. falciparum* is the most common species in tropical areas and the most dangerous clinically; and *P. ovale* and *P. malariae* are less prevalent. The summer weather in Hong Kong provides excellent conditions that encourage the breeding of mosquitoes and Hong Kong is an epidemic area of malaria.

In Australia, a climate modeling exercise showed that global warming would enlarge the potential range of the main vector, *Anopheles farauti sensu stricto*; and by year 2030 it could extend along the Queensland coast to Gladstone, 800 km south of its present limit. The vector distribution would change due to rise in temperature and sea-level. Global climate change could lead to more frequent tropical cyclones and floods which would increase vector density and the risk of malaria. Sea level rise would lead to inundation of more low-lying areas; and this would further promote the growth of malaria (Bryan et al., 1996).

Figure 4.8 shows the EP values for two common species of malaria. The maximum EP is found in the range of 29-33°C for malaria. This value is quite different from that of dengue fever. Martens, 1997, estimated that the EP of malaria transmission might increase by 12-27% in an epidemic area in the future. Based on the HadCM2 medium-high scenario, Rogers, 2000 estimated that the global potential exposure of human to malaria would increase by 23 millions (+0.84%). When the HadCM2 high scenario was adopted, the potential exposure would decrease by 25 millions (-0.92%) in 2050. Based on the HadCM3 scenario, Martens, 1999 reported climate change may result a much higher transmission. He predicted that the additional number of people at risk would be 150 million people for *P. vivax* and 300 million people for *P. falciparum* in 2080.

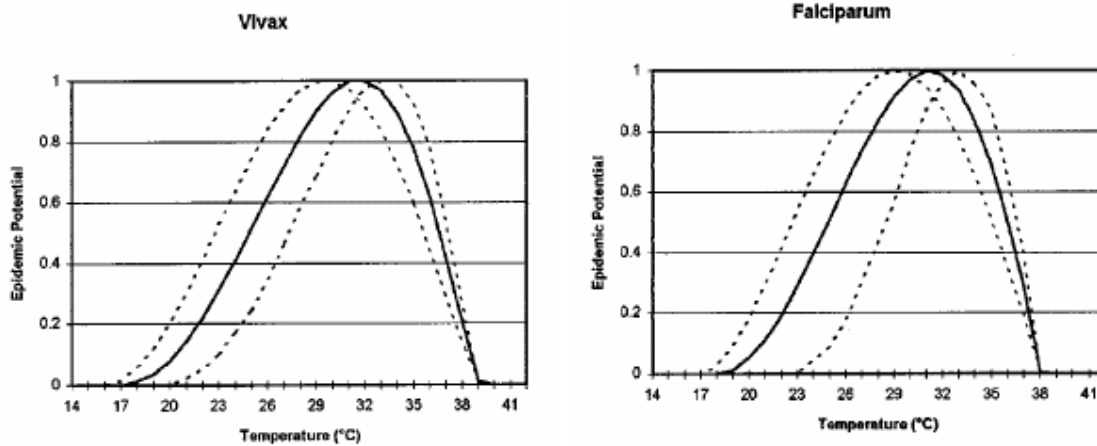


Figure 4.8 Epidemic Potential for *P. vivax* (right side) and *P. falciparum* (left side)

Impact of Temperature Rise on the Transmission of Malaria in Hong Kong

The transmission of malaria depends on population growth, temperature, rainfall, humidity and vector abundance. Under optimal conditions of rainfall and humidity, the probability of malaria transmission is correlated to temperature. To explore the impact of temperature rise on the EP of malaria, again population growth and other non-weather parameters are ignored. The aim of the following section is to find out ΔEP of malaria due to temperature rise.

Methodology

The computation of ΔEP of malaria is the same as that of dengue fever except that the curves of a , p and n curves of Malaria behave much better. The temperature curves of the 3 key parameters can be represented by analytical equations.

The relation between ambient temperature and latent period of parasite n can be calculated using a temperature sum (Macdonald, 1957):

$$n = \frac{D_m}{T - T_{\min,m}}$$

where n is the incubation period of the parasite inside the vector (in days), D_m is the number of degree-days required for the development of the parasite (105 °C days and 111°C days for *P. vivax* and *P. falciparum*, respectively). $T_{\min,m}$ the minimum temperature required for parasite development, is 14.5 °C and 16 °C for *P. vivax* and *P. falciparum*, respectively. T is the actual average temperature.

For a mosquito population, the frequency of the feeding interval u can be calculated by means of a temperature sum (Detinova et al., 1962):

$$u = \frac{D}{T - T_{\min}}$$

where D is the number of degree-days required for completion of the development. The values of T_{\min} and D are 9.9°C and 36.5°C days respectively for *An. maculipennis*.

The number of blood meals a mosquito takes from human beings depends on the frequency of feeding interval and the human blood index (HBI):

$$a = \frac{HBI}{u}$$

where HBI is set to 0.4, a value frequently found in malaria-endemic regions for a wide range of *Anopheles* species and u is the frequency of feeding intervals.

The daily survival probability p of mosquito is a function of temperature:

$$p = e^{\frac{-1}{(-4.4+1317-0.03T^2)}}$$

where p is the survival probability during one gonotrophic cycle and T is the ambient temperature. The relative humidity is assumed to remain at a favorable level for mosquito development and does not change with precipitation. A constant value k_1 and k_2 are used for analysis and listed as below:

$$\begin{aligned} k_1 &= 0.1668 \text{ for } P. \textit{vivax}, \text{ and} \\ k_1 &= 0.1451 \text{ for } P. \textit{falciparum} \end{aligned}$$

Next, we estimate the monthly EP of malaria and its percentage change when temperature increases by 1°C . Since $T_{\min,m}$ is 14.5°C for *P. vivax* and 16°C for *P. falciparum* respectively, in winter time when the average monthly temperature is below $T_{\min,m}$ for parasite development, the transmission of malaria will be zero. On the high temperature side, the proportion of parasites surviving decreases rapidly when temperatures are over 32°C (Figure 4.8). An extreme event such as El Nino in 1997 would suddenly influence the transmission of malaria in Hong Kong.

Findings

The monthly average temperature T , EP_T , ΔEP_{T+1} , ΔEP_{T+2} , and ΔEP_{T+3} , for *P. vivax* and *P. falciparum* for the year 2003 are shown in Table 4.8 and Table 4.9 respectively.

2003	avg. temp	EP _T	T+1	EP _{T+1}	ΔEP (%)	T+2	EP _{T+2}	ΔEP (%)	T+3	EP _{T+3}	ΔEP (%)
Jan	16.1	0.0002	17.10	0.0043	0.42	18.10	0.0002	2.10	19.10	0.0557	5.56
Feb	18.5	0.0328	19.50	0.0748	4.20	20.50	0.0328	10.20	21.50	0.2107	17.79
Mar	19.0	0.0514	20.00	0.1026	5.12	21.00	0.0514	11.94	22.00	0.2537	20.23
April	23.9	0.4398	24.90	0.5455	10.57	25.90	0.4398	21.13	26.90	0.7516	31.18
May	26.9	0.7516	27.90	0.8421	9.05	28.90	0.7516	16.55	29.90	0.9709	21.93
June	27.7	0.8250	28.70	0.9036	7.85	29.70	0.8250	13.71	30.70	0.9948	16.98
July	29.6	0.9573	30.60	0.9929	3.56	31.60	0.9573	4.03	32.60	0.9658	0.85
Aug	28.8	0.9104	29.80	0.9666	5.62	30.80	0.9104	8.61	31.80	0.9943	8.39
Sept	27.6	0.8163	28.60	0.8965	8.02	29.60	0.8163	14.10	30.60	0.9929	17.66
Oct	25.3	0.5880	26.30	0.6921	10.41	27.30	0.5880	20.13	28.30	0.8742	28.62
Nov	22.2	0.2718	23.20	0.3680	9.62	24.20	0.2718	19.94	25.20	0.5774	30.56
Dec	17.6	0.0107	18.60	0.0361	2.54	19.60	0.0107	6.92	20.60	0.1417	13.09

Table 4.8 The Monthly Averaged Temperature, Monthly EP for *P. vivax*, Hypothetical EP at T+1, T+2 and T+3 for the Year 2003.

2003	avg. temp	EP _T	T+1	EP _{T+1}	ΔEP (%)	T+2	EP _{T+2}	ΔEP (%)	T+3	EP _{T+3}	ΔEP (%)
Jan	16.1	0.0000	17.1	0.0000	0.00	18.1	0.0020	0.20	19.10	0.0168	1.68
Feb	18.5	0.0057	19.5	0.0286	2.30	20.5	0.0748	6.92	21.50	0.1435	13.79
Mar	19.0	0.0144	20.0	0.0488	3.44	21.0	0.1065	9.22	22.00	0.1852	17.08
April	23.9	0.3766	24.9	0.4900	11.34	25.9	0.6051	22.85	26.90	0.7162	33.96
May	26.9	0.7162	27.9	0.8172	10.10	28.9	0.9019	18.58	29.90	0.9639	24.77
June	27.7	0.7981	28.7	0.8866	8.85	29.7	0.9536	15.55	30.70	0.9927	19.46
July	29.6	0.9481	30.6	0.9902	4.22	31.6	0.9987	5.06	32.60	0.9676	1.95
Aug	28.8	0.8944	29.8	0.9589	6.45	30.8	0.9948	10.04	31.80	0.9958	10.14
Sept	27.6	0.7883	28.6	0.8786	9.03	29.6	0.9481	15.98	30.60	0.9902	20.19
Oct	25.3	0.5361	26.3	0.6503	11.42	27.3	0.7581	22.20	28.30	0.8534	31.73
Nov	22.2	0.2031	23.2	0.3012	9.81	24.2	0.4101	20.70	25.20	0.5246	32.15
Dec	17.6	0.0003	18.6	0.0070	0.67	19.6	0.0322	3.19	20.60	0.0807	8.05

Table 4.9 The Monthly Averaged Temperature, Monthly EP for *P. falciparum*, Hypothetical EP at T+1, T+2 and T+3 for the Year 2003.

The analysis was repeated for records in ten years. The ten years ΔEP_{T+1} , ΔEP_{T+2} , and ΔEP_{T+3} averages and their standard deviations of *P. falciparum* are shown in Table 4.10. The standard error for the whole year is between 0.16 and 1.53 for one degree Celsius increases. Similarly, the standard error of *P. vivax* is between 0.50 and 1.27. This regression analysis is statistically significant.

1994-2003	Average temp	Average ΔEP			Standard Deviation		
		T+1	T+2	T+3	T+1	T+2	T+3
January	16.62	0.26	1.71	5.24	0.28	1.05	2.11
February	16.87	1.00	3.67	6.96	1.09	3.17	5.73
March	19.39	5.07	12.19	21.05	2.34	4.47	6.18
April	23.11	10.61	21.61	32.45	1.56	2.43	2.67
May	25.78	10.69	20.41	28.51	0.57	1.73	3.67
June	28.15	7.80	13.14	15.38	1.22	2.81	4.77
July	28.71	6.45	10.06	10.21	1.47	3.31	5.52
August	28.57	6.86	10.99	11.75	1.23	2.78	4.64
September	27.61	9.16	16.31	20.80	0.79	1.90	3.35
October	25.51	11.16	21.41	30.13	0.24	0.76	1.58
November	21.99	9.78	20.59	31.90	1.10	1.79	2.05
December	18.30	2.40	6.88	13.51	1.61	3.53	5.37

Table 4.10 Ten Years Averaged ΔEP_{T+1} , ΔEP_{T+2} , and ΔEP_{T+3} of *P. falciparum* and their Standard Deviations

The seasonal variation of the ten years average ΔEP_{T+1} , ΔEP_{T+2} , and ΔEP_{T+3} listed in Table 4.10 is shown in Figure 4.9. The increase in transmission of malaria peaked in the spring and autumn seasons. The EP of malaria peaked at about 32°C. Unlike dengue fever, the transmission rate decreased in summer when the weather was too hot. The ten year mean temperature between March and May was 22.8°C and between September and November was 25°C. Thus temperature rise resulted in an increase of malaria transmission in Hong Kong during the spring and autumn seasons.

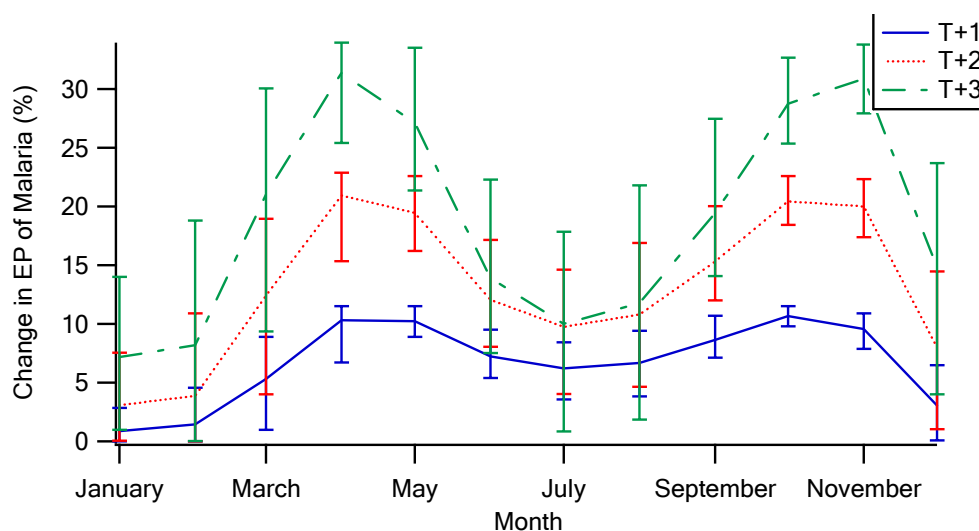


Figure 4.9 Monthly Average Percentage Change in Epidemic Potential of Malaria in 1994-2003. The error bars denote the maximum and minimum values.

The ten months average ΔEP of two species of malaria is summarized in Table 4.11. The ΔEP of malaria was estimated to be 6.7%, 13.0% and 18.7% for 1°C, 2°C and 3°C temperature rise in Hong Kong. The results showed that the risk of malaria would

increase due to global temperature rise. The impact was more significant than dengue fever.

Temperature increase	<i>P. vivax</i>	<i>P. falciparum</i>	Mean
1°C	6.63%(0.0047-10.62)	6.77%(0-11.52)	6.70% (0-11.52)
2°C	12.94%(0.27-21.13)	13.09%(0-22.90)	13.02% (0-22.90)
3°C	18.56%(0.85-31.39)	18.85%(0.004-33.96)	18.71%(0.004-33.96)

Table 4.11 Estimated Relative Percentage Change of the Epidemic Potential (ΔEP) of Malaria in Hong Kong, Compared to the Baseline (1994-2003 monthly mean temperature)

4.6 Present and Future Adaptation Measures in Hong Kong

Many government departments play different roles in mitigating the impact of climate change on public health.

Public health programs have been set up to monitor, quarantine, and treat the spread of infectious diseases and to respond to other health emergencies as they occur. Concerning preventive measures against dengue fever, HKSAR has initiated special anti-mosquitoes and cleansing operations. An innovative vector surveillance system has been in place since 2000. Ovitrap have been deployed in strategic locations throughout Hong Kong to monitor adult *Aedine* mosquitoes' population. Area and Monthly Ovitrap Indices are compiled and publicized. Prompt actions are taken by the management when the index is high. The Ovitrap Index can be classified into 4 levels. Specific preventive and control measures are initiated accordingly.

Figures 4.10 and 4.11 show that the Ovitrap index is highly correlated with the monthly mean temperature and monthly rainfall. In Hong Kong, mosquitoes are the most active in June.

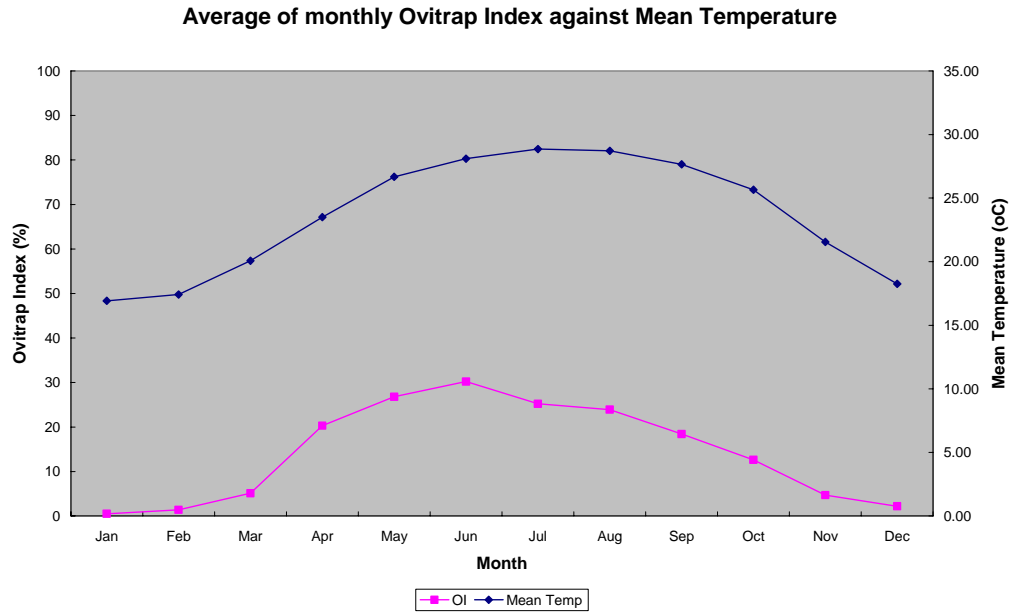


Figure 4.10 Average of Monthly Ovitrap Index (2000-2003) against Mean Temperature

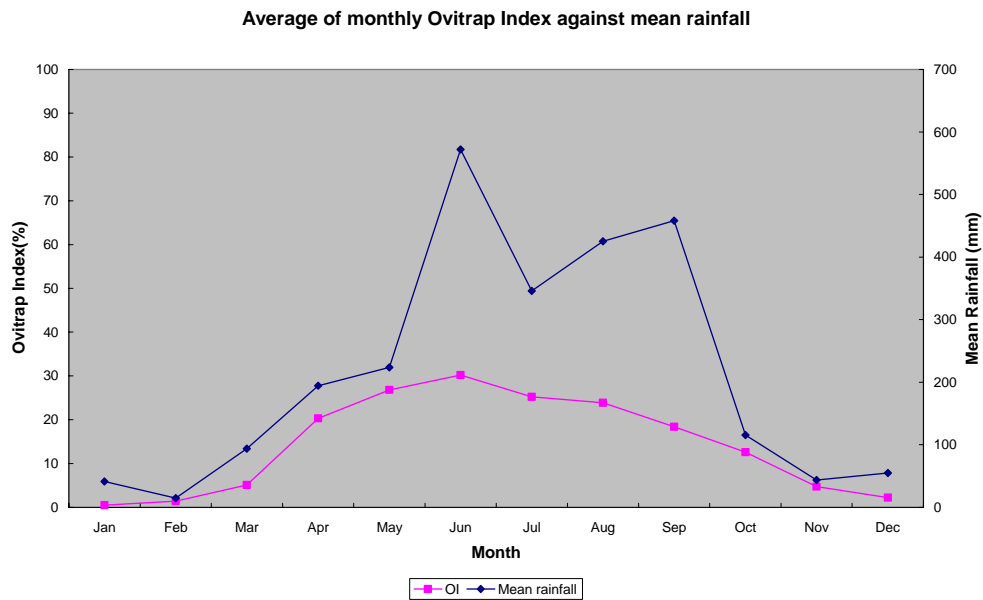


Figure 4.11 Average of Monthly Ovitrap Index (2000-2003) against Mean Rainfall

The Food and Environmental Hygiene Department, HKSAR, has been offering public education programs to the public on how to prevent the growth of mosquito larvae and adult mosquitoes and to protect themselves from adult mosquitoes. Officials and laborers have been employed to inspect stagnant water collections every week and to spray ponds and drainage with insecticide regularly.

The Department of Health is the enforcement body for preventing the transmission of communicable diseases (including air-borne, food-borne, vaccine-preventable, blood-borne and vector-borne diseases). To prevent the prevalence of these diseases and raise public awareness, many attractive advertisements have been broadcasted and posters have been posted to remind the public to eliminate mosquitoes. The Disease Prevention and Control Division under the Department of Health is in charge of public education concerning the prevention of infectious diseases. The division also inspects and manages suspected outbreaks of infectious disease. Although Hong Kong is located in a risk area of malaria, so far the number of infection has been low. According to the 2001/2002 statistics report of the Hospital Authority, there were only two death cases of malaria and 63 records of infection.

In conclusion, the impact on heat related diseases due to global warming is still unknown whereas the impact on dengue fever and malaria was successfully assessed. Both analyses indicated that the endemic potential of dengue fever and malaria would increase when the global temperature increases by 1°C to 3°C. HKSAR has a good public health system. Although Hong Kong is located in a risk area of dengue fever and malaria, human intervention has been keeping the infectious rate at a very low level.

In order to prevent the attack of these transmission diseases, a global climate change impact model should be established locally. Many databases that are needed for the impact model are available but many others are still outstanding. It is recommended that the HKSAR should streamline and centralize the important databases in Hong Kong. Many ad-hoc databases have been collected but they are not aligned to government objectives. The continuous development in GIS may help to improve this impact study. In the long term, having high quality databases is the key issue. The following Hong Kong databases are essential for future development:

- Geography
- Climate
- Health records
- Number of different infectious diseases notifications
- Resources and energy allocation
- Race and population distribution
- Cultural contexts of people related
- Practical behaviors of people related
- Economical situations of people related
- Living standards of people related
- Educational background of people related
- Knowledge levels of people related
- Hygiene practices of people related, and
- Sex and age of people related

The information and data can be collected via hospitals and public clinics.

4.7 References

1. Bryan J. H., Foley D.H., Sutherst R.W., Malaria transmission and climate change in Australia, *Medical Journal of Australia*, 164, 345-347, March 18, 1996.
2. Cox J., Mcmicheal A.J., Climate change and future populations at risk of malaria, *Global Environmental Change* 9, 89-107, 1999
3. Detinova T.S., Beklemishev W.N., Bertram D.S., Age-grouping Methods in Diptera of Medical Importance. WHO Monograph, 47, World Health Organisation, Geneva, 1962
4. Focks D.A., Daniels E., Haile D.G., Kessling J.E., A simulation model of the epidemiology of urban dengue fever: Literature analysis, Model Development, Preliminary Validation, and Samples of Simulation Results, *The American Society of Tropical Medicine and Hygiene* 53(5) 489-506, 1995.
5. Hajat S., Kovats R.S., Atkinson R.W., Hanes A., Impact of hot temperatures on death in London: a time series approach, *Journal of Epidemiology and Community Health* 56, 367-372, May 2002
6. Hales S., Potential effect of population and climate changes on global distribution of dengue fever: an empirical model, *The Lancet*, 360, 14 September, 2002.
7. IPCC, *Climate Change 2001: Impacts, Adaptation and Vulnerability*, 2001
8. MacDonald, G *The Epidemiology and control of malaria*. Oxford University Press, London, New York, 1957
9. Martens P., Kovats R.S., Nijhof S., Vries P.ed, Livermore M.T.J., Bradley D.J., Martens W.J.M., Global atmospheric change and human health: an integrated modeling approach, *Climate Research* 6, 107-112, 1996
10. Martens W.J.M, Jetten T.H., Focks D.A., Sensitivity of Malaria, Schistosomiasis and Dengue to Global warming, *Climatic Change* 35, 145-156, 1997
11. Patz J.A., Balbus J.M., Methods for assessing public health vulnerability to global climate change, *Climate Research* 6(2), 113-125, 1996
12. Rogers D.J., Randolph S.E., The global spread of Malaria in a Future, Warmer World, *Science* 289, 1763-1766 (in report) 8 September 2000
13. Rotmans J., Vries B. de, *Perspectives on global change: the TARGETS approach*, Cambridge University Press, Cambridge, 1997

Chapter5: Air Pollution

5.1 Introduction

The impact of global climate change on air quality is an unexplored topic. Pollution episodes in Hong Kong can be classified into three types: photochemical smog, aerosol smog and local urban air pollution. Photochemical smog is characterized by high ozone, poor visibility and characteristic meteorology. Aerosol smog is characterized by very poor visibility but not much ozone is detected. A massive amount of aerosol can be generated from either regional or long distance transportation. Local urban air pollution is often characterized by high level of NO_x or high level of PM₁₀. The visibility may not be too poor but the air pollution index is very high. This kind of air pollution is often observed in roadside stations. Under favorable meteorology, local urban air pollution can spread over a wide area of Hong Kong.

Publications were searched to find information on the relationship between global climate change and air pollution. The consultant was only able to find a few journal papers and conference proceedings that analyzed the correlation between the ambient temperature and surface ozone. Photochemical smog is an atmospheric chemistry phenomenon. It is the outcome of chemical reactions between OH⁻ radicals and ozone precursors under specific favorable meteorological conditions. There are reasons to believe that the occurrence of photochemical smog is related to the ambient temperature. Although the formation of aerosol smog also depends on specific meteorological conditions, it mainly depends on emission sources and their locations. The local urban air pollution mainly comes from vehicles. Their emission should have little relationship with the ambient temperature. The project team focused on the correlation between the surface ozone and temperature in Hong Kong and commented on the possible impacts due to climate changes.

A study on the relationship between diseases and air pollution was conducted by the Hong Kong University. It concluded that NO₂, SO₂, RSP (Respiratory suspended particulates), O₃ and FSP (Fine suspended particulates) would cause deaths with or without adjustment of co-pollutant. The effect of air pollutant on death was higher in the cool season than in the warm ones (Short-term Effects of Ambient Air Pollution on Public Health - An APHEA 2 Study).

5.2 Ozone Study

5.2.1 Exceedance of Surface Ozone in Hong Kong

Ozone is one of the core indicators quantifying the intensity of photochemical smog. According to the Hong Kong Air Quality Objectives, the hourly ozone standard was

set at $240\mu\text{g}/\text{m}^3$ (about 122 ppb). In Hong Kong, ozone exceedance has been recorded few times a year in many stations. It is defined as:

$$\text{percentage of exceedance} = \frac{\text{number of hours that exceed AQO O}_3 \text{ standard}}{\text{total number of hours}} * 100\%$$

Figure 5.1 shows the percentage of ozone exceedance in ten air monitoring stations for all collected valid data. The number of counts in Tung Chung, Tap Mun and Shatin is shown in Table 5.1. Ozone exceedance was the highest in the Tung Chung station. Thus the ozone data of Tung Chung station was selected to carry out further analysis.

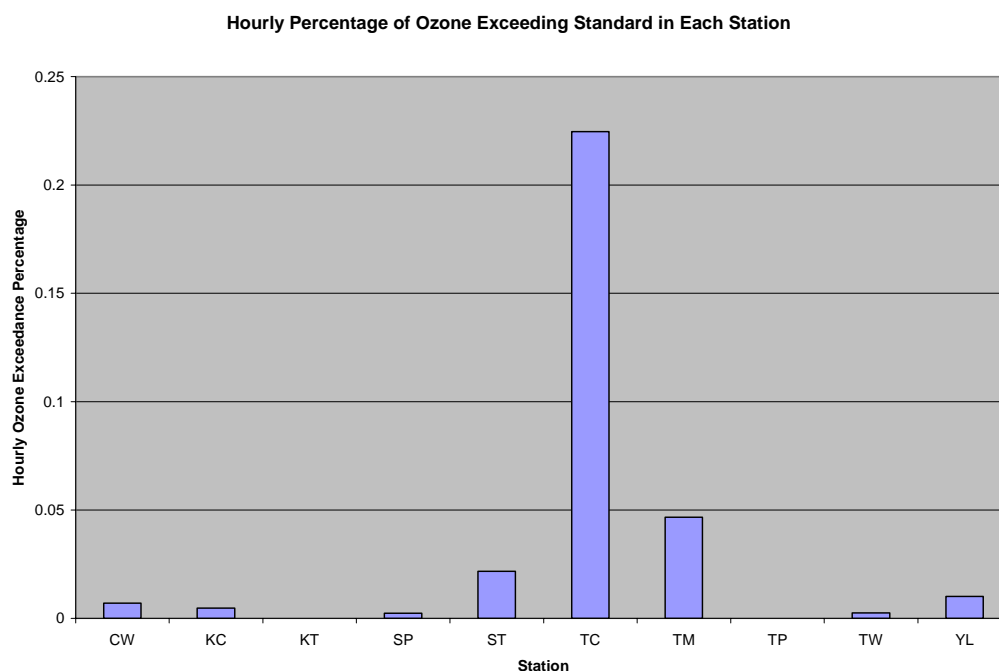


Figure 5.1 Percentage of O₃ Exceedance in EPD Air Monitoring Stations (CW states for Central/Western, KC states for Kwai Chung, KT states for Kwun Tong, SP states for Sham Shui Po, ST states for Sha Tin, TC states for Tung Chung, TM states for Tap Mum, TP states for Tai Po, TW states for Tsuen Wan, YL states for Yuen Long).

Station	Number of hourly counts exceed standard	Total hourly counts	Percentage of counting exceed $240\mu\text{g}/\text{m}^3$ O ₃
Tung Chung	71	31816	0.22%
Tap Mum	19	38575	0.049%
Sha Tin	11	46057	0.024%

Table 5.1 Hourly Percentage of Ozone Exceed Standard ($240\mu\text{g}/\text{m}^3$) in the First Three Stations

In the Tung Chung Station, out of 31,816 hours, there were a total of 71 hours when ozone exceeded $240\mu\text{g}/\text{m}^3$. The percentage of ozone exceedance was four times of

that in Tap Mum and more than ten times of that in the other stations. This was likely related to the locations of the major air pollution sources and the local meteorology. It is believed that under the conditions of land and sea breeze conditions, air dispersion in Tung Chung is much restricted. The monitoring program in Tung Chung started in April of 1999. The duration of the data set was about 3.5 years (April 1999 to December 2002).

5.2.2 Results

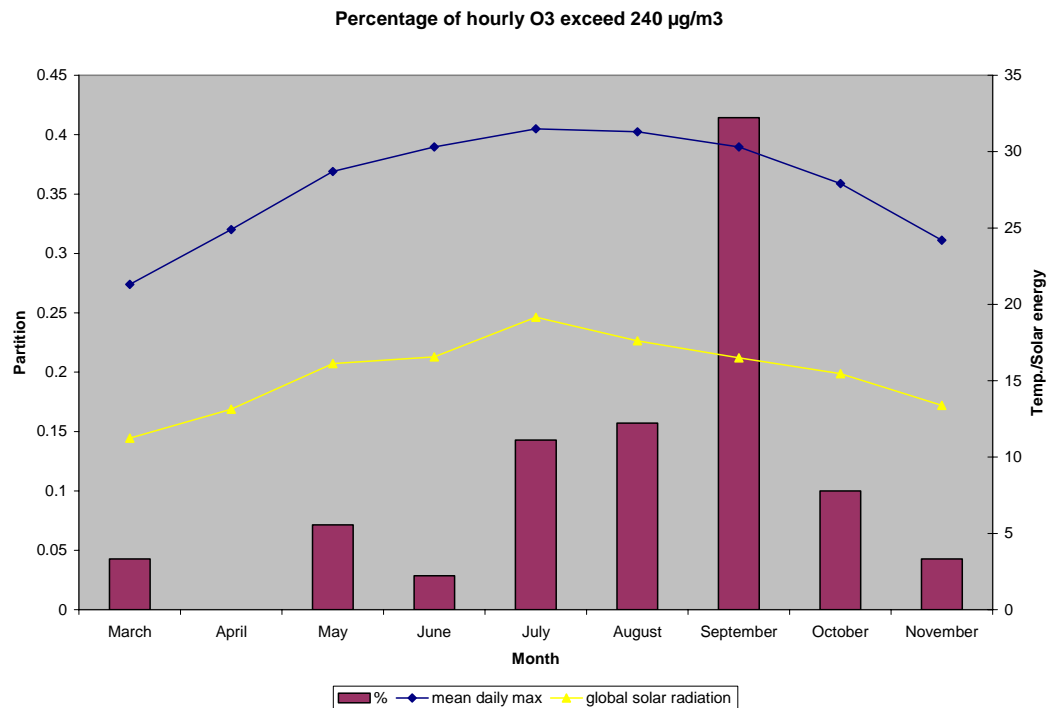


Figure 5.2 Seasonal Trends of O₃ exceedance, Ambient Temperature and Global Solar Radiation in the Tung Chung Station.

Figure 5.2 shows that O₃ exceedance was more frequent between July and October. The peak was in September. It appears that O₃ exceedance in Tung Chung exhibited correlations with temperature and solar radiation.

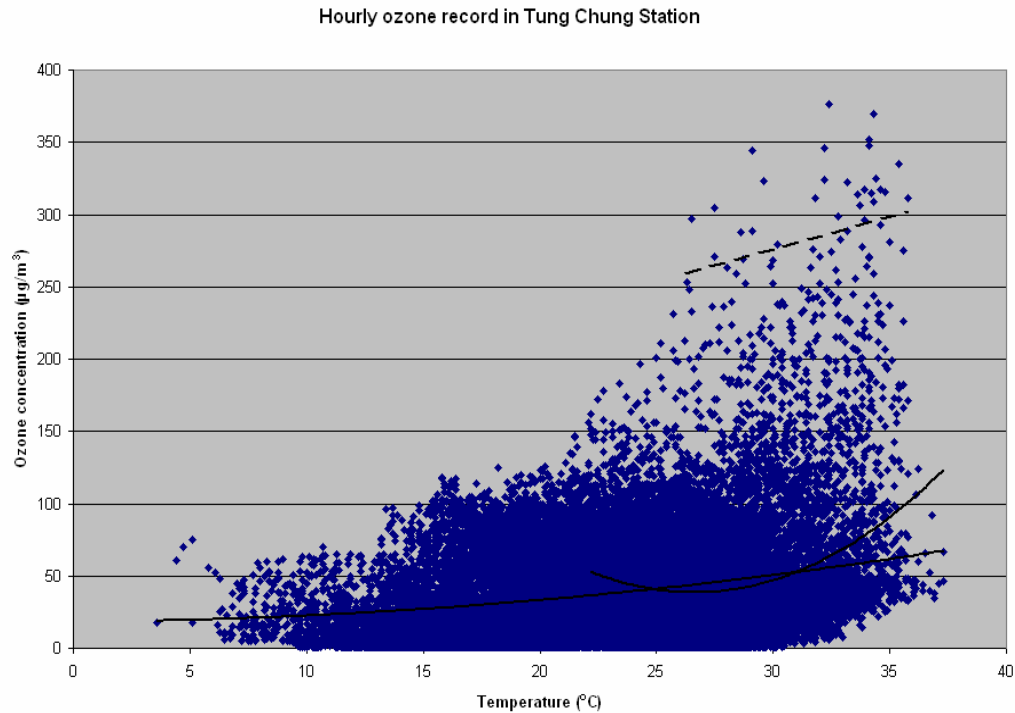


Figure 5.3 Hourly Ozone Concentration Against Ambient Temperature in the Tung Chung Station

The hourly average temperature was plotted against the hourly average ozone concentration in Tung Chung. Figure 5.3 shows that on the low temperature side, when the temperature was below 15°C, ozone concentration never exceeded 100 $\mu\text{g}/\text{m}^3$. Ozone levels higher than 150 $\mu\text{g}/\text{m}^3$ only occurred when the temperature exceeded 22°C. On the side with high temperature and high ozone level, when temperature exceeded 30°C, very high ozone level was detected. At this high end quadrant, the daily peak ozone concentration has a tendency to increase with temperature. This ozone-temperature correlation was more obvious on exceedance days. Wackter & Bayly, 1988 reported a linear relationship between ozone and temperature. IPCC also pointed out that the ozone level is highly associated with temperature when the temperature is greater than 32°C.

Regression was carried out 3 times. In the first time, the entire data set was studied. In the second time, the analysis was repeated using only those records with ozone that exceeded 240 $\mu\text{g}/\text{m}^3$. The third analysis was repeated using only those records with temperature that exceeded 32°C. The regression parameters included: ozone, temperature, wind speed and solar radiation. The statistical results of the three linear regressions are listed in Tables 5.2-5.7.

	Temperature	Wind Speed	Solar Radiation	All three parameters
R value of ozone regression	0.242 (a)	---	---	---
	---	0.437 (a)	---	---
	---	---	0.333 (a)	---
	---	---	---	0.510 (a)

Table 5.2 Correlation Coefficients of the Entire Data Set in the Tung Chung Station
a: statistically significant (significance of t value < 0.05)

Linear regression equations	Associated parameters
$O_3 = 2.411 (95\%CI\ 0.555\ to\ 4.268) + 1.584 (95\%CI\ 1.509\ to\ 1.659) * (Temp)$	$O_3, Temp$
$O_3 = 16.197 (95\%CI\ 15.488\ to\ 16.906) + 1.263 (95\%CI\ 1.232\ to\ 1.294) * (WS)$	O_3, WS
$O_3 = 32.930 (95\%CI\ 32.448\ to\ 33.412) + 0.512 (95\%CI\ 0.495\ to\ 0.529) * (SR)$	O_3, SR
$O_3 = -4.039 (95\%CI\ -5.793\ to\ -2.285) + 0.786 (95\%CI\ 0.714\ to\ 0.858) * (temp) + 1.087 (95\%CI\ 1.057\ to\ 1.117) * (WS) + 0.309 (95\%CI\ 0.292\ to\ 0.327) * (SR)$	$O_3, Temp, WS, SR$

Table 5.3 Linear Equations of Ozone Generated from the Entire Data Set in the Tung Chung Station

	Temperature	Wind Speed	Solar Radiation	All three parameters
R value of ozone regression	0.318 (a)	---	---	---
	---	0.064 (b)	---	---
	---	---	0.178 (b)	---
	---	---	---	0.341 (a)

Table 5.4 Correlation Coefficients when $O_3 > 240\mu g/m^3$ in the Tung Chung Station
a: statistically significant (significance of t value < 0.05)
b: statistically insignificant (significance of t value > 0.05)

Linear regression equations	Associated parameters
$O_3 = 137.339 (95\%CI\ 28.759\ to\ 245.919) + 4.613 (95\%CI\ 1.23\ to\ 7.995) * (Temp)$	$O_3, Temp$
$O_3 = 276.878 (95\%CI\ 244.678\ to\ 309.079) + 0.378 (95\%CI\ -1.068\ to\ 1.824) * (WS)$	O_3, WS
$O_3 = 271.297 (95\%CI\ 250.823\ to\ 291.771) + 0.276 (95\%CI\ -0.099\ to\ 0.651) * (SR)$	O_3, SR
$O_3 = 52.89 (95\%CI\ 39.57\ to\ 266.209) + 4.213 (95\%CI\ 0.626\ to\ 7.799) * (temp) - 0.787 (95\%CI\ -2.787\ to\ 1.213) * (WS) + 0.285 (95\%CI\ -0.255\ to\ 0.825) * (SR)$	$O_3, Temp, WS, SR$

Table 5.5 Linear Equations of Ozone when $O_3 > 240\mu g/m^3$ in the Tung Chung Station

	Temperature	Wind Speed	Solar Radiation	All three parameters
R value of ozone regression	0.166 (a)	---	---	---
	---	0.065 (a)	---	---
	---	---	0.139 (a)	---
	---	---	---	0.285 (a)

Table 5.6 Correlation Coefficients when the Temperature is Greater than 32°C
a: statistically significant (significance of t value < 0.05)

Linear regression equations	Associated parameters
$O_3 = -265.268 (95\%CI -373.334 \text{ to } -157.202) + 10.208 (95\%CI 6.962 \text{ to } 13.454) * (\text{Temp})$	O ₃ , Temp
$O_3 = 61.288 (95\%CI 49.966 \text{ to } 72.610) + 0.637 (95\%CI 0.113 \text{ to } 1.161) * (\text{WS})$	O ₃ , WS
$O_3 = 95.232 (95\%CI 86.629 \text{ to } 103.836) + -0.335 (95\%CI -0.463 \text{ to } -0.207) * (\text{SR})$	O ₃ , SR
$O_3 = -394.989 (95\%CI -504.485 \text{ to } -285.493) + 14.233 (95\%CI 10.951 \text{ to } 17.516) * (\text{temp}) + 1.495 (95\%CI 0.962 \text{ to } 2.028) * (\text{WS}) - 0.566 (95\%CI -0.7 \text{ to } -0.432) * (\text{SR})$	O ₃ , Temp, WS, SR

Table 5.7 Linear Equations of Ozone when the Temperature is Greater than 32°C in the Tung Chung Station

The results in Tables 5.2 and 5.3 imply that O₃ had correlation with temperature, wind speed and solar radiation. When all the data were included, wind speed had the highest correlation coefficient, while the correlation coefficient of solar radiation was lower and that of temperature was the lowest, but all 3 coefficients were statistically significant at 95% confidence. However, when O₃ exceeded 240µg/m³ (interpreted as ozone episode days), Table 5.4 shows that the temperature was highly correlated with O₃, while solar radiation and wind speed had no correlation with O₃. When only hot days were considered, Table 5.6 shows that all correlations coefficients decreased. Yet it remained that the temperature had the highest R, solar radiation had lower R and wind speed had no correlation. High ozone was attributed to high temperature and high solar radiation.

5.3 Impacts and Possible Adaptations

Photochemical smog is a highly undesirable by-product of human civilization. It has adverse effect on human health and results in poor visibility. It also causes damages to vegetations. Under ozone episode days, regression analysis yields the equation:

$$O_3 = 137.339 + 4.613 * (\text{Temp})$$

When the ambient temperature increases by 1°C, the ozone concentration will increase by about 4.6µg/m³ which is just 2% of the ozone standard of 240µg/m³. Thus the amount of ozone augmented during episode days due to climate change is insignificant. The more important point is whether the frequency of episode days is

increased due to climate change. Since temperature is correlated with ozone concentration in photochemical smog, it is likely that photochemical smog would occur more frequently in the future when temperature rises.

Global climate change may alter the ambient temperature, relative humidity, cloud amount, solar radiation and sea level. Higher temperature will result in more energy usage. More ozone precursors will be then emitted into the atmosphere. This has a direct impact on the primary air pollutants. On the other hand, higher temperature may increase heavy precipitation events and lower global solar radiation. These parameters will discourage the formation of photochemical smog. Exactly how global climate change affects air pollution in Hong Kong is still largely unknown.

The HKSAR has put in efforts in controlling air pollution in Hong Kong. As the manufacturing industry in Hong Kong has been phasing out, the Environmental Protection Department concentrates on vehicle emissions control. The government policies encourage the development of mass transit transportation in Hong Kong. Top priority has been given to the use of electric trains and public buses. For motor vehicle control, all private motor vehicles must be installed with catalytic converter and satisfy stringent emission standard before they can be imported. Ultra low sulfur diesel has been used in public buses since 1996. An emission standard of diesel vehicles has been introduced, ranging from Euro I in 1992 to Euro IV in 2003. Taxis have been fully switched to LPG fuel in 2004 and similar conversion is being implemented in public light buses. The government has also introduced an incentive scheme to encourage the use of electric motor vehicles. Unfortunately, it is not quite successful. Research has been actively carried out on alternative fuels for vehicles, such as natural gas. These programs will reduce significantly the emission of air pollutants by the end of 2005. Despite the presence of global climate change, Hong Kong has adapted to such change by introducing measures to mitigate air pollution.

5.4 References

1. Wackter, D.J. & Bayly P.V., The Effectiveness of emission controls on reducing ozone levels in Connecticut from 1976 through 1987, *The scientific and Tech. Issue Facing post-1987 ozone control strategies*, 398-415. 1988
2. Short-term Effects of Ambient Air Pollution on Public Health - An APHEA 2 Study, May 1999 by HKU, EPD Air Study Report (http://www.epd.gov.hk/epd/english/environmentinhk/air/studyreports/effect_ambient_ap.html)

Chapter 6. Tourism Industry

6.1 Introduction (eco-tour)

Tourism is an important economic source of income in Hong Kong. A total of 16,566,382 tourists visited Hong Kong in year 2002. The total tourism expenditure associated with inbound tourism amounted to HK\$77,410 million in 2002. The GDP at factor cost in 2002 was HK\$1205.9 billion. Tourism contributed to about 6.4% of the local economy.

This chapter only focuses on eco-tourism rather than the whole industry including hotel renting, retail industry and air-line flights. In a survey conducted by the Hong Kong Tourism Board (HKTB) in 2000, 24% of the visitors were interested in eco-tourism and 15% were interested in “hiking in the countryside” (Table 6.1). In 2001, the Government announced a HK\$18 billion plan to boost tourism in which specific emphasis was put on ecological and cultural tourism. Eco-tourism would be expanded to include hiking, cycling, migratory birds watching, dolphins watching, coastal and freshwater-related tourism, nature experience and education experience, such as museum and natural reserve visits.

Special Interest Activities	% of visitors
Gourmet Dining	43
Heritage	27
Traditional Chinese Festivals	26
Green Tourism/Eco-tourism	24
Art/ Cultural Exhibits	22
Major Sport competition	19
Art Festival	19
Content (International)	16
Broadway Music	15
Hiking in countryside	15
House Racing	13
Aquatic Activities	12
Arts & Crafts Demonstration	12
Film / TV Studio Visit	12
Performing Arts – Chinese (excl. Broadway Musicals & Concerts)	11

Table 6.1 Special Interest Activities of Visitors in Hong Kong in 2001
(source: Hong Kong Tourism Board)

One of the major eco-tourism facilities is the Hong Kong Wetland Park adjacent to Mai Po and the Inner Deep Bay RAMSAR site, set to open in late 2005. The Wetland development (0.65 km²) will host migratory birds and waterfowls. It is forecasted to attract 500,000 students and visitors every year. This not only helps meet the growing demand on eco-tourism, but also alleviates human interference to the neighboring Mai Po reserve that has an annual visiting quota of only 50,000.

Other important eco-tourism sites are located on the eastern side of Hong Kong, such as Sai Kung in New Territories. Sai Kung is the "Leisure Garden of Hong Kong". It has long been one of the most beautiful tourist sites in Hong Kong. It has a total area of 126 km². Sai Kung is famous for its natural mountains and ocean views and it has many small islands. Trails have been maintained along the country parks and High Island Reservoirs for hiking and sightseeing. The eastern water is open to the South China Sea and is less polluted. The clear water and a serenity environment nurture the growth of many marine species such as coral reefs and fishes. Popular underwater tourist spots include Hoi Ha Wan, Tung Ping Chau and Double Haven.

Climate changes may have direct and indirect impacts on eco-tourism. In the following sections, the impacts on different types of eco-tourism in Hong Kong will be discussed.

6.2 Impacts on Migratory Birds Watching

Although it is still uncertain, there is a potential loss in coastal wetlands. Under such a scenario, migratory birds may fly to other wetlands. It is possible to quantify indirectly the social economic impact due to global climate change on Hong Kong's bird watching tourism. At present, the HKTB organizes bird-watching tour for eco-visitors. The visitors travel to the fish ponds and ancient shrimp ponds near the Mai Po wetland site and watch birds through the border fence. The tour price is HK\$360 per person. According to the statistics from the HKTB, about 24% of tourists were interested in eco-activities. Based on the figure of 16,566,382 visitors in 2002, about 4 million tourists were interested in joining local eco-tours while visiting Hong Kong. Assuming 5% of all eco-interested tourists would join bird-watching tour, the related eco-tourism income is estimated to be about HK\$72 million per year. If 50% of all eco-interested tourists would join bird-watching tour, the related eco-tourism income is estimated to be about HK\$720 million per year. In reality, the economic loss due to climate change will not be the total amount of potential income but it is impossible to estimate the percentage of loss.

6.3 Impacts on Dolphin Watching

Hong Kong Dolphinwatch Limited estimated that over 570 dolphin watching trips involving approximately 20,000 people were run during 1995-1999. Assuming the charging rate of each activity is HK\$250 per head, this eco-tourism income would be estimated at about HK\$1 million per year (Hong Kong Dolphinwatch Limited), without taking into account other social and environmental impacts. Under the worse scenario, most Chinese Dolphin emigrated and local dolphin-watch tourism might eventually terminate.

6.4 Impacts on Mountain Related Tourism

Based upon the observation by the U.S. Environmental Protection Agency, trees of the same species will shift northward by about 300 Km in 100 years to adapt to 2°C rise in temperature. Unfortunately, this scenario will not occur in Hong Kong. Since Hong Kong is located in a sub-tropical region, mountains and hills are covered by mixed species of trees. It is difficult for different species to shift at the same time. Rise in temperature of 1°C in Hong Kong may result in two scenarios : 1.) increase in species and quantity of trees due to warmer weather, and 2.) reduction in species due to an increase in population of some species that can adapt to the temperature rise and occupy the space of those less adaptive. The former case will enhance the value of country parks and the latter will have negative effect on it. Therefore, it is difficult to conclude the impact on mountain related tourism due to climate change.

The HKTB organizes hiking tours in Hong Kong. Adopting the same approach in section 6.2, about 4 million tourists were interested in joining local eco-tours while visiting Hong Kong. The tour price was HK\$ 595 per person. Assuming 5% of all eco-interested tourists would join hiking tour, the eco-tourism income was estimated to be about HK\$118 million per year. Assuming 50% of all eco-interested tourists would join hiking tour, the eco-tourism income was estimated to be about HK\$1.2 billion per year. In reality, the economic loss due to climate change will not be the total amount of potential income but it is impossible to estimate the percentage of loss.

Apart from serving foreign visitors, country parks also provide entertainment to local residents. According to the AFCD statistics, about 11 million local people visited country parks in 2002 (AFCD annual report, 2001-2002). Assume each person would spend HK\$30 on average on preparing food and drinks in one day, this would generate about HK\$330 million income to the retail industry annually.

6.5 Modeling of Economic Loss of Tourism

Exactly how global climate change affects Hong Kong's tourism is largely unknown. The literature search of the consultant only came up with one comprehensive study that was conducted by economist. In the US, the linear demand model and loglinear demand model were used to estimate the economic impact on outdoor recreation due to climate changes. Mendelsohn & Neumann developed an empirical formula to estimate the economic impact on tourism in the US due to climate change. The formula of the US's tourism is:

$$R_{t,k} = \exp \left[\left\{ \frac{\text{POP}_k(t)}{\text{POP}_k(t_0)} \right\} \left\{ a_k + 0.31 T_k - 0.0101 T_k^2 \right\} \right]$$

where

$R_{t,k}$	= the values (\$) of tourism in country k,
$\text{POP}_k(t)$	= population in country k,
a_k	= empirical constant (depends on country),
T_k	= annual temperature (°C).

The coefficients of 0.31 and 0.0101 in the above mathematical approach were established through factor analysis. The above models are empirical and very complicated. They require the use of GDP values for local visitor and oversea travelers, local population, price of hotel and travel activity, weather, pollutions, climate variables and areas of activities (such as wetlands, mangroves and forest).

Modeling results indicated that Fishing and Boating were anticipated to experience positive impact under the scenarios of rising temperature and rainfall. In U.S., the benefit was about US\$22.2billion and US\$13.1billion respectively. Camping was, however, anticipated to experience negative impact with an economic loss of US\$1.7billion. The overall economic impact was positive due to climate changes in the US (Mendelsohn & Neumann, 1999).

The empirical constants used in the models are based on the US statistics. The above empirical constants are probably not the same in Hong Kong. The consultants of this project are unable to apply these models to Hong Kong because not all input parameters are available. If we want to do the same thing for Hong Kong, it is necessary to build up a similar database first. The database that generated the two constants should be set up by gathering tourist information using questionnaires. The information collected should include: sex and age of visitors; salary ranges, country of origin; purposes of visiting (sight-seeing, shopping, visiting relatives, and eco-tour); season of traveling (spring, summer, autumn, or winter); eco-tour (for migratory birds watching, pink dolphins watching, butterfly watching, marine parks, country parks, etc), and facilities (adequate transportation and accommodation services). An integrated data collection system should be established to collect the multidisciplinary information (i.e. GDP) in Hong Kong.

6.6 References

1. A statistical Review of Hong Kong Tourism 2001, Hong Kong Tourism Board.
2. Department Annual Report 2001-2002, AFCD , Agriculture, Fisheries and Conservation Department
3. Green Tour of Hong Kong Tourism Board
<http://www.discoverhongkong.com/eng/touring/city/index.jhtml>
4. Hong Kong Dolphinwatch Limited
<http://www.hkdolphinwatch.com/>
5. Mendelsohn R. & Neumann J.E., The Impact of Climate Change on the United States Economy, Cambridge University Press, 265-314,, 1999

Chapter7. Agricultures and Water Resources

7.1 Agricultures

Hong Kong consists largely of steep, unproductive hillsides. Under the threat of human encroachment, cultivated land area has dwindled by about 43% over the past decade. At present, 24 km² of land area are being cultivated engaging 5800 farmers and workers which represent 0.17% of the total workforce. At the end of 2003, the land used for vegetables, flowers, field crops, and orchards was 350 ha, 240 ha, 40 ha and 450 ha respectively. Local consumers are provided with high quality fresh food through intensive land use and production methods. Market gardening crop is currently one of the most important users of agricultural land. Local production of agricultural food in 2002 is listed in Table 7.1. In 2003, the gross value of agricultural production was HK\$ 1,052 million. Local production accounted for 5 percent of fresh vegetables, 23 percent of live poultry and 32 percent of live pigs of the local consumption.

Local agricultural production	Gross value (million)
Crop production*	272
Livestock	529
Poultry	251

* Crop production includes leafy vegetables, high-value cut flowers and fruits

Table 7.1 Production of Local Agricultural Food

The service sector is a major constituent of Hong Kong's economy, about 86.5%. Agricultural and fishing industries in Hong Kong are phasing out, and in 2001 they contributed only 0.1% of the total GDP in Hong Kong (Table 7.2). Thus it is considered that the direct impact of global climate change on Hong Kong's agricultural industry is minimal. Under the sores scenario where climate change destroys all agriculture the maximum loss is only 0.1% of Hong Kong's economy. Nevertheless, we should not ignore the indirect impact, given that most of the agricultural food is imported from Mainland China.

Between 1992 and 1994 there was about 10% of land area in the mainland China being dedicated as crop lands (95,145 x 10³ ha), in which the northern parts of China contained two-thirds of the country's cropland (IPCC 2001). Zhai et al., 1999 reported that while western northwest China was having positive trends in rainfall, northeastern China, southeastern China and northern China were all showing negative trends over the past decades. Water resources and subsequent food production yields in the North China region, would be hard hit by climate change. It will experience more droughts and receive less precipitation in this century. This will lead to a significant secondary impact on Hong Kong's food supply.

	1997	2000	2001*
Percentage contribution of economic activities to GDP at current factor cost (%)			
Agriculture and fishing	0.1	0.1	0.1
Mining and quarrying	---	---	---
Manufacturing	6.4	5.8	5.2
Electricity, gas and water	2.6	3.2	3.3
Construction	5.7	5.2	4.8
Services	85.1	85.7	86.5
Wholesale, retail and import/export trades, restaurants and hotels	25.7	26.4	26.7
Transport, storage and communications	9.1	10.2	10.2
Financing, insurance, real estate and business services	26.5	23.7	22.6
Community, social and personal services	17.4	20.5	21.8
Ownership of premises	13.5	12.6	13.1
<i>Less: Adjustment for financial intermediation services indirectly measured</i>	<i>7.1</i>	<i>7.8</i>	<i>7.9</i>
Total	100.0	100.0	100.0
GDP at factor cost (HK\$ billion)	1,267.5	1,228.9	1,216.4

Table 7.2 GDP by Economic Activity at Current Prices (Hong Kong Yearbook, 2002)

7.2 Water Resources

Water resources problems concern about fresh water supply, its distribution and its demand. It involves the water cycle - precipitation, flood, catchments, drought, soil moisture and evaporation. Water demand is of great concern in the world. Factors which have effect on water resources are population growth, urbanization, flooding, farming, storage and global warming.

In Hong Kong, the average annual rainfall is about 2,214 millimeters. This amount was insufficient to meet annual demand of 946 million cubic meters (mcm) in 2002. 80% of water supply in Hong Kong comes from Guangdong and the rest is supplied by local reservoirs. There are 17 local reservoirs with a total storage capacity of 586 million cubic meters. The capacity of Hong Kong reservoirs is listed in Table 7.3.

Reservoir	Storage *	Reservoir	Storage *
Pok Fu Lam	231,000	Aberdeen (2 reservoirs)	1,259,000
Tai Tam	1,490,000	Kowloon Byewash	800,000
Tai Tam Byewash	80,000	Shing Mun (Jubilee)	13,279,000
Tai Tam Intermediate	686,000	Tai Lam Chung	20,490,000
Kowloon	1,578,000	Shek Pik	24,461,000
Tai Tam Tuk	6,047,000	Lower Shing Mun	4,299,000
Shek Lei Pui	374,000	Plover Cove	229,729,000
Reception	121,000	High Island	281,124,000

* Storage in cubic meters

Table 7.3 Capacity of Hong Kong reservoirs (Water Supplies Department, HKSAR)

The population in Hong Kong is about 6.9 million. The average daily consumption of fresh water and sea water in 2001 were 2.57 mcm and 0.65 mcm respectively (Figure 7.1). To secure a stable long term supply of fresh water, the HKSAR has made agreements with Guangdong province since early 1960. The fresh water supply from Dongjiang has increased from 23 mcm per year in the 1960s to 790 mcm per year in 2001. It will further increase annually by 10 million cubic meters to 820 mcm in 2004. Ultimately a maximum of 1100 mcm/yr Dongjiang water can be delivered to the HKSAR. The current price of purchasing Dongjiang water is HK\$3.085/m³.

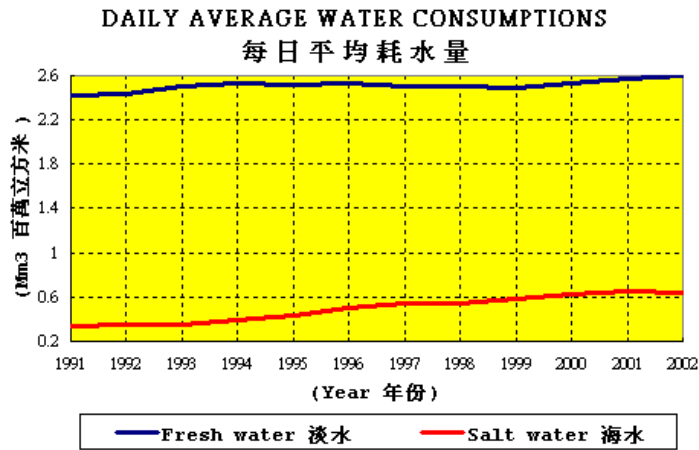


Figure 7.1 Daily Average Water Consumption

Factors controlling water demand are population growth, economic situation and the improvement on the standard of living. The population in Hong Kong will be continuing to increase as a result of the immigration policy. The industrial water consumption may decrease due to the emigration of local industries to the PRD region. In the coming century, it is predicted that the water demand for domestic use may continue to rise. Figure 7.2 shows that the annual fresh water demand is forecasted to increase to 1050 mcm by year 2020. This demand could be met by both local resource of 295 mcm/yr and imported water of 1100 mcm/yr (ACQWS Paper No. 12).

In the US, one national model was adopted to estimate the impact on water resources. The model assumes that the water institution will respond to change in economic conditions which will transmit these economic signals to water users. This model anticipates positive impact on water resources when temperature has risen by 1.5°C while the impact would be negative when there is 5°C temperature rise. (Mendelsohn and Neumann, 1999)

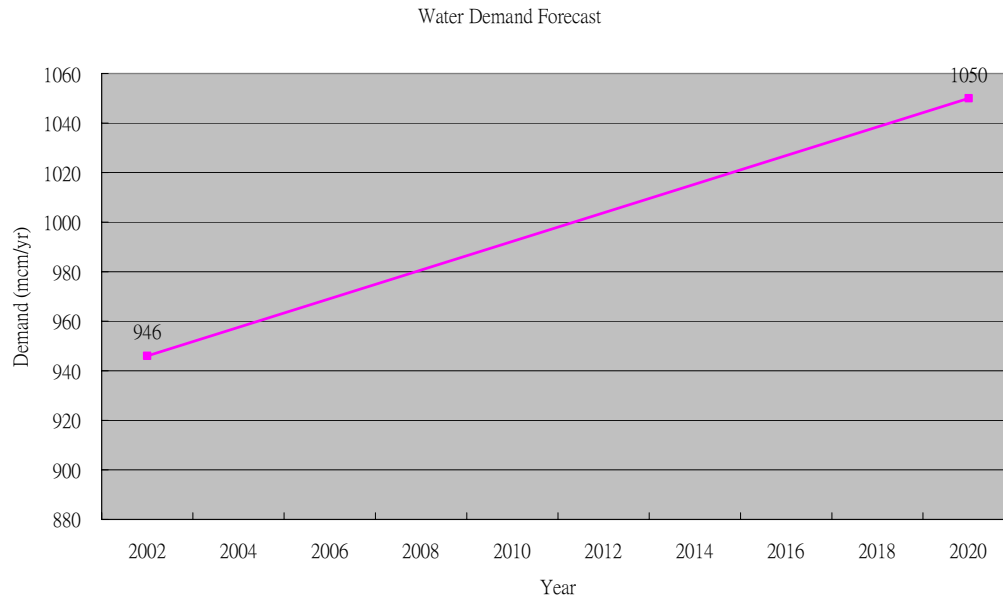


Figure 7.2 HKSAR's Fresh Water Demand in the Future

The other major impact of climate change on Hong Kong's water resources is on fresh water collection. Owing to urbanization, catchment area would be diminished. There will be less ground water resources due to run-off. Hotter climate may induce more water consumption, thus domestic demand may increase.

Another impact is on income which is generated from eco-tourism. Water is essential to the ecosystem. When water supply to the wetlands is reduced, many natural habitats will shrink. Wild life, especially migrant birds, may migrate to other locations.

To mitigate the problems of water shortage in Hong Kong, the HKSAR has studied three potential new fresh water resources together with the rearrangement of water supply with the Guangdong Authority. The studies include the feasibility of wastewater recycling; expansion of water gathering ground to all country parks and other undeveloped areas, and desalination plant for seawater, which had once been commissioned in 1976, but mothballed 1-2 year after because of high cost and strong public opposition. The unit cost of collecting surface water from new water gathering grounds, desalination, recycling effluent and importing more Dongjiang water from Guangdong are HK\$9.1/m³, HK\$7.7/m³, HK\$5.3/m³ and 4.5/m³ respectively. (ACQWS Paper No.12). It came to a conclusion that the most effective and economic approach for preventing water resources shortage is by purchasing and treating Dongjiang water to portable standard. Nevertheless, reliance on Dongjiang water is not without worries. Under global warming, there is also a potential water shortage problem in Guangdong where demand is outstripping supply due to the affluence of the society, influx of transient labors and booming industries.

Apart from taking measures on the supply side, the HKSAR has also controlled the demand side. Hong Kong has stringent water pollution control measures in place.

High drinking water quality is assured by an agreement reached with the Guangdong authority which requires the conformation of Dongjiang water to Environmental Quality Standard of Surface Water. The potable water quality in Hong Kong complies with the standard of the World Health Organization (WHO, 1993) and is suitable for consumption without further treatment. In this context, further efforts have been stepped up, including the commissioning of biological nitrification plant and desilting (removal of sediment) of the Shenzhen reservoir, and water pollution control at the upstream of Dongjiang river. Further improvement in water quality is achieved, upon the completion of closed aqueduct construction between Dongjiang and Shenzhen in 2003. Therefore, it is anticipated that Hong Kong should be able to cope with the challenge imposed by climate change.

7.3 Flooding

Flooding depends on the frequency and intensity of rainfall. It also depends on the storm drain capacity and their maintenance. Most of the rainfall in Hong Kong is brought by the low pressure troughs (most intense in May), thunderstorms (associated with summer monsoon) and tropical cyclones. Hong Kong is on the common track of tropical cyclones. Every year, it is expected that two to three tropical cyclones will come close or pass through Hong Kong. During these rainstorms, the rural low-lying areas and natural flood-plains in the northern part of the territory and some locations in the older urban areas suffer serious flooding. The main affected areas include Yuen Long, Kam Tin, San Tin, Ho Sheung Heung (rural areas), Mong Kok, Yau Ma Tei, Sham Shui Po and Tsim Sha Tsui (urban areas).

Changing the land use pattern, especially the conversion of agricultural land to fish ponds and for urban development has resulted in a significant loss of flood storage plain and increasing runoff over the past 40 years. Most of the rain falls on the New Territories of Hong Kong. According to HKO's record, 62% of the total annual rainfall (3091mm) in June 2001 was fallen on the northern New Territories. Climate change may increase the rainfall amount and exacerbate the flooding problems.

Hong Kong does not have official record on the actual number of flooding each year. The number of flooding can be inferred by the number of heavy rain each year. Figure 7.3 shows the number of rainstorm warnings between 1995 and 2003. Year 2001 was a very wet year.

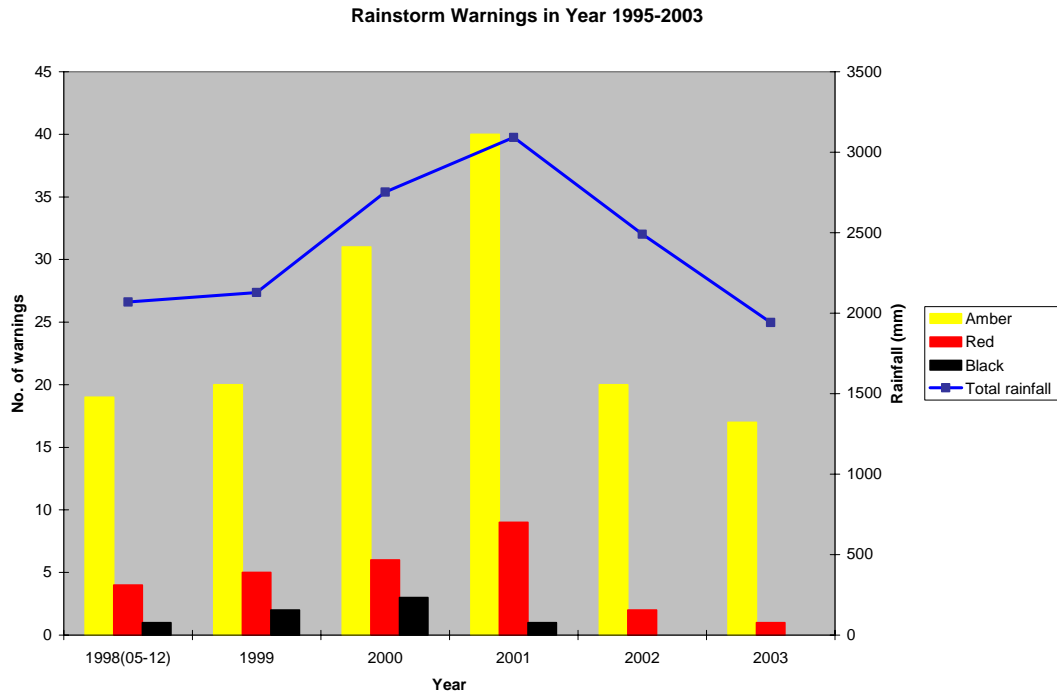


Figure 7.3 The Number of Rainstorm Warning in Hong Kong Between 1995 and 2003

The number of flooding can also be inferred by the number of flooding announcements in each year. However, the number of flooding announcements is not the actual number of flooding because there could be many flooding sites at the same time or at different hours of the same day. Figure 7.4 shows the number of flooding announcement in the northern territories between 1995 and 2003.

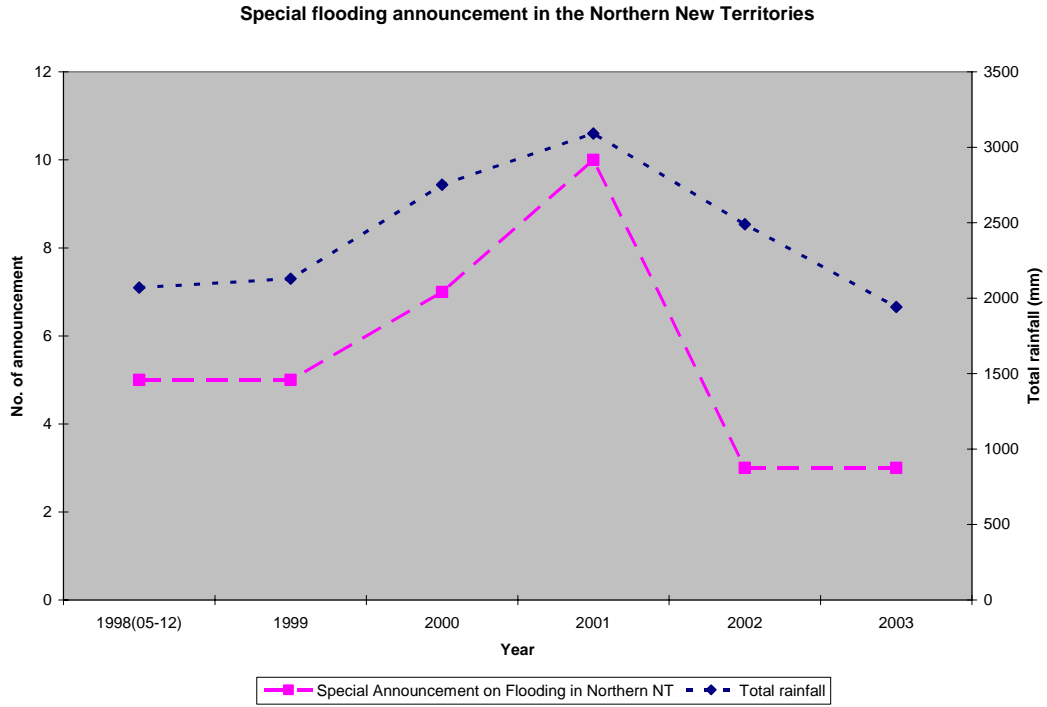


Figure 7.4 The Number of Flooding Announcements in the Northern Territories in Hong Kong Between 1995 and 2003

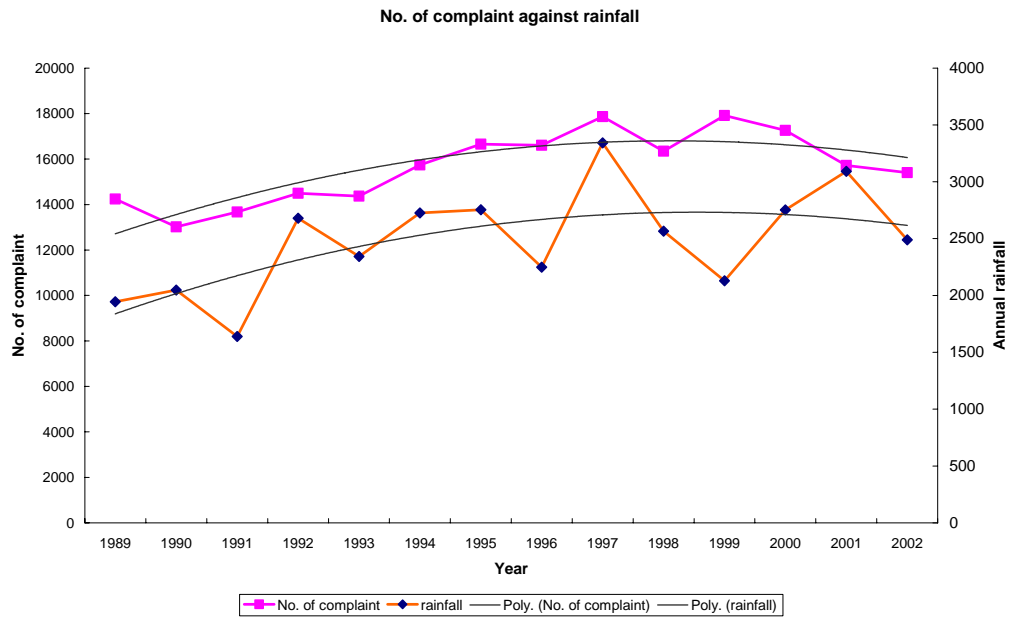


Figure 7.5 A Time Series of Annual Rainfall and Number of Flooding Complaints in Between 1989 and 2002

Figure 7.5 shows that the number of flooding complaints is associated with the annual rainfall. The number of flooding complaints is counted by the number of public help calls (including minor or major flooding within all regions). This number does not account for the actual number of flooding or the seriousness of each flooding. Figure 7.5 also shows that the number of flooding complaints has been decreasing since 1997.

To combat the flooding problem, the HKSAR established the Drainage Services Department (DSD) in September 1989 to take up the overall responsibility of providing an efficient approach to resolve both the flooding and sewage problems in Hong Kong. Four strategies of flooding prevention have been introduced. They include the long term improvement measures, on-going improvement and mitigation measures, preventive maintenance, and land use management and legislation. Continuous master planning (long term improvement) has alleviated the flooding problems. HKSAR has launched three Rural Drainage Rehabilitation Schemes: 1.Nam Hang drainage improvement (Stage 2, phase 1), 2.rehabilitation works at Ng Tung River (Stage 1, phase 1A) and 3.rehabilitation works at Sheung Yue River (Stage 1, phase 1B). The total cost was HK\$ 313.5 million. Figure 7.6 shows that there was a sharp drop in the number of flooding complaints in 2002. This was due to the progressive completion of the flooding prevention programs. The modified Shenzhen River, as example, is shown in Figure 7.7.

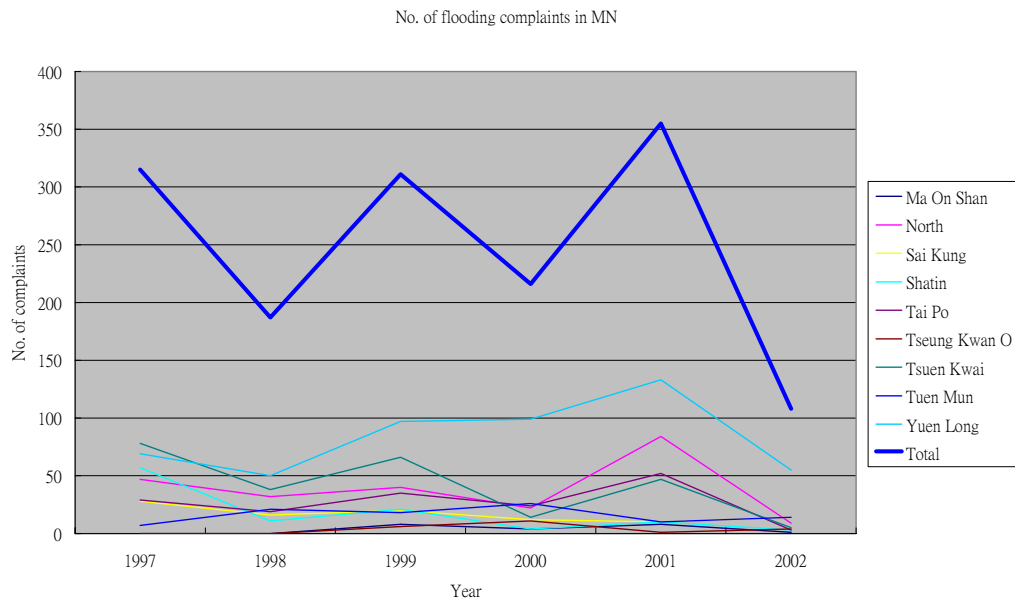


Figure 7.6 The Number of Flooding Complaints in Different Districts in the Northern Part of Hong Kong Between 1997 and 2002



Figure 7.7 Extensive Flooding in Shenzhen River and Ma Tso Lung areas, Sheung Shui, during Typhoon Dot in 1993 (left) and The Completed Shenzhen River Regulation Project Stages I & II (right)

The Drainage Services Department (DSD) has developed a number of measures, including real time flood warning systems, village polder schemes, river training, stormwater diversion and storage system. Additional resources would be put to continually upgrade the existing flood prevention infrastructure and improve the flood warning dissemination. Further research into methods of coastal engineering leading to design guidelines for coastal defenses is needed. The HKSAR has already introduced mitigation measures to alleviate flooding problem in the future. It is anticipated that Hong Kong could adapt to this impact of climate change. To further adapt to future flooding, the DSD has incorporated design standards to prevent flooding with different return periods (Table 7.4).

Types of Drainage	Years
Urban drainage trunk systems	200
Urban drainage branch systems	50
Main rural catchment drainage channels	50
Village drainage	10
Intensively used agricultural land	2-5

Table 7.4 Average Recurrence Interval of Flooding Prevention in Hong Kong Drainage Systems

The Guangdong province has studied in great details the impact of climate change on PRD coastal resources. Further discussions on flooding impact can be found in Chapter 11.

7.4 References

1. ACQWS Paper No. 12, Strategy for Long-term Fresh Water Resource, Water Supplies Department, Personal Communication, March 2002
2. Department Annual Report 2001-2002, AFCD , Agriculture, Fisheries and Conservation Department
3. Department Annual Report 2002-2003, WSD, Water Supplies Department
4. Hong Kong Yearbook 2002, HKSAR
5. IPCC, Climate Change 2001, Impacts, Adaptation, and Vulnerability
6. Mendelsohn R. and Neumann J. E., The Impact of Climate Change on the United States Economy: Cambridge University Press, 133-177, 1999
7. Website of AFCD,
http://www.afcd.gov.hk/agriculture/arch_e.htm
8. Website of WSD,
<http://www.info.gov.hk/wsd/en/html/water/index.htm>
9. WHO, World Health Organization Guidelines for Drinking-Water Quality, 1993
10. Zhai P., Sun A., Ren F., Liu X., Gao B. and Zhang Q., Changes of climate Extremes in China, Climatic Change 42, 203-218, 1999

Chapter 8. Ecosystems

8.1 Introduction

According to the WWF Hong Kong's ecological databases published in 1993, Hong Kong is surprisingly green and has a surprisingly large number of wildlife species. The HKSAR has an excellent achievement in environmental conservation. Despite the enormous pressure due to large population to land area ratio, only about 21% of land in Hong Kong is urbanized. About 40% of land use is protected as country parks, Sites of Special Scientific Interests (SSSI) and RAMSAR sites. The numbers of selected ecological species found in Hong Kong are highlighted in Table 8.1.

Category	no.	Category	no.	Category	no.
Seaweed	310	Ferns	175	Flowering plant	1,900
Orchid	120	Moth	2,000	Bird	422
Dragonfly	93	Butterfly	200	Freshwater fish	96
Amphibian	23	Reptile	78	Mammal	57

Table 8.1 Category of Ecological Species in Hong Kong

Recent surveys indicate that there had been further increase in the numbers of some local species: 2900 species of flora, 107 species of dragonflies, 232 species of butterflies (one sixth of the total butterfly species in China) and 452 species of birds (one-third of the total bird species in China and 5% of the world's total). The primeval forest, which is dominated by the oak and laurel families, has a wide mix of species. The number of local primeval plant species is estimated to be about 3,100.

As ecosystem is a very broad topic, this chapter will focus on two specific areas: the birds and hill fires in Hong Kong.

8.2 Migratory and Local Birds

Every year, more than 100 species of birds descend on the marshes in Hong Kong before setting off across the South China Sea. Mai Po acts as a refueling station and wintering site for thousands of migratory birds during their migrations between the Arctic Russia and Australia. Over 120,000 migratory birds visit Mai Po every winter and up to 68,000 waterbirds have been observed using these wetlands. It also hosts 14 globally endangered species, including the Black-faced Spoonbill (*Platalea minor*) and Spotted Greenshank (*Tringa guttifer*) and so on. Some 25% of the black-faced spoonbill, estimated at about 700 birds in 2002, shelter in Mai Po in winter, where large mangrove stands, fishponds, gei wais (240 ha) and reed beds (45 ha) provide ample foods and habitats for migratory birds. The count of 24 selected species is shown in Table 8.2. The conservation of wetlands is, therefore, very important for ecological habitats.

Climate change is likely to have both direct and indirect impacts on migratory birds. It could alter their habits due to the lack of land, food supply or weather change. The potential loss of estuarine beaches caused by sea level rise would decrease available habitats for the endangered species; it may decrease feeding areas for shore birds that rely on shrimps, horseshoe crabs and other organisms found in inter-tidal areas. Another indirect impacts resulted from the shrinkage of coastal wetlands are a decrease in estuarine fish and shellfish populations, which may tighten available food supplies. As a result, some of the migratory birds are forced to find new habitats. Global warming will also change the timing of seasonal cycles. Shorter winter and longer summer may change the time schedule of their migration and nesting.

Hong Kong is an urbanized city. Highways and concrete roads will prohibit the retreat of mangroves inland. Impact of global climate change on Hong Kong's migratory birds is still uncertain. Mangroves might be able to adapt or it might shrink due to sea level rise. Owing to the urbanization of Shenzhen and PRD, more and more migratory birds stop at Mai Po. Both food supply and living area are stressed due to this immigration.

NAME OF SPECIES	DECEMBER - MARCH		
	2000 - 2001	2001 - 2002	2002 - 2003
Great Cormorant	7142	6230	7959
Dalmatian Pelican	16	16	-
Chinese Pond Heron	297	297	307
Little Egret	1631	1343	1653
Great Egret	1150	1239	1421
Grey Heron	1064	1297	930
Black-faced Spoonbill	179	183	203
Common Shelduck	373	268	192
Eurasian Wigeon	6705	4752	4080
Common Teal	2509	3147	3826
Northern Pintail	3435	-	4381
Northern Shoveler	6414	-	4271
Eurasian Coot	534	54	54
Pied Avocet	1926	1957	5846
Kentish Plover	2372	2418	378
Grey Plover	312	294	295
Dunlin	3100	2968	11
Black-tailed Godwit	317	320	340
Eurasian Curlew	810	558	1040
Spotted Redshank	512	2500	450
Marsh Sandpiper	1171	153	1760
Common Greenshank	290	376	67
Saunders' Gulls	43	60	35
Black-headed Gull	13500	13009	12601

Table 8.2 Numbers of 24 Migration Birds in Hong Kong

A more imminent issue is the urbanization and pollution problem in Deep Bay that has already seen a reduction of 12,830 birds in its first count round Mai Po in 1979 down to 68,000 birds in 1997 to the present 54,000 birds (Hong Kong Bird Watching Society). Using Saunder's gulls as an example, there has been a general decline in the

peak winter count since the peak of 172 in 1993-94 (Table 8.3). The change of visiting birds' population depends on the genetic acclimatization of species.

Year	92 - 93	93 - 94	94 -95	95 - 96	96 - 97	97-98	98-99	99-00	00-01	01-02
No. of bird	107	172	131	113	127	91	73	58	43	60

Table 8.3 Numbers of Saunders' Gulls in Past Ten Years

Both the non-government organizations and the HKSAR have indulged great efforts in the protection of migratory birds in Hong Kong. On 4 September 1995, Mai Po and Inner Deep Bay (1,500 ha) were listed as RAMSAR Sites. WWF Hong Kong was established in 1961 and has been performing maintenance and conservation in Mai Po. In 1996, the Agricultural and Fisheries Conservation Department (AFCD) took over 60% of the annual habitat management works at the Reserve.

In mitigation, many environmental organizations and the HKSAR invested heavily in public education through school and public programs, online education and out-going activities. These programs introduce the importance of wetlands for the migration birds and ecology, the path of birds' migration, and different types of waterbirds such as endangered Black-faced Spoonbill, Chinese Bulbul, Spotted Dove and Yellow-bellied Prinia.

To promote environmental awareness, the "Big Bird Race" was organized by WWF Hong Kong and has been held in Hong Kong every year since 1984. A significant amount of the operational funding of Mai Po has been raised from this "Big Bird Race". In 2004, it raised about HK\$1.0 million and 206 species of birds were spotted. This fund has been used in converting the traditional shrimp ponds (gei wai) in the Reserve for education and conservation purposes. More recently, the funds have also been used to cover running costs and the construction of new facilities.

Hong Kong also keeps a good inventory on migratory birds. The AFCD and the WWF Hong Kong closely monitor the population and number of species. Non-government organizations such as the Hong Kong Bird Watching Society also participate actively in archiving the bird records in Hong Kong. Both (AFCD & WWF) societies and the Big Bird Race contribute to an excellent bird inventory in Hong Kong without using public fund.

Other measures for further protection of migratory birds in Hong Kong have been implemented. They include education, town planning and legislation. To enlarge the natural habitat for migratory birds, the possibility of converting some existing reservoirs and land on the eastern part of Hong Kong to wetland has been studied.

8.3 Hill Fires

In recent years, severe forest fires broke out in Australia and United States causing great damages as well as the loss of life. It is suspected that higher global temperature might conduce to more hill fires in the world. There have been many hill fires

occurring in Hong Kong over the last two decades (Table 8.4). Hill fire in country parks annihilates all grassland, trees and animals within the burnt area and it takes decades for the country parks to recover. It is not uncommon in a few popular fire spots that hill fires have occurred several times within a decade and these spots never recover.

Year	1991	1992	1993	1994	1995	1996	1997	1998	1999	2000	2001	2002
No. of hill fire	139	188	156	53	178	107	45	82	193	65	105	78

Table 8.4 Number of hill Fires Between 1991 and 2002

In Hong Kong, hill fire is also quite a common phenomenon. A preliminary analysis was done to explore whether there was any evidence on the relationship between temperature/relative humidity and number of hill fires in Hong Kong. The Hong Kong hill fire statistics between 1997 and 2001 is shown in Figures 8.1. Figure 8.1 shows that hill fires in Hong Kong occurred between October and April. The number of hill fires depends on rainfall, ambient temperature, relative humidity, shrub or grass density, frequency of lightning strike and anthropogenic influence. The monthly averaged relative humidity and monthly rainfall of Hong Kong are shown in Figure 8.1 and Figure 8.2 respectively. Both RH and rainfall in Hong Kong have a distinguishable cycle. The winter in Hong Kong is dry with low RH and low rainfall and the summer is wet with high RH and high rainfall. In general, hill fires occur in fall and winter. It is unusual that a large number of hill fires occurred in April in 1998 and 1999.

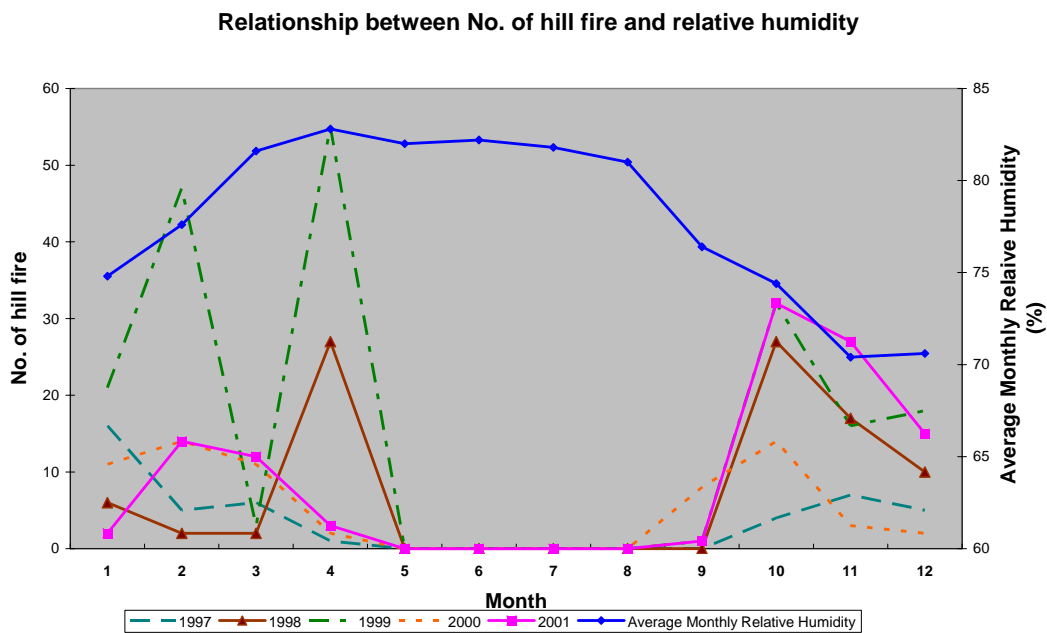


Figure 8.1 Relationship Between Hill Fires and Relative Humidity

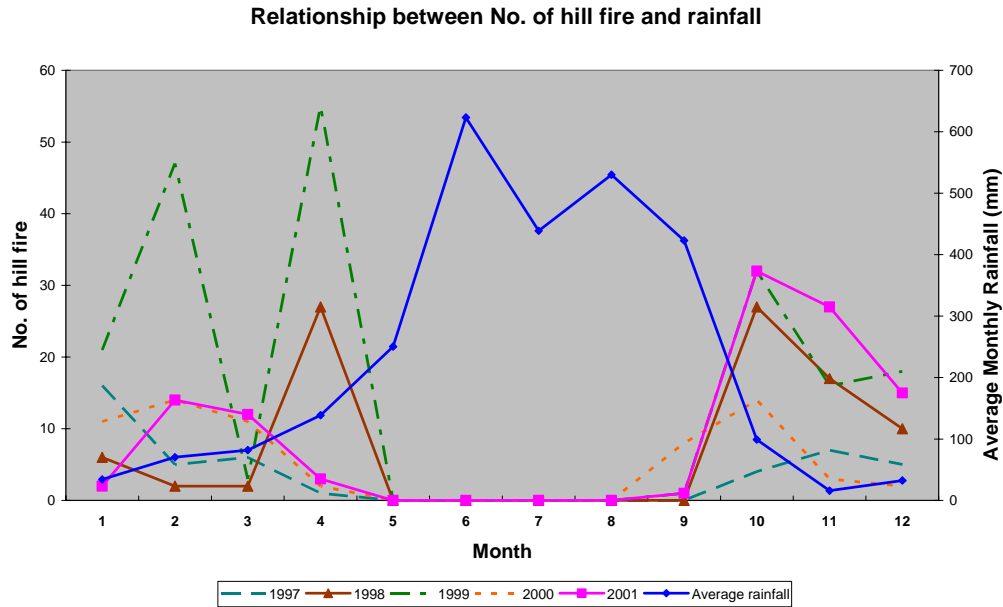


Figure 8.2 Relationship Between Hill Fires and Rainfall

Multiple regression analysis was carried out between the temperature, RH and number of hill fires using SPSS. No significant correlation can be identified (Table 8.5). It is shown in Figure 8.1 and 8.2 that the monthly variation of rainfall and RH are smooth curves whereas the numbers of hill fires are rather random and have great variability. The frequency distribution of the number of hill fires is dominated by many zeros and large proportion of large numbers. The non-normal distribution is highly skewed. Thus it is difficult to find good correlations with other more well behaved parameters.

	R value	Significant
Temp	0.52	0.394
RH	0.96	0.117

Table 8.5 Linear Regression Between the Number of Hill Fires, Temperature and Relative Humidity

Anthropogenic influence is another explanation for the poor correlations. Not all hill fire records are caused by nature. Actually most of them are caused by negligence and arson. In general, the number of hill fire should also depend on factors such as number of people visiting the countryside, citizen education level and behaviors of country park visitors. Many of these factors are random, difficult to quantify and measure.

The direct way to estimate the economic loss due to hill fire is to multiply the total number of trees burnt by the replanting cost of each tree. Other costs include loss of life and lost of properties. However, these figures are not available. A trial was undertaken to estimate the economic loss by an indirect approach. We multiplied the number of trees planted each year with the replanting cost of trees in restoration program and treated it as the loss due to hill fire. Figure 8.3 shows the approximate

number of trees planted between 1997 and 2001. This methodology was not successful because we found out that the planting cost of trees was reducing in recent years (Figure 8.4) and also the number of trees planted each year did not follow the trend of number of hill fires each year. Figure 8.3 shows that the number of tree planted has been increasing since 1997 whereas the number of hill fires did not have this trend. It is obvious that the increasing number of trees planted per year is due to human intervention and market drive. Not only the HKSAR has increased its restoration effort, the cost of tree planting also has been decreasing. In summary, the number of trees planted per year cannot represent the number of trees burnt in that year or the year before. This method can only be applied to estimate the cost of hill fire for a much longer period such as one decade.

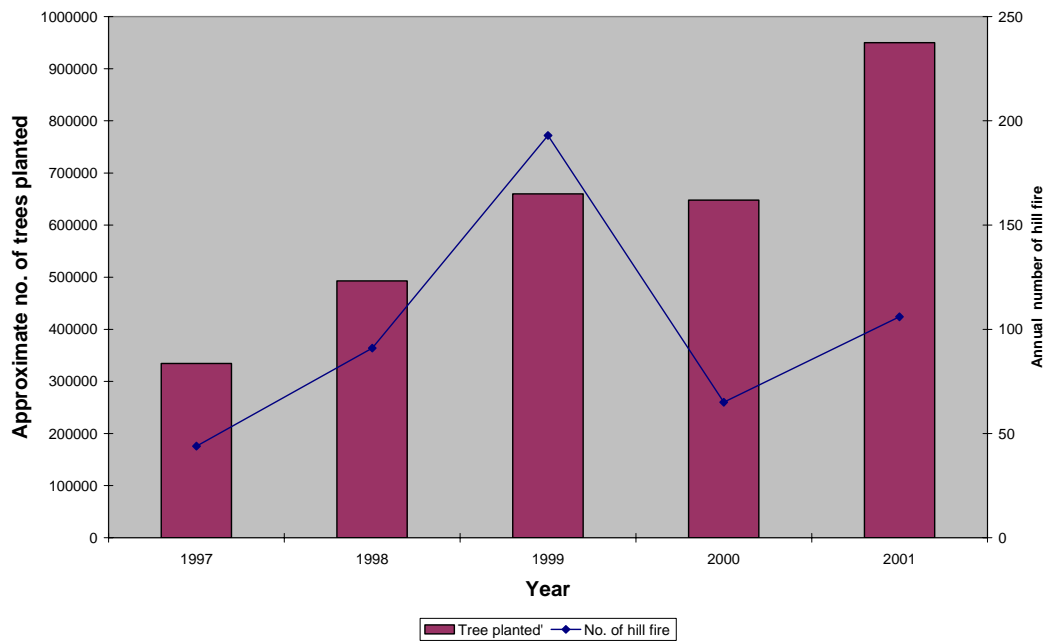


Figure 8.3 Approximate Number of Trees Planted Against the Number of Hill Fires Between 1997 and 2001

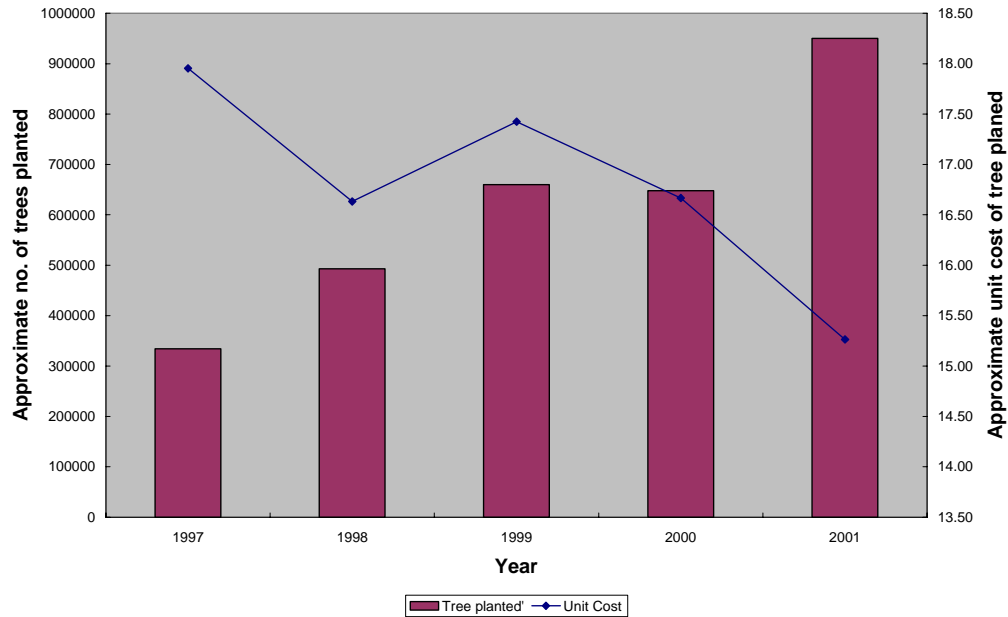


Figure 8.4 Approximate Number of Trees Planted And its Unit Cost in Tree-Planting Program Between 1997 and 2001

The HKSAR has spent great effort in restoration. Tree planting program is instituted to alleviate the loss of woodland and countryside and promote a greener HKSAR. Each year 600,000 trees, mostly native, are planted for soil protection, greening needs and education. In 2000, the AFCD organized Green Hong Kong Campaign to promote public awareness of environmental protection through greening activities involving 760,000 participants of all ages. The Government Flying Service cooperated with the AFCD to make announcements to hikers on the prevention of hill fires and to keep country parks clean using aircraft on public holidays. In addition, the AFCD has established and maintained a Computerized Tree Inventory System that assists in taking stock of tree species and formulating policies on tree management in the long run.

8.4 References

1. Agriculture, Fisheries and Conservation Department
http://www.afcd.gov.hk/index_e.htm
2. Hong Kong Observatory website
<http://www.hko.gov.hk/contente.htm>
3. Hong Kong Bird Watching Society
<http://www.hkbws.org.hk/>
4. World Wide Fund For Nature Hong Kong
<http://www.wwf.org.hk/chi/index.html>

Chapter9. Coastal Zones and Marine Life

9.1 Introduction

There are many valuable plants and mammals within the HKSAR water boundaries. In this chapter, we focus on mangroves, dolphins and coral reefs.

9.2 Impact on Coral reefs



Figure 9.1 Healthy (left and middle sides) and Bleached (right side) Corals in Hong Kong Waters

Hong Kong is located at the northern edge of the tropical Indo-Pacific region. There are 2 km² of reef areas but no true reef structure in Hong Kong waters. About 84 species of reef-building corals are recognized from 28 genera of 12 families and about 10 species of non-reef-building corals from 4 genera. Corals are mainly located in the north-eastern part of Hong Kong and outlying islands. The depth distribution of stony corals is confined to about -1 m to -3 m Chart Datum¹ (C.D.) and unlikely extends to more than -10 m C.D due to high turbidity levels. Corals provide food and habitat to marine life. The richest coral communities can be found in the northeastern water which is generally free from the silty water floods from the Pearl River.

The impact of global warming on corals is still largely unknown. It is difficult to find literature discussing the impact of global climate change on corals. Despite the lack of knowledge in this area, one factor is certain – corals are vulnerable to extreme events. Corals are sensitive to water temperature and water quality. Serious coral bleaching was first recorded in Hong Kong in 1996. Figure 9.1 displays the healthy and bleached corals within Hong Kong Waters. High water temperatures and low salinity in shallow waters due to exceptionally heavy rainfall in June and July are believed to have caused the bleaching. Sixteen species from five genera showed some bleaching and 12 suffered some mortality as a result. The most severely affected species was *Montipora*, with more than 50% of colonies dying at 3 shallow sites in eastern waters.

¹ Chart Datum is 0.146 m below Principal Datum (PD).

Two shallow mixed species coral communities in southern waters, which are less optimal for coral growth due to the influence of the Pearl River, suffered more than 90% mortality. Conditions started to return to normal following Typhoon Victor in August which caused physical mixing of the shallow hyposaline waters with deeper, cooler, ambient salinity water. Most bleached colonies not suffering mortality recovered 4-8 weeks afterwards (McCorry, 2002).

Regarding the impact of sea level rise, if the vertical accretion of coral reefs can keep up with the predicted rate of sea level rise, the impact on reefs would be negligible. According to IPCC IS92a scenario, the rate of sea level rise range from 1.6mm per year to 8mm per year but the rate of upward accretion in reef lagoon is only 0.6mm/year, while coral reef flats have rates around 3mm/year and areas of coral thickets have rates of about 7mm/year.

In respect to the impact of temperature rise, the sea water temperature should in turn rise along with global warming. It might lead to coral bleaching. In Hong Kong, the maximum monthly sea water temperature recorded at Waglan Island was 27.7°C in summer and 14°C in winter. Judging from the large difference in sea water temperature in Hong Kong between summer and winter, it is believed that coral species are capable of tolerating different sea water temperature provided that the temperature change is gradual. The key parameter that governs the health of corals is the fluctuation of sea water temperature. The lethal limits temperature is about 2°C higher than mean sea surface temperature. A sudden change of temperature, only a few days to temperature elevations of 3 to 4°C above normal summer ambient maxima or several weeks to elevations of only 1 to 2°C above summer ambient, can cause coral bleach (Raton, 1995). This impact varies geographically and is correlated with normal summer ambient maximum sea temperatures. Arabian Gulf corals could expose to 34°C for weeks while Hawaii corals could expose to temperature of 31°C for prolonged period. At present, the lethal limits temperature in Hong Kong is estimated at about 30°C. Any extreme event that causes sea water temperature fluctuations of 2°C or more is likely to cause damage. How this lethal limit change with long term sea water temperature rise in the future is still unknown.

Another indirect impact is that seawater temperature rise may reduce CO₂ level in seawater and thus, the growth of reef which relies on the availability of CaCO₃ would slow down and could not keep pace with the sea level rise. Temperature rise in atmosphere melts icebergs in the poles and reduces salinity of the seas. Decrease of salinity together with the rise of seawater temperature may cause coral breaching and kill the species that rely on the coral. In actual fact, anthropogenic influence on the health of corals far exceeds the cause by nature. Reclamation, pollution, overfishing and marine tourism all pose serious threat to coral communities. The death of coral community and vanishing of coral species imply the lost of the coastal resources and tourist value of marine parks. The impacts on local coral due to climate change or human activities should be studied.

To conserve the marine eco-systems in the HKSAR, four marine parks and one marine reserve have been designated. In total, they cover totally around 2,430 hectares, or about 1.3% of local waters. Marine Parks have been established for conservation and recreation purposes.

Four legislations have been introduced to provide effective protections for coral communities and associated faunas. Two key government departments, the AFCD and the EPD are responsible to enforce these legislations. These legislations include Marine Parks Ordinances(1995), Fishery Protection Ordinances(1962), The Animals and Plants (Protection of Endangered Species) Ordinances(1976) and Water Pollution Control Ordinances(1981). These legislations are adaptation measures taken by the HKSAR to mitigate the impact on marine eco-systems caused by nature or human threats. The introduction of Marine Parks Ordinances is to provide designation, control and management of marine parks and marine reserves, and for the purposes in the connection with the aforesaid. The other three ordinances are introduced to promote the conservation of fish and other forms of aquatic life within the waters of Hong Kong. They regulate fishing practices and prohibit activities detrimental to the fishing industry; “to restrict the importation, exportation and possession of certain animals and plants, and parts of such animals and plants, and to provide for matters connected therewith; and to control the pollution of the waters of Hong Kong accordingly.

Monitoring programs have been introduced to manage the health of marine eco-systems. The Chinese University of Hong Kong, The University of Hong Kong and the AFCD collaborate to monitor corals, fishes and basic environmental parameters. A Reef Check survey has been conducted annually since 2000 by the AFCD in collaboration with the Reef Check Foundation. The survey reported that coral cover in Hong Kong has improved slightly over the past few years, ranging from 12.5% to 77.5% in 32 sites in 2003. 22 of these sites have high coral cover (>50%). Apart from the Reef Check, the AFCD also commissioned a study on coral communities in coastal waters of Hong Kong. With the monitoring network in place, timely warning and conservation efforts could be taken before conditions deteriorate.

Apart from post-active measures, pro-active methodologies have been also adopted. The AFCD initiated the artificial reef deployment project in 1996 with the aim of enhancing local marine and fisheries resources. Main deployed areas include Marine Parks, Long Harbour and Outer Port Shelter. Other artificial reefs have been constructed and maintained by local universities. The main objective of building artificial reef is to enrich marine eco-systems in Hong Kong. The program should enhance the quantity of fisheries and provide food resources for Chinese White Dolphins’ habitats. By 2003, artificial reefs reached 168,000 cubic meters within Hong Kong waters (AFCD Press Releases). These programs may also transplant the reefs to fit their livable temperature and water depth.

Hoi Ha Wan Marine Park in Sai Kung was established by the WWF HK together with the HKSAR in 1988. A new Marine Life Center will be completed in 2004. The aim of this center is to provide a study tour for the public to appreciate the coral reef and promote the conservation of Hong Kong’s marine environment and heritage.

9.3 Impact on Coastal Wetlands / Mangroves / Mudflats

The relationship between mangrove and migratory birds has been discussed in chapter 8. The significance of wetlands, mangroves and mudflats in coastal resources will be discussed in this section.

Mai Po Ramsar Site covers an area of 15 km². It is the sixth largest coastal wetlands in China. In Hong Kong, there are 8 true mangroves species in 44 clusters covering areas of about 2.9 km². They are distributed in six districts: Sai Kung, Northeast New Territories, Tolo Harbour, Deep Bay, Lantau Island and Hong Kong Island. Mangroves have high ecological values. It plays an important role in maintaining biological diversity by providing a diverse habitat for many plants and animal species. It also maintains the ecological balance of coastal and marine ecosystems.

Concerning the impacts of global climate change, the main threat to Mai Po comes from the sea level rise. In general, mangroves are sensitive to the sea level as it dwells in estuary mud-land that is immersed during high tide and totally exposed during low tide. Hypothetically, sea level rise could damage mangroves' habitat along coastal areas. At the outermost perimeter of Mai Po, the root of mangroves will be immersed thoroughly for a whole day. Some species of mangrove will be depleted due to the shortage of oxygen. As the sea rises, the outer boundary of these wetlands will erode. By the force of nature, tidal waves will open the estuary upstream causing an inland retreat of mangrove. New wetlands will form inland as previously dry areas are flooded by the higher water levels. In rural areas in other countries, the impact of sea level rise would be minimal because nature will convert dry land into wetland when shore line retreat. Adaptation of mangroves depends on the rate of sea level rise and shoreline geology.

Hong Kong is an urbanized area, artificial barriers such as concrete roads and anti-wave structures may restrict the migration of mangrove. Bulkheads, dikes, and other structures keep new wetlands from forming inland. Even in the case of no restriction, both the irregular coastline and topography of Hong Kong tend to compress mangrove stand. Most of the Estuaries in Hong Kong are fan shaped. By geometry, the amount of newly created wetlands will be smaller than the area of wetlands that are lost. Many mangrove clusters in Sai Kung cannot retreat due to the terrain. Sea level rise will increase the removal ability of detritus and sediment from the mangal edge by waves (Raton, 1995).

If adaptive measures are not taken, there is a possibility that mangroves in Hong Kong may be inundated by the sea in the future and may suffer reduction in species diversity owing to sea level rise. Whether this will happen, there are two schools of thoughts. Pessimists anticipated that when sea level rises by one meter in Hong Kong, all mangroves would be inundated since mangroves retreats are restricted by concrete structures. With no mud land exposed in low tide, there is a break in the food chain. Mai Po eco-system will be annihilated though some species of mangrove still survive. This situation can be seen in a few mangrove clusters in Sai Kung. On the contrary, optimists anticipated that mangroves in Mai Po should be able to adapt. It is universally agreed that there is little room for coastal wetlands to retreat in Hong

Kong. However, if the land rise vertically copes with sea level rise, Mai Po could sustain. There is a continuous reclamation in coastal wetlands. Silt and sediment carried down by rivers is a commonly known source. Mangroves take in carbon dioxide from the atmosphere and build wood and leaves. Fallen leaves, branches and dead animals also contribute to a net gain in land. The fate of the coastal wetlands in Hong Kong remains a subject of investigation.

To manage the impact on coastal wetlands, it is necessary to identify the areas flooded when sea level rises by one meter. The latest approach is to use GIS to estimate the land loss. One way is to calculate the difference between the land bounded by the present coastline and the land bounded by the new coastline when sea level rises by one meter. The consultants of this project have made an unsuccessful attempt. The digital map of Hong Kong was acquired from the Lands Department. Unfortunately, the highest resolution in contour line is 2m. The digital map is not fine enough to carry out this study. Other techniques should be employed in further studies.

The WWF Hong Kong has conducted a survey to predict the inundation of Mai Po and Deep Bay mudflat, where the areas would be confounded by the increased rate of siltation of the mudflat itself. It pointed out that the estimated rate of siltation of mudflat is around 3cm per year. The AFCD is beginning to collect preliminary data on contour of mudflat in Hong Kong. It is very useful for long-term analysis of mudflat development and the change of contour due to sea level rise. Until now, there is no accurate methodology to estimate the land loss due to climate change in Hong Kong.

9.4 Impact on Dolphins

Chinese white dolphins (also known as Indo-pacific humpback dolphin) and finless porpoises are the only two marine mammals species sighted throughout the year in Hong Kong's water. Chinese white dolphins belong to the *Sousa Chinensis* species. It can be found in South Africa, Australia and throughout Southeast Asia. The Pearl River Estuary provides a favorable shallow, sheltered and estuary environment for the dolphins and its population is estimated at over 1000 individuals. Chinese white dolphins often stay in the western waters of Hong Kong within the Pearl River Delta area. Peak abundance occurs in summer (145 individuals) under greater Pearl River influence during the summer monsoon season, while about 92 individuals can be observed in winter.

Finless porpoises center round the southern and eastern oceanic waters of Hong Kong. They can be found in warm coastal Indo-Pacific fresh and marine waters and range from Central Japan to the Persian Gulf. Preliminary survey indicated its abundance of at least 217 individuals in Hong Kong's water. Seasonal movement is observed in this species with peak abundance in spring (152 individuals) and a dramatic decline in number in summer and autumn.

Seasonal change in abundance of Chinese White Dolphin has a significant correlation with water temperature (positively) and salinity (negatively), whereas the abundance

of Finless porpoises are correlated with water temperature (negatively) and salinity (positively) and also with the number of reported neonatal porpoises strandings (Parsons, 1998). Climate change may alter the sighting seasons of dolphins and regional abundance, but may not pose a direct threat to their lives as these species may migrate to other water areas when water temperature changes.

Of particular concern is our degrading marine environment and diminishing fisheries resources under the pressure of coastal developments, overfishing, destructive fishing practices and marine pollution. Catches, demersal fish in particular because of its commercial value, have decreased by 40% since 1976. It was reported that annual strandings of Chinese white dolphins have increased rapidly from <3 per year in 1985 to 15 strandings in 1996. 22 of strandings occurred between January 1996 and March 1998, 59% were neonates, suggesting that the high mortality rates of newborns, as is the case for most cetaceans (Jefferson 1998). Post-mortem in stranded dolphins identified bacterial disease and elevated levels of organic contaminants. This has prompted widespread concern about the water pollution damage to the habitats of Chinese White Dolphins (Parsons 1997). Other anthropogenic influence such as the construction of bridges and reclamation works forced the dolphins to shift their living zone. Some of the dolphins may not adapt such changes and die. It is believed that anthropogenic impact far exceeds impact due to nature.

In mitigation, the AFCD has initiated various programs to replenish fishery stock and to protect our marine habitats. The construction of artificial reefs has been mentioned in chapter 8. Others include trial release of fish fry, stricter enforcement of the Fisheries Protection Ordinance against destructive fishing practices, study on viability of offshore fishing and education. Between July 1996 and November 2001, four marine parks and one marine reserve covering 2,430 hectares were designated. They include the Hoi Ha Wan Marine Park, Yan Chau Tong Marine Park, Sha Chau and Lung Kwu Chau Marine Park, the Tung Ping Chau Marine Park and the Cape D'Aguilar Marine Reserve. The aim of those parks and reserves is to protect the marine life and raise the public awareness on marine conservation in Hong Kong. A 12km² Marine Park - also known as a 'the Dolphin Sanctuary' - was designated in 1996 in accordance with the Marine Park Ordinance, in which trawling was banned and a number of artificial reefs were employed to enhance the fish stock. A Marine Mammals Conservation Working Group was formed under the AFCD with participation from various concerned parties in an effort to increase dolphin's population.

The impact of sea level rise in the Pearl River Delta region has been studied thoroughly by the Government of Guangdong Province. The report was published by the Guangdong Science publishing company. The impact of sea level rise has been estimated in separate parts with possible migrations recommended for the future 2030. The report is very informative and worthwhile to extract some information that is relevant to Hong Kong. The information is summarized in Chapter 11 of this report.

9.5 References

1. AFCD Press Releases
(<http://www.afcd.gov.hk/news/epress/pr387.htm>)
2. Chinese-White Dolphin Net
(<http://www.chinese-white-dolphin.net/>)
3. Department Annual Report 2001-2002, Agriculture, Fisheries and Conservation
(http://www.afcd.gov.hk/downloads/textannualreport2002/eng_txt/app.html)
4. Jefferson T.A., Population Ecology of the Indo-Pacific Hump-backed Dolphin (*Sousa chinensis* Osbeck, 1765) in Hong Kong waters: final Report, Ocean Park Conservation Foundation, April 1998
5. McCorry, D., Hong Kong's scleractinian coral communities: status, threats and proposals for management. PhD Dissertation. University of Hong Kong, Hong Kong, 2002
6. Parsons E.C.M., The behavior of Hong Kong's resident cetaceans: the Indo-Pacific hump-backed dolphin and the finless porpoise. *Aquatic Mammals* 24(3): 91-108, 1998
7. Parsons, E.C.M., Hong Kong's cetaceans: the biology, ecology and behavior of *Sousa chinensis* and *Neophocoena phocaenoides*. PhD Dissertation, University of Hong Kong, Hong Kong. 1997
8. Raton B., *Climate Change: Impact on Coastal Habitation*, Lewis Publishers, 209-234, 1995

Chapter10. Sea level Rise Extracted from “Guangdong

Haipingmian Bianhua Jiqi Yingxiang Yu Duice”

Hong Kong is a coastal city. The impact of sea level rise is one of the key issues. The Guangdong Province is also very concerned in this subject. The Guangdong government carried out a thorough study and published a textbook which incorporated technical reports from a total of thirteen research institutes and government departments. The English translation of the Chinese title is – “The Changes in Guangdong Sea Level, Their Impacts and Adaptations”. This book is a valuable reference for those who are interested in the impact of sea level rise. But it covers the whole of Guangdong, with a lot of materials not related to Hong Kong. It took quite a bit of time to interpret the report regarding the impact on Hong Kong. In this chapter, the consultant extracted, interpreted and translated the content from simplified Chinese into English. For any doubts or unclear points, readers may refer to the original Chinese textbook. For abbreviation, the “Guangdong Haipingmian Bianhua Jiqi Yingxiang Yu Duicis” will be referred as the “Guangdong book” in this chapter.

This chapter is extracted from the Guangdong book on predicted sea level rise and tide wave and their impacts on Hong Kong by 2030. Focus is put on the impacts on the present marine life zone, beaches and infrastructures.

10.1 Introduction

The Guangdong Province predicted that, by the year 2030 the sea level rise may range between 9cm and 31cm. IPCC (1995) predicted the sea level rise along the Guangdong coastal area to be 8 cm by 2030 and the rising rate to be 3.0 mm per year. Based on the Hong Kong local tidal data at the North Point/Quarry Bay station, the HKO reported that the mean rise in sea level was 7 to 14 mm per decade between 1957 and 2002. Ding 2001 reported that the current rate of sea level rise is about 19mm per decade. The most conservative estimate indicated that by 2030 the mean sea level rise in Hong Kong will exceed 5.7cm.

The Guangdong book discussed seven impacts of sea level rise: (1) storm tides, (2) water level of the Pearl River, (3) lake and sea dam, (4) saline water intrusion, (5) beach and shore, (6) drainage and water environment, (7) coastal engineering design standard.

The Guangdong government takes the relative sea level rise to be the sum of four components. These include the theoretical sea level rise, abnormal relative sea level amplitude, additional value due to flood and tidewater level, and relative

topographical change. The Guangdong Province is classified into three regions: Guangdong east (Yuedong), Pearl River Estuary and Guangdong west (Yuexi).

10.2 The Impact on Storm Tide

Storm tide is one of the major natural disasters in the Guangdong coastal regions. 66% of the tropical cyclones that made landfall in China entered through the Guangdong Province. The Guangdong government estimated that on average the economic loss caused by each tropical cyclone landing was over three hundred million Yuan. Global warming may result in higher frequency and strength of storms. (There is no evidence that the number of tropical cyclone will increase in Guangdong in the future, chapter 2, section 2.6). Severe storms and heavy rain will destroy seawall, agriculture, and cause life loss.

Sea level rise will result in higher tidal positions in all regions. Tidal positions are designated by 5 parameters:

- (1) mean high water spring (MHWS) – highest sea level at spring tides,
- (2) mean high water neap (MHWN) – highest sea level at neap tides,
- (3) mean sea level (MSL),
- (4) mean low water spring (MLWS) – lowest sea level at spring tides,
- (5) mean low water neap (MLWN) – lowest sea level at neap tides,

Tidal positions can be predicted by:

$$\text{MHWS} = \text{MSL} + 1/2S_g$$

where S_g is the average amplitude of the spring tides.

$$S_g = [M_n - \frac{H_{S2}^2}{2H_{M2}}] + [1.96 - 0.08(\frac{H_{k1} + H_{01}}{H_{M2}})^2]H_{S2}$$

$$M_n = 2H_{M2} + \frac{1}{2H_{M2}}(1.0712H_{S2}^2 + 0.963H_{N2}^2 + 1.077H_{k2}^2 + 0.231H_{01}^2 + 0.266H_{p1}^2 + 0.214H_{q1}^2)$$

M_n is the average amplitude of normal tides, and H_{M2} , H_{S2} , ..., H_{q1} are the amplitudes of eight harmonic constants. The equations for neap tides were not given in the Guangdong book but they should be very similar. The average mean sea level and the constants can be derived from long term tidal records.

When sea level rises, all 5 tidal positions will rise but their rates of increase are non-linear. Locations that are dry at present may be immersed during high tides. The tidal positions are also related to the intensity of the storm and the volume flow of the Pearl River as well. The modeling results show that when the sea level rises by 0.3m, under normal river volume/normal storm strength, low river volume/large storm strength, and flooding river volume/normal tides, the MHWS at Guangzhou will rise by 0.3m, 0.27m and 0.17m respectively. Taking Guangzhou as an example, at present the MHWS and MHWN computed by the above model are 0.763m and 0.464m (reference to Macau CP). When the sea level rises by 0.3m, the MHWS and MHWN will be 1.063m and 0.764m respectively. Thus the new neap tide high position will be

higher than the present spring tide high position. Furthermore, the MHWS of 1.063m at Guangzhou is close to the astronomical high tide position of 1.373m. Similar to Guangzhou, many locations in the Pearl River Delta region will have drainage difficulty.

Similar prediction on tidal position has not been done for Hong Kong. However, according to the Guangdong book, the MHWS at the outer edge locations of the Pearl River is 1.8 times higher than average. The MHWS and MHWN in Macau computed by the above model are 2.63m and 1.92m respectively. When the sea level rises by 0.3m, the new Macau MHWS and MHWN will become 2.93m and 2.22m respectively. Thus the impact of sea level rise in Macau is not very significant as indicated by the large numbers. Hong Kong is on the eastern side of the Pearl River estuary. The tidal positions are less affected by the volume flow of the Pearl River. It is anticipated that the impact of sea level rise on tidal positions in Hong Kong is also not significant.

A critical parameter in Hong Kong is the storm tidal position. The storm tidal position is calculated as follows:

$$H_p = \Delta h_p + \text{MHWS}$$

where H_p is the storm tidal position at a certain frequency p and Δh_p is the relative increment at that frequency. Frequency is used as the return period T_R of storm tide where $T_R = 100/p$. It carries a sense of storm intensity. Table 10.1 shows that the impact of sea level rise on Δh_p is in terms of a few meters. This is much larger than the change in tidal positions. For a once per 100 years large storm, the highest tide position is 4.88 m higher than the MHWS. Most of the reclaimed land in Hong Kong will be flooded by sea water. For a once in 50 years storm, some reclaimed land will be affected.

Station	Frequency p					
	0.1% (1000 yrs)	0.5% (200 yrs)	1% (100 yrs)	2% (50 yrs)	5% (20 yrs)	10% (10 yrs)
North Point	4.62	4.17	3.98	3.79	3.53	3.33
Tai Po Kau	5.94	5.20	4.88	4.56	4.14	3.81

Table 10.1 Current Storm Tide Increment Δh_p (in meter) in Hong Kong at Different Frequencies

Present Frequency	0.5% (200 year)			1% (100 year)			2% (50 year)			5% (20 year)		
	0.1	0.2	0.3	0.1	0.2	0.3	0.1	0.2	0.3	0.1	0.2	0.3
Sea level rise (m)												
North Point (years)	135	95	70	70	48	37	35	25	18	15	9	6
Tai Po Kau	160	135	105	80	65	52	40	35	28	15	10	6

Table 10.2 Predicted Change in Return Period of Storm Tide due to Sea Level Rise

Sea level rise will cause higher storm tidal position and shorten the return period of storm tides. The more the rise in sea level, the more the return period will be shortened. For a rise of 0.3m sea level, the return period of 20-years storm tides will be shortened to 6-years.

Hong Kong has painful experience on storm surge. The HKSAR has adopted stringent design standards for coastal infrastructures to fight against storms. Reclamation is raised +4 m above CD to cater for the settlement of the reclaimed land and sea level rise. A world class storm warning system has been installed to monitor and forecast stormy weather. Physical models and computational models are widely applied for the design of bridges, coastal infrastructures and drainage.

10.3 The impact on Water Level in the Pearl River Estuary

Based on the records in 40 years of 48 tidal gauges in the Pearl River estuary, almost all of the stations observed a rise in the river level. 82% of the stations observed a rising trend in high tide positions and 73% observed a rising trend in low tide positions. The rising rate of the average high tide or low tide positions is about 1 mm to 3 mm per year. The rising rate of the highest high tide position is about 2 mm to 6 mm per year.

The flood-tide level at a certain station depends on the sea level and river flow volume flow. The relationship is:

$$Z_2 = C_1 Z_1 + \beta Q + \alpha Z_1 Q + C_2$$

where Z_2 is the flood-tide level, Z_1 is the high tide level in SanDu station (三杜站), Q is the flow rate in MaKou station (馬口站) and C_1 , C_2 , α , β are constants that are acquired from correlation analysis. The relationship between sea level rise and flood-tide level can be derived from the above equation.

$$\Delta Z_2 = (\alpha Q + C_1) \Delta Z_1$$

Usually α is a negative constant and C_1 is a positive constant. The impact of sea level rise depends on Q . When the river volume flow Q equals $-C_1/\alpha$ then ΔZ_2 becomes zero. When Q exceeds $-C_1/\alpha$, ΔZ_2 becomes negative. Thus the impact of sea level rise is not significant in high flow seasons. It is important in the low flow seasons.

Sea level rise will shift the tidal flow boundary upstream. Firstly, when the sea level rises, the water depth will increase (assuming cross section of the channel remains unchanged). The tidal wave propagation velocity will increase. Secondly, the difference between the high tide positions and the low tide positions will increase because the low tide positions rise at a lower rate whereas the high tide positions rise at a faster rate.

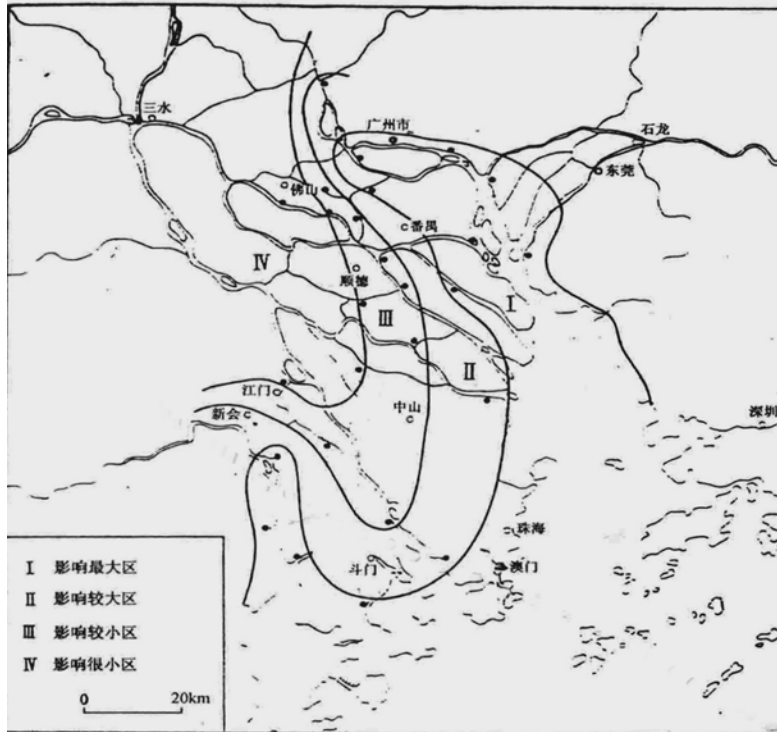


Figure 10.1 Four Influence Zones of Flooding / Tidal Level due to Sea Level Rise in the Pearl River Delta

Based upon the above analysis and considering the vulnerability of dams, the regions around the Pearl River is divided into four zones according to the degree of influence of flooding/tidal level. The areas of zone 1 to zone 4 are shown in Figure 10.1. Zone I suffers the most serious impact and Zone IV is not influenced by sea level rise at all. The farmland and coastal infrastructures in zone I will experience more frequent and frontline impact of flooding. The quality and quantity of harvest will be affected. The existing defense capacity of the coastal seawall is relatively weak against this rate of sea level rise. A series of adaptation measures have been introduced to reduce the impact of sea level rise in the Guangdong Province. The Guangdong Province has also rectified the standard of seawall according to the predicted sea level rise.

The Guangdong book has not classified Hong Kong into any zone. However, it is believed that the influence of sea level rise on flooding/tidal level is relatively low and is only limited to the wetlands in the northwestern territory of Hong Kong.

10.4 The Impact of Sea Level Rise on Seawall and Dam

Within the Guangdong Province, there are 4,321 numbers of dams and seawalls. Their total length is 15,829 km long. These seawalls protect 11300 km² of farmland and 20.7 million of people. These infrastructures are crucial in defense against floods and storm tides. Defense standards depend on the return period of flooding/storm and the maximum tidal height. The standards for flood-proof and sea-proof are different. In general, there are five levels of standards of dams and seawalls (Table 10.3).

Level and Standard of dams against flooding				Protected Object					
Level	Return Period (year)	Excess height of dam top	Top Apron width	Protected Farmland (x104hm ²)	Protected people (in million)	Cities	Protected people (in million)	Main Area	Supplement Area
1	≥200	2.0	8	≥20	≤25	Very important	≥15	---	---
2	200~100	2.0~1.5	8~7	20~6.67	25~10	Important	15~5	Huge	---
3	100~50	1.5	7~6	6.67~1.33	10~2	Minor Important	5~2	Large	Huge
4	50~20	1.5~1.2	6~4	1.33~0.07	2~0.1	General	2~0.1	Middle	Large
5	≤20	1.0	4~3	≤0.07	≤0.1	Small town	≤0.1	Small	Middle/ Small
Level and Standard of seawalls against storm tide				Protected Object					
Level	Return Period	Excess height of dam top	Top Apron width	Protected Farmland (x104hm ²)	Protected people (in million)	Cities	Protected people (in million)	Main Area	Supplement Area
1	≥200	1.0	8	≥20	≤25	Very important	≥15	---	---
2	200~100	0.8	8~7	20~6.67	25~10	Important	15~5	Huge	---
3	100~50	0.7	7~6	6.67~1.33	10~2	Minor Important	5~2	Large	Huge
4	50~20	0.6	6~4	1.33~0.07	2~0.1	General	2~0.1	Middle	Large
5	≤20	0.5	4~3	≤0.07	≤0.1	Small town	≤0.1	Small	Middle/ Small

Table 10.3 Standard of Dam and Seawall in the Guangdong Province (1995)

In Hong Kong, the flooding protection standards of public storm drainage systems adopted by Drainage Service Department are shown in Table 10.4. There are five main types of drainage designs based upon the types of land use, economic growth, socio-economic needs, consequences of flooding, and cost-benefit analysis of flood mitigation measures. Similar to the Guangdong standards, most of the important areas in Hong Kong are protected by designs which cater for a return period of 200 years. However, the 2-5 year return period design for the protection of agricultural land is below the Guangdong standards (≤ 20 years return period).

Types of Drainage	Years
Urban drainage trunk systems	200
Urban drainage branch systems	50
Main rural catchment drainage channels	50
Village drainage	10
Intensively used agricultural land	2-5

Table 10.4 Design Standards of Drainage in Hong Kong

When the sea level rises, the defense ability against flooding and storm is reduced. In zone 1 (Figure 10.1), 100-years storm tides may become 50-years storm tides (Table 10.2). The design of marine infrastructures should be adjusted to adapt to sea level rise. Table 10.5 illustrates the design return period of storms in the present and future system. The return period of storms will be greatly reduced in 2030.

Station	燈龍山 (deng long shan)	西炮台 (xi pao tai)	橫門 (heng men)	南沙 (nan sha)
Design high tide level (m)	2.38	2.68	2.36	2.55
Present Return Period (year)	100	100	100	100
Predicted Return Period in 2030 (year)	36	43	23	28

Table 10.5 Change in Design of Return Period of Storm in the Pearl River Estuary Stations (0.3m sea level rise)

Furthermore, high tide positions will be much enhanced. At present, the Port Work Manual of the Civil Engineering Department (CED) has stipulated the design wave height. Many existing coastal infrastructures in Hong Kong were designed according to the present wave height together with a safety factor (Table 10.7). Not all current marine/coastal structures can withstand the wave impact in the future. The CED will have to conduct port maintenance and monitoring programs to ensure safe and efficient

port operations. Nevertheless, the port work design standards in Hong Kong can already cope with the present 100-years return period flooding. The present geotechnical design standards and port work designs should be able to adapt to a 0.3 m rise in sea level by 2030.

Zone	Station	Rise in Storm level in different return period			Reduction in defense ability of seawall/dam (Shorten return period)
		100	50	20	
Most Serious Influence	南沙 (nan sha)	0.306	0.303	0.303	100→20,50→10
	三沙口 (san sha kau)	0.312	0.309	0.303	100→<20,50→<10
	黃埔 (huang bu)	0.336	0.330	0.324	100→<10,50→<10
	西炮台 (xi pao tai)	0.336	0.336	0.333	100→10,50→<10
	三灶 (san zao)	0.300	0.300	0.300	100→20,50→10
Serious Influence	燈籠山 (deng don shan)	0.231	0.237	0.240	100→20,50→10
	橫山 (heng shan)	0.210	0.219	0.225	100→20,50→10
	橫門 (heng men)	0.231	0.234	0.240	100→20,50→10
Minor Influence	竹銀 (zhu yin)	0.093	0.105	0.120	100→50,50→20
	睦洲 (mu zhou)	0.093	0.108	0.123	100→50,50→20
	板沙尾 (ban shan wei)	0.096	0.111	0.126	100→50,50→20
	三善滘 (san shan jiao)	0.063	0.078	0.093	100→50,50→20

Table 10.6 Impact on the Storm Tidal Level of the Pearl River Delta according to a 0.3m Rise in Sea Level

Location	The Island, Hong Kong		Power Generation (Daya Bay nuclear plant)	
Current design water depth	9.00m		2.99m	
Current design wave height (for 50-years storm)	7.00m		2.34m	
Sea level rise	0.2m	0.3m	0.2m	0.3m
Predicted design wave height	7.19	7.27	2.49	2.57
Additional wave height after sea level rise	0.19	0.27	0.15	0.23

Table 10.7 Design Standards of Tide Wave Height at Present and in 2030

10.5 The Impact of Sea Level Rise on Saline Water Intrusion

The Pearl River Delta is the major saline water intrusion zone in the Guangdong Province. Saline water intrusion affects the drinking water, agricultural irrigation and industrial water usage. The salination of the Pearl River is inversely proportional to the flow rate of the river and directly proportional to the rise in sea level. Sea level rise will enhance the effects of saline water intrusion. When the sea level rises by 0.2m, the salinity will increase by about 40%. This increase is roughly the same under different river flow volumes.

The impact of saline water intrusion in Hong Kong is minimal. Fresh water supply mainly comes from the Dongjiang via enclosed ducts. Agriculture and industries have almost been phased out. The main areas influenced by saline water intrusion are the High Island Reservoir, fish ponds and wetlands in the northwestern part of Hong Kong. The major economic loss due to an increase in salinity is the corrosion of materials in coastal infrastructures.

10.6 The Impact of Sea Level Rise on Beach and Shore

Beaches and shores are important resources in the Guangdong Province. By 1995, the Guangdong government had developed 2,028 km² of beaches and shore land. 1,213 km² of land is being used for agriculture (59.8%), while 546 km² is being used for aquaculture (27%) and 268 km² for other uses (13.2%). Usually, beaches and shores land grow in river deltas due to sedimentation. In the Guangdong coastal area, the rising rates of beaches/shores relative to the mean sea level are 5 ~ 7.5 mm per year. These rising rates of beaches and shores are four times of that of sea level rise. As the rise of beaches and shores is offset by sea level rise, Table 10.8 shows that area of new

beaches and shores will reduce by 29% when sea level rises by 0.3m. The reduced resources are equivalent to about 7.7% of the current profit.

Ocean Zone	Percent Area	No sea level rise	Sea level rise					
		Fill up area	10cm		20cm		30cm	
			Fill up area (km ²)	Difference (%)	Fill up area (km ²)	Difference (%)	Fill up area (km ²)	Difference (%)
伶仃洋 (ling ding yang)	280.7	80.0	72.2	9.7	64.3	19.6	57.2	28.5
磨刀門 (mo dao men)	139.3	45.4	42.8	4.8	40.1	11.7	37.4	17.6
雞啼門 (ji ti men)	15.3	26.5	25.0	5.7	23.5	11.3	22.0	17.0
黃茅海 (huang mao hai)	11.2	72.0	66.5	7.6	61.0	15.3	55.0	23.6
Total	547.3	233.9	206.5	7.8	188.9	15.6	171.6	23.4

Notes: Beach and shore area is measured as -2.0mCD of Pearl River Delta Foundation

Table 10.8 Reduction of Beaches and Shores Area due to Sea Level Rise in 2030
(unit of area : km²)

Although Hong Kong has a very long coast line, the impact of sea level rise on the natural build up of new beaches and shores should be minimal. This is mainly due to human intervention. The growth of new land gained from reclamation projects far exceeds the natural growth.

10.7 The Impact of Sea Level Rise on Coastal Eco-system and Aquaculture

Coastal animals are sensitive to storm tides and the amplitude of tidal waves. The maximum tidal difference is between 1.5m and 6.6m in different tidal zones, as shown in Figure 10.2. Although the water depth of marine habitats will be increased by 0.3m by 2030, the coastal wildlife will adapt to this gradual environmental change. The

reason is that the lifetime of coastal animals is short when compared to the time scale of sea level rise.

Sea level rise has positive and negative impacts on the aquaculture industry. The types and the habitat environment of marine fishes will change due to changes in salinity and storm tides. Overall, the quantity of aquatic production may remain the same, but the types of products may be substituted by others species due to changes in nutrition. The characteristics of pond fishes will suffer the most due to saline intrusion. This problem of salination can only be solved by building seawalls.

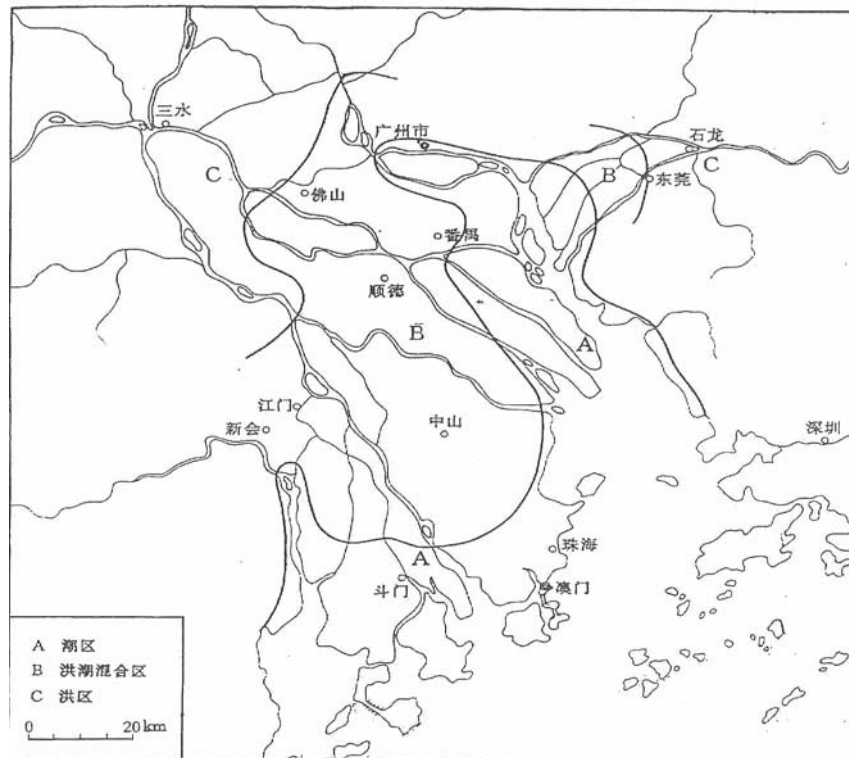


Figure 10.2 Distribution of Tide, Mixed and Flooding Zones in the Pearl River Delta

In Hong Kong, the Mai Po wetland is a rich coastal eco-system. The impact of anticipated sea level rise of 30 cm by 2030 on coastal animals should be insignificant. The lifetime of living organisms is in the order of days or months whilst the time scale of sea level rise is in terms of decades. The coastal animals have sufficient time to adapt to the warmer sea water. The effect of salt water intrusion on fresh water aquaculture in the northern part of the New Territories will be observable. Either the aquaculture industry should adapt to this change by engineering measures or this sunset industry will be terminated.

The possible horizontal erosion distance of beaches and shores in Hong Kong due to sea level rise can be estimated. Figure 10.3 shows the cross section of a beach.

By simple geometry:

$$R = \frac{L}{(B+h)} S = \frac{S}{\tan \theta}$$

where R is the horizontal erosion distance of beaches (in meter), S is the rise in sea level, B is the height of beach edge, h is the water depth alongshore, L is the horizontal distance between the beach and the water depth of h, $\tan \theta$ is the average slope of beaches and $\tan \theta \approx (B+h)/L$ respectively

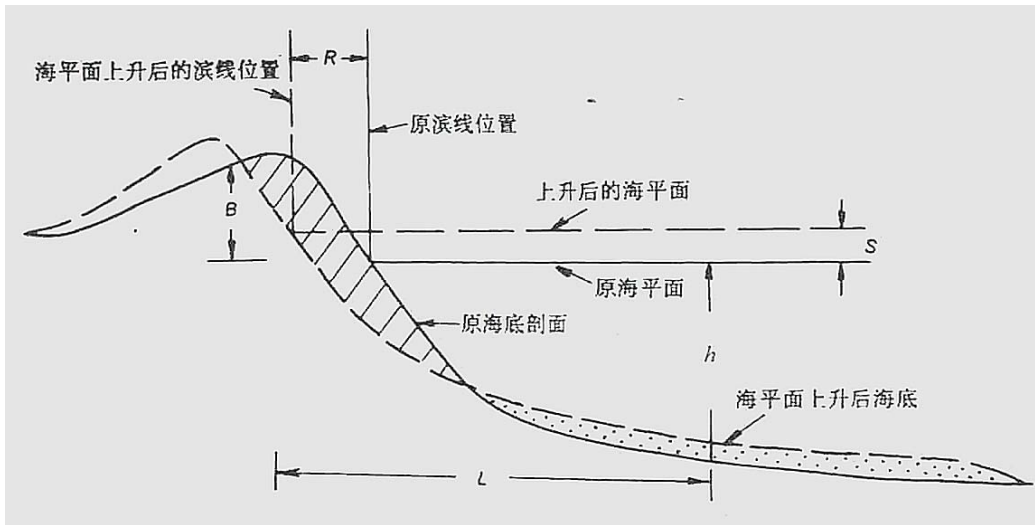


Figure 10.3 Shoreline Retreat of Beaches and Sea Level Rise

If beaches are composed of sandstones and with slope of 1/100~1/200, the horizontal erosion loss of beaches is about 15 m to 30 m with sea level rise of 30 cm. In general, beaches with gentler slopes have greater erosion loss.

Table 10.9 lists the horizontal erosion distance of beaches in Hong Kong due to sea level rise. Most of the beaches at locations such as the Repulse Bay, Stanley Bay, Shek O, Clear Water Bay, and Silverstrand will be eroded. In summary, the predicted horizontal erosion distance of beaches is in the range of 0.6 ~ 10.5 m in 2030. The impact of horizontal erosion in steep-sloped beaches is insignificant in Hong Kong. Further technical information of beaches in Hong Kong can be found in the Port Works Design Manual Part 5 (Civil Engineering Department, HKSAR).

Beaches Features		Sea level rise in 2030			
		Guangdong province		IPCC	Dr. Ding study
Sand, D50 (mm)	Lower Slope	20 cm	30 cm	12 cm	5.7 cm
<0.2	1/35	7 m	10.5 m	4.2 m	2 m
	1/20	4.0 m	6 m	2.4 m	1.1 m
0.2~0.5	1/20	4.0 m	6 m	2.4 m	1.1 m
	1/15	3.0 m	4.5 m	2.2 m	0.9 m
>0.5	1/15	3.0 m	4.5 m	2.2 m	0.9 m
	1/10	2.0m	3 m	1.2 m	0.6 m
Range		2.0 ~ 7 m	3 ~ 10.5 m	1.2 ~ 4.2 m	0.6 ~ 2 m

Table 10.9 Horizontal Erosion Distance of Beaches due to Sea Level Rise in 2030

10.8 Conclusion

The impacts of sea level rise on the Pearl River Delta region are summarized. The major impacts of sea level rise on Hong Kong are reduction in the return period of tides and increase in tidal height. If the sea level rises by 0.3m, the return period of tide will be shortened in most areas in the Pearl River Delta and the maximum tidal height will be increased by 0.19-0.27 m. The coastal defense system should be rectified based on the present observations in order to reach the standards in 2030 or later. The impact on organisms in the marine zone is not significant since the lifetime of organisms is shorter than the timescale of sea level rise. The quantity of aquaculture products should remain more or less the same. The quality of these products will be influenced by salinity intrusion. Continuous management and adaptation measures are necessary to prevent or minimize salination. The predicted horizontal erosion of beaches in Hong Kong is 0.6 m to 10.6 m. This impact is not significant. The present coastal defense system is able to cope with the sea level rise predicted in 2030 but the present standards will be outdated in 2030. In summary, the northwestern part of Hong Kong will be affected. Further studies should be carried out to study the impacts on Mai Po RAMSAR site. Coastal defense systems and design standards should be developed to adapt to changes in storm tides and tidal positions.

10.9 References

Books

1. Guangdong Haipingmian Bianhua Jiqi Yingxiang Yu Duice (廣東海平面變化及其影響與對策), 黃鎮國著, 廣東科技出版社, 2000
2. Port Works Manual (Design, Construction and Maintenance), Department of Civil Engineering Department, HKSAR
3. Port Works Design Manual Part 5 (Guide to Design of Beaches), Department of Civil Engineering Department, HKSAR

Website

4. Flood protection standards for the planning and design of the public stormwater drainage systems, Drainage Service Department, HKSAR
(http://www.dsd.gov.hk/flood_prevention/flood_protection_standards/index.htm)

Chapter 11 Conclusion

Characterization of Urban Heat Island

The characterization of UHI in Hong Kong was successfully carried out. Land based mobile experiments were carried out in summer, fall and winter. The UHI in the urban areas in the Kowloon Peninsular and the northern part of Hong Kong Island was about 2.17°C. The largest UHI occurred in the mixed commercial urban areas, including Causeway Bay, Yau Ma Tei and Mongkok. The average UHI values were 2.12°C in summer, 3.04°C in autumn and 1.35°C in winter.

Characterization of Long Term Climate Change in Hong Kong

The urban and rural temperature is rising at 0.2°C and 0.6°C per decade respectively in Hong Kong. And the daily diurnal range is decreasing by 0.28°C per decade. Urbanization increases the concentration of suspended particulates, and decrease the percentage of time with reduced visibility at the rate of 1.9% per decade. The increased in cloud amount by 1.8% per decade and the decrease in global solar radiation by 26% will reduce evaporation by 40%. Moreover, the frequency of heavy rain and thunderstorms increases by 0.4day and 1.7days per decade respectively. The number of tropical cyclones decreases by 0.17 per decade. The sea level rise is at the rate of 2.3mm per year for the past 50 years.

Characterization of Global Warming Impact

Energy Industries

The consultant believes that the major impact of global warming on Hong Kong is on the energy sector. Rising the ambient temperature by 1°C will increase electricity consumption by 9.02%, 3.13%, and 2.64% in the domestic, commercial and industrial sectors respectively. However, the gas consumption will decrease when the ambient temperature increases. For 1°C rise in temperature, the gas demand will be reduced by 2.39% in the domestic sector. The gas consumption rates in the commercial and industrial sectors and the consumption of oil products do not depend on the ambient temperature. Therefore, they are not affected by climate change. For 1°C rise in temperature, the total energy cost of Hong Kong will increase by HK\$1.65 billion.

Dengue Fever and Malaria

The impact of temperature rise on the transmission of dengue fever and malaria in Hong Kong was successfully quantified. The ΔEP of dengue fever was estimated to be 1.24%, 2.62% and 4.12% for 1°C, 2°C and 3°C rise in temperature respectively in Hong Kong. The results showed that the risk of dengue would increase due to global

temperature rise but the impact was not significant. The increase was only in a few percentage. The ΔEP of malaria was estimated to be 6.7%, 13.0% and 18.7% for 1°C, 2°C and 3°C rise in temperature respectively in Hong Kong. The risk of malaria would also increase with temperature rise. The impact of malaria was more significant than that on dengue fever. The maximum impact on dengue fever was in summer months while the maximum impact on malaria was in spring and fall.

Air Pollution

The impact of global warming on air quality in Hong Kong is still largely unknown. It was discovered that the ozone level in Tung Chung had correlations with temperature, wind speed and solar radiation. When the ambient temperature increased by 1°C, the ozone concentration increased by about $4.6\mu\text{g}/\text{m}^3$ which was just 2% of the ozone standard of $240\mu\text{g}/\text{m}^3$. Thus the amount of ozone augmented during the episode days due to climate change was insignificant. The more important point is whether the frequency of episode days will increase due to climate change. Since temperature is associated with ozone concentration in photochemical smog, it is likely that photochemical smog will occur more frequently in the future when temperature rises.

Others

Other topics that have been explored include agriculture, water resources, flooding, migratory birds, hill fire, coral reef, mangrove, dolphins, eco-tourisms and sea-level rise. This project is only able to give an account of the existing adaptation measures and report the potential ones. Exploratory works were limited to elementary statistics compilation and regression analysis.

Extreme events such as tropical storms or heavy rainfall may bring more flooding problems to Hong Kong. The maximum tidal height when the sea level rises by 0.3 m may be increased by 0.19-0.27m. This will cause higher storm tidal position and shorten the return period of storm tides. Most of the reclaimed land in Hong Kong will be flooded by sea water during storms. The impacts of coastal infrastructure will become more serious in future. It is believed that the influence of sea level rise on flooding/tide level is relatively low and it is only limited to the wetlands in the northwestern territory of Hong Kong.

Agriculture has been phasing out in Hong Kong. The total value of agriculture in 2002 was about \$1.1 billion (< 0.1% of GDP). The impact of global warming on agriculture is considered insignificant. The eco-tourism values of migration birds watching, dolphin watching, and hiking are estimated to be \$72 – 720 million, \$1 million and \$118 to 1180 million respectively. The impact on them are also considered minor.

Negative impacts on wetlands, mangroves, corals due to global warming are anticipated.

Acknowledgements

The project team would like to express sincere thanks to the EMSD for their support in the energy impact work. Acknowledgement is also due to Simon Hales, Ecology and Health Research Centre, Wellington School of Medicine & Health Sciences, The University of Otago, New Zealand for his guidance on human health.

We are deeply indebted to Dr. Chen Wu of the Department of Land Surveying and Geophysical Information, PolyU, GPS operation supports. Without this support, the UHI mobile experiment would not be carried out.

End of final report